TOPOLOGICAL CHARACTERIZATIONS OF THE CONTROLLABILITY OF COMPLEX NETWORKS

by

Baike She

A thesis submitted in partial fulfillment
of the requirements for the Doctor of Philosophy
degree in Mechanical Engineering in the
Graduate College of
The University of Iowa

May 2020

Thesis Committee: Zhen Kan, Thesis Supervisor
Shaoping Xiao, Thesis Supervisor
Er-Wei Bai
Siddhartha Mehta
Venanzio Cichella

This dissertation is dedicated to my mother Shuyu Zheng, my father Jun She, for their unconditional love and support.

ACKNOWLEDGMENTS

I would like to express my gratitude and sincere thanks to my advisor Dr. Zhen Kan for providing me valuable guidance and regular suggestions throughout my whole Ph.D. study. With his inspiration and encouragement, I could complete my degree successfully. I am really appreciated that he could devote his time to my research, from discussing fundamental ideas to helping paper revisions. In addition, I feel grateful that his training is always in line with my career goals.

I am thankful to my research collaborator and committee member Dr. Siddhartha Mehta, for his timely assistance and guidance. Meanwhile, I would like to extend my gratitude to other committee members. I am deeply grateful to Dr. Shaoping Xiao, for his supervision and help during my last semester. I am also thankful to Dr. Er-Wei Bai and Dr. Venanzio Cichella for contributing many valuable comments that improved my presentation and contents of this dissertation.

I would also like to thank all of the research opportunities provided by the department of mechanical engineering at the University of Iowa, University of Iowa Technology Institute and University of Florida Research and Engineering Education Facility.

I am indebted my parents for their encouragement and unconditional love through my entire life. I owe special thanks to all of my friends for being stuck with me throughout my life.

ABSTRACT

Complex networks composed of units dynamically interacting among themselves have been found broad applications in brain networks, social networks, multi-agent networks, and power networks. Owing to tremendous application potential, growing research has been devoted to investigating structural and functional properties of complex networks. The focus of this dissertation is to characterize classical controllability and generalized controllability of complex networks from graph-theoretic perspectives.

Classical controllability of complex networks is studied in Chapter 2. By exploring connections among leaders and followers, leader selection algorithm is developed through graph topology to guarantee networked systems with both cooperative and antagonistic interactions to be controllable. Energy-related controllability is investigated from Chapter 3 to Chapter 5. In chapter 3, energy-related controllability of complex networks is studied through individual performance of leaders. Followed by the results in Chapter 3, a novel leader selection method using graph distance to ensure network controllability with better energy-related performance is proposed in Chapter 4. Further, Chapter 5 analyzes energy-related performance of composite networks via graph product. Chapter 6 introduces a relaxed controllability referred to as herdability. Generalized Equitable partition is utilized to characterize herdability of complex networks in Chapter 6, while graph walk is applied to leader selection to ensure herdability of complex networks in Chapter 7. Chapter 8 characterizes structural balance of signed networks via algebraic topology. Chapter 9 concludes the dissertation by summarizing the work and discussing the open problems that require further investigation.

PUBLIC ABSTRACT

Complex networks composed of units dynamically interacting among themselves have been found broad applications in brain networks, social networks, multi-agent networks, and power networks. Owing to tremendous application potential, growing research has been devoted to investigating structural and functional properties of complex networks. The complexity of complex networks lays down a challenge for analysis and design networked dynamical systems through traditional tools. Hence, the focus of this dissertation is to characterize properties and performance of networked dynamical systems from graph-theoretic perspectives. The gaps between system performance and network structures are built to facilitate the design of networked systems, which can be applied to social network analysis and swarm robotics.

TABLE OF CONTENTS

page

LIST OF TABLES

LIST OF FIGURES

CHAPTER 1
INTRODUCTION

1.1 Motivation

Complex networks composed of units dynamically interacting among themselves have been found broad applications in biological networks, social networks, multi-agent systems, and urban networks. Owing to tremendous application potential, growing research has been devoted to investigating structural and functional properties of complex networks. In such applications, one popular approach is to cast the network control problem on complex networks into a leader-follower framework, wherein the leaders dictate the overall behavior of a network by influencing the followers via the connectivity characteristics of the network. Leader-follower systems that coordinate and cooperate over information exchange networks have been increasingly applied in both science and engineering. Typical applications of leader-follower systems include:

- Robotic Networks: Distributed Coordination and Formation Control;
- Social Networks: Propagation and Consensus/Clustering of Opinions;
- Biological Networks: Analysis of Biochemical Reaction and Brain Functions.

The ability to steer a networked system to a desired behavior via external controls, referred to as network controllability, is of fundamental significance to achieve system functionalities. For most applications, networked control systems are required to be maneuvered by external inputs to achieve designed tasks and functions, where network controllability ensures the goal of driving a networked control system to any desired state. Classical control theory provides abundant tools via linear algebra and matrix analysis to check the controllability of a system. However, due to the complexity and higher dimension of complex networks, adopting classical ways to check network controllability is of great computation and is obscure for designing networked control systems. Compared to traditional ways of checking network controllability, researchers have been trying to investigate the controllability of complex networks from topological perspectives. Complex networks fully captured by graphs provide insights on interactions among individuals as well as structures of systems. Evolution on network controllability via topology remarkably

facilitates analysis and design of networked control systems. More importantly, existing algorithms developed on detection and exploration of topological properties of complex networks can be borrowed to help dig the characteristics of network controllability.

Along with controllability of complex networks, two important aspects stem from practical applicability. One is the dynamic performance of a networked system. This is particularly critical in a situation where a network might be controllable by a selected leader group but the system performance might be infeasible to allocate in practice. For example, a designed control input may exceed the limitations of the actuators. To this effect, investigation on the energy-related controllability of complex networks is necessary. In the other circumstance, requiring a networked system to be fully controllable could be nonessential. For example, in applying adaptive cruise control to a platoon of autonomous vehicles, the vehicles are often required to maintain a desired positive speed. In a political election, a candidate aims to drive the supportive rate above a positive percentage in order to win. In such cases, a relaxed controllability referred to as herdability that drives the system states to a specific subset, rather than the entire state space, as in classical controllability, is of more practical significance.

Given the importance of controllability of complex networks, this dissertation is motivated by the following questions:

1. Under what topological conditions are complex networks fully controllable?
2. How to characterize the energy-related controllability of complex networks from topological perspective?
3. How to develop criteria to capture a relaxed controllability, i.e., network herdability from graph-theoretic perspectives?

1.2 Problem Statement

Network controllability of leader-follower complex networks highly depends on the network structure and locations of leaders. In this dissertation, complex networks with both cooperative and antagonistic interactions are considered. This requires networks to capture the interactions among units using positive and negative edge weights. Network controllability, energy-related

controllability and network herdability are characterized from graph topological perspectives, leading to new insight into the influence of network topology and location of leaders on system performance of networked control systems.

1.3 Literature Review

This section provides a review of relevant literature for each chapter.

Classical Controllability of Complex Networks: Two types of interactions can be captured in complex networks without considering the edge weights, named as cooperative and antagonistic interactions. Networks with only cooperative interactions are commonly modeled as unsigned graphs containing only positive edge weights, where positive weights indicate cooperative relationships. Average consensus is a typical example of cooperative networks, where units within a network positively value information collected from their neighbors and achieve group consensus via collaboration [1]. If a graph allows to admit negative edge weights, it is called a signed graph. Signed graphs are widely used to represent networks with both cooperative and antagonistic interactions [2]. For instance, positive/negative weights in signed graphs can be used to model friend/adversary relationships in social networks [3] and collaborative/competitive relationships in multi-agent systems [4].

Controllability of cooperative networks has been extensively studied in the literature. Leader-follower controllability was considered for the first time in [5], where the network controllability was characterized based on the spectral analysis of the system matrix. Graph-theoretic approaches were then explored to provide characterizations of network controllability. For instance, it was established in [6] that network symmetry with respect to leader groups can potentially lead to uncontrollability. Topological characterizations of network controllability were investigated in [7] and [8]. Graph-distance based lower bounds on the rank of the controllability matrix were developed in [9]. Necessary and sufficient conditions for network controllability were developed for tree topology [10], grid graphs [11], and path and cycle graphs [12]. Other than graphical characterizations of network controllability, structural properties of cooperative

networks were also exploited from matrix-theoretical perspectives in the works of [13–21] to reveal the connections between network controllability and underlying graphs. Other representative works that investigated network controllability include the results in [22–24]. Besides characterizing network controllability, various methods, e.g., combinatorial [25] and heuristic [26] methods, were developed to select leaders to ensure controllability of given networks. Other representative works regarding leader selection for network controllability include [27–29].

To ensure controllability of complex networks with both cooperative and antagonistic interactions, several theorems in regards to network controllability are developed on particular graphs, i.e. signed path and cycle graphs in Chapter 2. A leader selection method is proposed on complex networks with Laplacian dynamics by partitioning a network into sub-networks. This is based on the invariance of the network controllability via alterations of leader-to-leader connections.

Energy-Related Controllability of Complex Networks: Characterizations of Energy-Related Metrics: Various metrics of network performance have been developed through controllability Gramian to characterize control energy metrics of complex networks. The structure of controllability Gramian relates to the energy-related metrics of the network controllability. The properties of controllability Gramian, such as its minimum eigenvalue, the trace of its inverse, and the condition number, have been explored in the works of [30–32] to characterize the energy-related performance in network control. Control energy metrics can also be characterized via spectral analysis of system matrices which have been found to hold a relationship with the controllability Gramian. In [33], it was discovered that the minimal control energy is related to the distribution of the eigenvalues of the system matrix. In [34], the leading right and left eigenvectors of the system matrix were found to play a crucial role in quantifying how much each node contributes to the network in terms of controllability and control energy metric. Other representative approaches include optimization-based leader group selection for minimal control energy [35–37], graph-theoretical characterizations of energy-constrained controllability [38–40], and network design methods for improved controllability and energy efficiency [41]. Nodal

centrality (i.e., a measure of individual contributions of nodes in networked control systems) was previously investigated in the works of [31, 32, 42–47]. In [42], network vulnerability was investigated in terms of the minimum average control energy required for the adversary to drive a system away from synchronization. Similar energy metrics were also investigated independently via submodular set function [31], the joint centrality measure for reduced control energy [43], the nodal communicability to support actuator selection [44, 45], and the reachability metrics for bilinear networks [46]. A common approach employed in the aforementioned results is the exploitation of the controllability Gramian-based energy metrics.

Chapter 3 investigates the energy-related controllability of complex networks, where the network units interact via neighbor-based Laplacian dynamics and the network allows both positive and negative edges to capture cooperative and antagonistic interactions among network units. The energy-related controllability jointly considers network controllability (i.e., the ability to drive the network to a desired state by a leader group) and energy-related performance (i.e., the energy-related metrics incurred by the selected leaders in steering the network to a desired state). Specifically, energy-related measures, average controllability, average control energy, volumetric control energy, are considered. These measures are then characterized in relation to signed graph Laplacian to gain topological insights into the energy-related controllability of complex networks.

Energy-Related Controllability of Complex Networks: Leader Selection: Followed by the previous section, to investigate control energy metrics of complex networks, controllability Gramian-based metrics, such as the worst case control energy, average control energy, average controllability, and volumetric control energy, have been studied in the works of [31, 32, 48, 49] to provide quantitative measures of energy-related metrics in networked control systems. Based on these energy-related metrics, the leader group identification problem was investigated in [39, 41, 42, 50, 51]. In [50], a projected gradient method was developed to determine the key nodes with minimum control cost in complex networks. The relationship between network structure and minimum energy required to control networked systems was studied in [39] to

facilitate the identification of the leader group. In [41], controllability Gramian-based metrics were employed to improve system performance via the design of system dynamics and network topology.

Chapter 4 jointly investigates network controllability and control energy metrics for leader group selection in complex networks with Laplacian dynamics. A networked system with signed acyclic topology is considered. Graph inspired characterizations of the energy-related controllability are developed based on the interactions between the network topology and network dynamics. The developed topological characterizations are then exploited to derive leader selection algorithms on signed acyclic graphs.

Energy-Related Controllability of Complex Networks: Composite Complex Networks Via Graph Product: Followed by previous two sections, it has been observed that many complex systems can be constructed and analyzed through simple subsystems (i.e., factors), where core properties of factors are preserved in the composite system. For example, controllability and observability of factor systems are preserved under series-parallel connections [52]. Stability of composite feedback systems can be analyzed based on its factor systems via small-gain theorem and composite Lyapunov functions [53]. Recently, graph products have been explored to construct and reveal structural and functional relationships between factor systems and the associated composite system. Cartesian product, direct product, and strong product are typical graph products that are used to obtain a composite network from simple factor networks. In [11, 21, 54, 55], classical controllability and observability of a composite network were characterized based on its factor networks. In [56], the verification and prediction of the structural balance of signed networks was studied via Cartesian product. In a recent work [57], generalized graph product, including Cartesian, direct, and strong product, were utilized to reveal spectral and controllability properties of composite systems.

Chapter 5 characterizes the energy-related controllability of composite complex networks. A class of composite networks constructed from simple factor networks via graph product, such as Cartesian product, direct product, and strong product are considered. The considered factor

networks are leader-follower signed networks with neighbor-based Laplacian dynamics, adopting positive and negative edges to capture cooperative and competitive interactions among network units. The results reveal how the energy-related controllability of a composite network can be inferred from the spectral properties of the local factor systems. These results are then extended to layered control networks, a special, yet widely used, network structure in many man-made systems. Besides Cartesian product, developed results are generalized on direct and strong graph product. A necessary and sufficient condition to verify the structural balance of composite signed networks is also developed, which is applicable to general graph product.

Herdability on Complex Networks: Controllable Subspace and Generalized Equitable Partition: Instead of studying classical controllability problem as in Chapter 2, Chapter 6 investigates a relaxed controllability referred to as herdability. A concept that drives the system states to a specific subset, rather than the entire state space. Both herdability and controllability concern the ability to drive system states in a controllable subspace, therefore, the literature on the controllability of networked systems is first reviewed. The influence of network topological structures on network controllability has been investigated using a variety of tools, such as graph-theoretic approaches [8, 9, 18, 21, 58], structural controllability [13, 16, 17, 19, 20], and consensus based results [22–24]. With respect to non-cooperative networks, the controllability of signed networks has been investigated via structural balance in [40, 59–61]. Network controllability is closely related to the underlying graph topology, hence, graph partition (cf. [62] and [63]) was exploited to characterize network controllability from topological perspectives. In [6] and [64], equitable partition and almost equitable partition were used to develop conditions that render cooperative networks (i.e., unsigned graphs) uncontrollable. In [65], necessary conditions of uncontrollable networks were developed via almost equitable partition. These graph partition-based results were extended to investigate non-cooperative networks (i.e., signed unweighted graphs) in [59]. Upper and lower bounds of the controllable subspace of networked systems were characterized based on graph partitions in [66–68].

Chapter 6 studies network herdability. Herdability is an ability to drive system states to a specific subset in the state space. A positive subset of the state space was considered in [69], where the system states are controlled to be element-wise above a positive threshold. Positive systems are a particular class of systems where, provided positive initial states, the states remain positive during evolution [70]. Necessary and sufficient conditions for a herdable positive networked system were developed based on controllable subspace and graph walks in [69]. The results of [69] were then extended to characterize the herdability of linear systems based on sign patterns and graph structures in [71] and [72]. Followed by this, Chapter 6 characterizes the controllable subspace and herdability of signed weighted networks. Graph partitions are exploited to characterize the controllable subspace of the system, from which sufficient conditions on quotient graphs are derived to render the system herdable.

Herdability on Complex Networks: Graph Walks and Structural Balance: The literature reviews of Chapter 6 and Chapter 7 overlap with each other. Followed by Chapter 6, Chapter 7 proposes several leader selection methods on complex networks through graph walks. In particular, graph walk is exploited to develop sufficient conditions ensuring the herdability of general signed networks. The results are then extended to structurally balanced networks to refine leader groups.

Algebraic Topological Characterizations of Structural Balance on Complex Networks: Structural balance is a topological characterization of signed networks [73]. Recent research shows that the structural balance is crucial in determining network performances. For instance, a bipartite consensus over a network with antagonistic interactions was established in [2], provided that the network is structurally balanced. The developed bipartite consensus was then extended for signed directed networks [74], signed switching networks [75], general linear agents [76], and high-order system dynamics [77]. Despite various system dynamics and network topology, the structural balance is a common necessary condition for achieving bipartite consensus in the aforementioned results [2, 74–77]. Besides engineering applications, the structural balance has also been explored in the context of social and opinion networks [78–81] to reveal the

evolution of individual's social states in the presence of trustful and distrustful interactions. Recent research also indicates that the structural balance provides insights in addressing network stability and controllability [40, 59, 60, 82, 83]. The verification and prediction of the structural balance in signed networks were investigated from a data-driven perspective in [56].

Due to the significance of the structural balance in network performances, Chapters 8 is particularly motivated to investigate the fundamental relationship between the structural balance and the underlying topological structure of signed networks.

1.4 Contributions

The contributions of Chapters 2-8 are discussed as follows:

1. **Classical Controllability of Complex Networks:** Controllability ensured leader group selection on signed networks is considered. Despite extensive study of controllability of unsigned networks, relatively few research effort focuses on signed networks. Specifically, leader selection rules are developed for signed path and cycle networks in Chapter 2, which provides constructive approaches to select leaders for network controllability. Some networks can be considered as a combination of path and cycle networks, therefore, the developed leader selection rules on path and cycle networks can be potentially extended to more complex and sophisticated networks. In contrast to most existing matrix-theoretical approaches to characterize network controllability, graph-inspired understandings of network controllability are realized in Chapter 2. Specifically, Chapter 2 investigates the relationship between the network controllability and the underlying topology, revealing how leader-to-leader and leader-to-follower connections affect the controllability of signed networks with Laplacian dynamics. Such graphical characterizations of network controllability are able to provide more intuitive and effective means in selecting leaders for network controllability.
2. **Energy-Related Controllability of Complex Networks: Characterization of Energy-Related Metrics:** Energy-related controllability of signed complex networks with Laplacian dynamics is studied in Chapter 3. It is revealed that the inverse signed graph

Laplacian can be used to quantify how the leaders individually contribute to network performance in terms of energy-related controllability. Aligned with these efforts, Chapter 3 moves forward in relating the controllability Gramian-based energy metrics to the graph Laplacian. Different from discrete systems (e.g., [32, 43, 46]) or single leader cases (e.g., [42, 44, 45]) in the literature, this work considers complex networks evolving with continuous signed Laplacian dynamics and multiple leaders. Through the global topological property of a network, the developed characterizations reveal how the energy-related controllability is influenced by the network topology. It is revealed that, for structurally unbalanced signed graphs, the energy-related controllability is closely related to the diagonal entries of the inverse of the graph Laplacian. This provides insights into how much an individual leader contributes to the network's overall energy-related performance. The revealed relation can be potentially leveraged to characterize energy-related controllability from topological perspectives via effective resistance, since the inverse graph Laplacian is closely related to effective resistances [84], as shown in Chapter 4.

3. **Energy-Related Controllability of Complex Networks: Leader Selection:** Chapter 4 characterizes network controllability and energy-related performance on signed networks, where classical methods are no longer applicable due to the presence of cooperative and antagonistic interactions. Graph-inspired understandings of the relationship between leader roles and network topology are developed to facilitate the development of leader selection rules. The rules jointly consider network controllability and energy-related performance. In particular, effective resistance and graph distance are considered to characterize energy-related performance from leaders to followers. In addition, constructive examples are provided to illustrate how the developed leader group selection algorithms can be applied to general signed acyclic networks.
4. **Energy-Related Controllability of Complex Networks: Composite Complex Networks Via Graph Product:** Chapter 5 characterizes energy-related controllability of complex

composite networks via graph product approaches. A crucial benefit of using graph product is that the global properties, such as average controllability, average control energy, and volumetric control energy, of the composite networks can be inferred from its local factor graphs. This provides a practical means to analyze large-scale and complicated networks from its relatively simple factor systems. It is revealed that the eigenvalues and eigenvectors of factor systems can be used to characterize energy-related controllability of composite networks. Applications, such as network topology design and leader selection, are discussed to demonstrate how factor graphs can be individually designed based on the developed characterizations to improve overall energy-related controllability of the composite systems.

5. **Herdability on Complex Networks: Controllable Subspace and Generalized Equitable Partition:** Chapter 6 characterizes the herdability of general undirected signed weighted networked systems. Topological characterizations of network herdability are developed using graph partitions. Since previous research mainly focused on unsigned networks or signed unweighted networks, generalized equitable partitions are developed in Chapter 6 to take into account the edge weights of signed networks. Differing from Chapter 2-5 and most graph partition-based results that consider Laplacian dynamics [6, 59, 64–68], Chapter 6 considers the linear dynamics depending on the adjacency matrix of the underlying graph. This type of network dynamics has many applications in nature (e.g. brain networks [85]) and man-made systems (e.g., multi-agent networks [86]). The controllable subspace of such dynamics is then derived based on the generalized equitable partition. In addition, it is revealed that the quotient graph can be used to infer the herdability of the original graph, where herdability of quotient graphs criteria is developed based on positive systems.
6. **Herdability on Complex Networks: Graph Walks and Structural Balance:** Chapter 6 studies the herdability of signed leader-follower networks through graph walk. To develop

sufficient conditions ensuring the herdability of signed networks, graph walks, such as 1-walk and 2-walk are adopted. Controllability of complex networks is shown to be invariant under structurally balanced networks in Chapter 3. However, herdability of complex networks does not satisfy this condition anymore. The results developed through graph walks are then extended to facilitate leader selection for the herdability of structurally balanced signed networks.

7. **Algebraic Topological Characterizations of Structural Balance on Complex Networks:** Simplicial complexes are used as a novel modeling approach to represent and analyze complex networks in Chapter 8. Compared to conventional graphical models, simplicial complexes generalize graphical models in the sense that, in addition to the binary relations between nodes as in standard graphs, they also capture the higher-order topological relations among them [87]. Consequently, simplicial complexes are able to provide insights into network topologies that are unobtainable from standard graphs or other traditional modeling and analysis methods. Other than that, the use of the simplicial complex opens a new door to investigate networks, where new sets of analysis tools from algebraic topology become available. In particular, as topological invariants that can only be extracted from simplicial complexes, homology and cohomology are exploited to unravel the fundamental relationship between the structural balance and the network topology. Motivated by the recent research of using homology to verify sensor network coverage [88–90], the homology and cohomology are extended in Chapter 8 to unravel the topological properties of signed networks, which has received little research attention in the literature.

1.5 Dissertation Outline

Chapter 1 serves as an introduction, where the motivation, problem statement, literature review and the contributions of the dissertation are discussed.

Chapter 2 investigates leader-follower controllability of signed networks. Leader-follower controllability is interpreted as identifying a small subset of nodes in signed networks, such that

the selected leaders are able to drive the network to any desired behavior, even in the presence of antagonistic interactions. In particular, graphical characterizations of the controllability of signed networks are developed based on the investigation of the interaction between network topology and dynamics. Along with illustrative examples, heuristic algorithms are also developed showing how leader selection methods developed for signed path and cycle graphs can be potentially extended to more general signed networks.

Chapter 3 studies the energy-related measures of controllability for signed networks and characterizes these measures in relation to graph Laplacian to gain topological insights into controllability. Controllability Gramian-based metrics, namely, average controllability, average control energy, and volumetric control energy, are exploited for general signed networks in this Chapter to quantify the energy-related performance incurred by the leaders.

Chapter 4 investigates a leader group selection approach that jointly considers network controllability and energy-related performance. Specifically, a networked system with signed acyclic topology is considered. The developed topological characterizations are exploited to derive heuristic leader selection algorithms on signed acyclic networks. Illustrative examples are provided to demonstrate the effectiveness of the developed leader group selection methods.

Chapter 5 studies the energy-related controllability of composite networks through the corresponding factor networks. Graph product, including Cartesian product, direct product and strong product are utilized to analyze the control energy metrics of the composite networks.

Chapter 6 is practically motivated to characterize the herdability of networked systems from graph topological perspectives. By considering the herdability of signed weighted networked systems, a generalized equitable partition is exploited to characterize the controllable subspace of the system, from which sufficient conditions are derived to render the system herdable.

Chapter 7 proposes leader group selection methods to ensure herdability of complex networks on both general signed graphs and structurally balanced signed graphs. Graph walks are exploited to help determine the suitable leaders. For balanced networks, leaders are determined through the particular structure of networks and are shown to be refined through graph walks.

Chapter 8 draws on techniques from algebraic topological spaces and invariants to extract the topological properties of the structural balance in complex networks. Specifically, instead of using conventional graphs, simplicial complexes are employed as the primary tool to model signed networks. Topological invariants, such as homology and cohomology, are then explored to extract topological characterizations of the structural balance from the simplicial-complex-based models.

Chapter 9 concludes the dissertation by summarizing the work and discussing some remaining open problems that require further investigation.

CHAPTER 2
CONTROLLABILITY OF COMPLEX NETWORKS

Leader-follower controllability of signed networks is investigated in this chapter. Specifically, we consider a dynamic signed multi-agent network, where the agents interact via neighbor-based Laplacian dynamics and the network allows positive and negative edges to capture cooperative and antagonistic interactions among agents. The agents are classified as either leaders or followers, thus forming a leader-follower signed network. To enable full control of leader-follower signed networks, controllability ensured leader group selection approaches are investigated in this Chapter, i.e., identifying a small subset of nodes in a signed network, such that the selected nodes are able to drive the network to a desired behavior, even in the presence of antagonistic interactions. In particular, graphical characterizations of the controllability of signed networks are first developed based on the investigation of the interactions between network topology and agent dynamics. Since signed path and cycle graphs are basic building blocks for a variety of networks, the developed topological characterizations are then exploited to develop leader selection methods for signed path and cycle graphs to ensure leader-follower controllability. Along with illustrative examples, heuristic algorithms are also developed to show how leader selection methods developed for path and cycle graphs can be potentially extended to more general signed networks. In contrast to existing results that mainly focus on unsigned networks, this Chapter characterizes controllability and develops leader selection methods for signed networks.

2.1 Problem Formulation

Consider a multi-agent networked system represented by an undirected signed graph $\mathcal{G} = (\mathcal{V}, \mathcal{E}, \mathcal{A})$, where the node set $\mathcal{V} = \{v_1, \ldots, v_n\}$ and the edge set $\mathcal{E} \subset \mathcal{V} \times \mathcal{V}$ represent the agents and the interactions between pairs of agents, respectively. An undirected edge $(v_i, v_j) \in \mathcal{E}$ indicates that v_i and v_j are able to interact with each other (e.g., mutual information exchange). The potential interactions among agents are captured by the adjacency matrix $\mathcal{A} \in \mathbb{R}^{n\times n}$, where $a_{ij} \neq 0$ if $(v_j, v_i) \in \mathcal{E}$ and $a_{ij} = 0$ otherwise. No self-loop is considered,

i.e., $a_{ii} = 0 \, \forall i = 1, \ldots, n$. Different from classical unsigned graphs that contain non-negative adjacency matrix, $a_{ij} \colon \mathcal{E} \to \{\pm 1\}$ in this Chapter admits positive or negative weight to capture collaborative or competitive relationships between agents, thus resulting in a signed graph $\mathcal{G}$. Specifically, v_i and v_j are called positive neighbors of each other if $a_{ij} = 1$ and negative neighbors if $a_{ij} = -1$, where positive neighborhood indicates cooperative interactions while negative neighborhood indicates non-cooperative interactions between v_i and v_j, respectively.

Some terms are defined for later use. A path of length $k-1$ in $\mathcal{G}$ is a concatenation of distinct edges $\{(v_1, v_2), (v_2, v_3), \cdots, (v_{k-1}, v_k)\} \subset \mathcal{E}$. A cycle is a path with identical starting and end node, i.e, $v_1 = v_k$. Graph $\mathcal{G}$ is connected if there exists a path between any pair of nodes in $\mathcal{V}$. The neighbor set of v_i is defined as $\mathcal{N}_i = \{v_j | (v_j, v_i) \in \mathcal{E}\}$, and the degree of v_i, denoted as $d_i \in \mathbb{Z}^+$, is defined as the number of its neighbors, i.e., $d_i = |\mathcal{N}_i| = \sum_{j \in \mathcal{N}_i} abs(a_{ij})$, where $|\mathcal{N}_i|$ denotes the cardinality of $\mathcal{N}_i$ and $abs(a_{ij})$ denotes the absolute value of a_{ij}. The signed graph Laplacian of $\mathcal{G}$ is defined as $\mathcal{L}(\mathcal{G}) \triangleq \mathcal{D} - \mathcal{A}$, where $\mathcal{D} \triangleq diag\{d_1, \ldots, d_n\}$ is a diagonal matrix. Due to the consideration of negative weights, unlike unsigned graphs, $-\mathcal{L}(\mathcal{G})$ in (2–1) is no longer a Metzler matrix[1] and its row/column sums are not necessary zero.

Let $x(t) = [x_1(t), \ldots, x_n(t)]^T \in \mathbb{R}^n$ denote the stacked system states[2] , where each entry $x_i(t) \in \mathbb{R}$ represents the state of agent v_i. Suppose the system states evolve according to the following Laplacian dynamics,

$$\dot{x}(t) = -\mathcal{L}(\mathcal{G}) x(t), \tag{2–1}$$

where the graph Laplacian $\mathcal{L}(\mathcal{G})$ indicates that each agent v_i updates its state x_i only taking into account the states of its neighboring agents, i.e., $x_j \in \mathcal{N}_i$. Various networked systems feature the

[1] Metzler matrices are matrices with nonnegative off-diagonal entries [62].

[2] If multi-dimensional system states (e.g., $x_i \in \mathbb{R}^m$) are considered, the Laplacian dynamics in (2–1) can be trivially extended to $\dot{x}(t) = -\mathbb{L}(\mathcal{G}) x(t)$, where $\mathcal{L}(\mathcal{G})$ is augmented to $\mathbb{L}(\mathcal{G}) \triangleq \mathcal{L}(\mathcal{G}) \otimes I_m$ by the m-dimensional identity I_m and the matrix Kronecker product $\otimes$. Without loss of generality, the subsequent development will focus on the case that $x_i \in \mathbb{R}$ for ease of presentation.

Laplacian dynamics described in (2–1). For instance, formation control [91], flocking [92], and consensus [1,93] are typical applications of the Laplacian dynamics.

Suppose the agent set $\mathcal{V}$ is classified into a leader set $\mathcal{V}_l \subset \mathcal{V}$ and a follower set $\mathcal{V}_f \subset \mathcal{V}$ with $\mathcal{V}_l \cup \mathcal{V}_f = \mathcal{V}$, thus forming a typical leader-follower network. Without loss of generality, assume that the first m agents form the follower set $\mathcal{V}_f = \{v_1, \ldots, v_m\}$, while the remaining agents form the leader set $\mathcal{V}_l = \{v_{m+1}, \ldots, v_n\}$. Let $x(t) = \left[x_f^T(t), x_l^T(t)\right]^T \in \mathbb{R}^n$ be the aggregated system states, where $x_f(t) \in \mathbb{R}^m$ and $x_l(t) \in \mathbb{R}^{n-m}$ represent the aggregated states of followers and leaders, respectively. Similar to [6], the graph Laplacian in (2–1) can be partitioned as

$$\mathcal{L}(\mathcal{G}) = \left[\begin{array}{c|c} \mathcal{L}_f(\mathcal{G}) & \mathcal{L}_{fl}(\mathcal{G}) \\ \hline \mathcal{L}_{lf}(\mathcal{G}) & \mathcal{L}_l(\mathcal{G}) \end{array}\right], \tag{2–2}$$

with $\mathcal{L}_f(\mathcal{G}) \in \mathbb{R}^{m\times m}$, $\mathcal{L}_{fl}(\mathcal{G}) = \mathcal{L}_{lf}^T(\mathcal{G}) \in \mathbb{R}^{m\times(n-m)}$, and $\mathcal{L}_l(\mathcal{G}) \in \mathbb{R}^{(n-m)\times(n-m)}$. Based on (2–1) and (2–2), the dynamics of the followers become

$$\dot{x}_f(t) = -\mathcal{L}_f(\mathcal{G})\, x_f - \mathcal{L}_{fl}(\mathcal{G})\, u(t), \tag{2–3}$$

where $u(t) \triangleq x_l(t)$ denotes the exogenous control signal dictated by the leaders. In leader-follower networks, leaders are tasked to direct the overall behavior of the network by influencing the followers. The dynamics in (2–3) signify that the followers are influenced or controlled by the leaders via the connectivity of the network, where the exogenous signal becomes the leaders' control input.

Definition 2.1 (Leader-Follower Controllability)**.** Provided that the leaders are completely controllable and dictated by exogenous input $u(t)$, a leader-follower network with dynamics of (2–1) is called controllable, if the followers' state $x_f(t)$ in (2–3) can be driven to any target state by a proper design of $u(t)$. Mathematically, if the controllability matrix

$$\mathcal{C} = \left[\begin{array}{cccc} -\mathcal{L}_{fl} & \mathcal{L}_f\mathcal{L}_{fl} & \cdots & (-1)^m \mathcal{L}_f^{m-1}\mathcal{L}_{fl} \end{array}\right]$$

has full row rank, the leader-follower system in (2–3) is controllable.

From Definition 2.1, the leader-follower controllability is dependent on the system matrices $\mathcal{L}_f$ and $\mathcal{L}_{fl}$ in (2–3). Since $\mathcal{L}(\mathcal{G})$ is determined by the topological structure of $\mathcal{G}$ and the roles of nodes, i.e., leaders or followers, $\mathcal{L}(\mathcal{G})$ can vary significantly with different leader set, resulting either a controllable or uncontrollable network. Therefore, the primary objective of this Chapter is to characterize the relationship between leader-follower controllability and network topology and identify a subgroup of nodes (i.e., the leader set) in $\mathcal{G}$ such that leader-follower controllability in Definition 2.1 is ensured.

Remark 2.1. Different from the dynamics in (2–3) where the leaders' states are directly influenced by external control input, an alternative leader-follower network model employed in the works [12, 59, 60] and Chapter 3 to Chapter 5 is

$$\dot{x}(t) = -\mathcal{L}x(t) + Bu(t), \tag{2–4}$$

where $B = \begin{bmatrix} e_1 & \cdots & e_m \end{bmatrix} \in \mathbb{R}^{n\times m}$ is the input matrix with basis vectors e_i, $i = 1, \ldots, m$, indicating that the ith node is endowed with external controls $u(t) \in \mathbb{R}^m$. The model in (2–4) indicates that the external control input indirectly influences the states of leaders and followers through network dynamics. Despite different representations in (2–3) and (2–4), the discussion in [12] indicates the two different models can be equivalently reformulated into each other, thus yielding the same controllability. In other words, if the selected leaders yield a controllable leader-follower network with dynamics (2–3), the controllability result holds for the same set of leaders on a network with dynamics (2–4).

2.2 Topological Characterization of Leader-Follower Controllability

Lemma 2.1. *[94] Consider a linear time-invariant system*

$$\dot{x}(t) = Ax(t) + Bu(t), \tag{2–5}$$

where $A \in \mathbb{R}^{n\times n}$ is the system matrix, $B \in \mathbb{R}^{n\times m}$ is the input matrix, and $x(t) \in \mathbb{R}^n$ and $u(t) \in \mathbb{R}^m$ represent the system states and the control input, respectively. Let $E(\cdot)$ denote the set of left eigenvectors of a matrix. Per the well-known eigenvector test, the system in (2–5) is

uncontrollable if and only if there exists a left eigenvector $\nu \in E(A)$ *(i.e.,* $\nu^T A = \lambda \nu^T$ *for some eigenvalue* λ*) such that* $\nu^T B = 0_m$*, where* 0_m *is an* m*-dimensional vector of all zeros. In other words, the system (2–5) is controllable if and only if* $\nu \notin \ker\left(B^T\right)$, $\forall \nu \in E(A)$*, where* $\ker(\cdot)$ *indicates the kernel space.*

Proposition 2.1. *Consider a signed leader-follower network* $\mathcal{G}$ *where the followers evolve according to (2–3) and the leaders are driven by an exogenous input, i.e.,* $x_l(t) = u(t)$*. Provided that the follower-to-follower and leader-to-follower connections are intact, the leader-follower controllability is invariant to any addition, removal, or change of weight in leader-to-leader connections.*

Note that the follower dynamics (2–3) can be represented using (2–5), which indicates that the leader-follower controllability is only dependent on the system matrices $\mathcal{L}_f$ and $\mathcal{L}_{fl}$. Since any change to leader-to-leader connections within $\mathcal{G}$ can only affect the structure of $\mathcal{L}_l(\mathcal{G})$ while $\mathcal{L}_{fl}(\mathcal{G})$ and $\mathcal{L}_f(\mathcal{G})$ remain the same, Proposition 2.1 is an immediate consequence of Definition 2.1 and Lemma 2.1.

Example 2.1. Proposition 2.1 implies that leader-to-leader connections can be freely altered without affecting the controllability of the original network. To illustrate this idea, consider a controllable signed graph with the leader set $\{3, 4, 5\}$ in Fig. 2-1 (a), where negative edges are labeled with -1 and positive edges are not labeled for the simplicity of presentation. According to Proposition 2.1, it can be verified that the network in Fig. 2-1 (b) remains controllable if any leader-to-leader connections (i.e., dashed lines) are removed.

As an immediate consequence of Lemma 2.1, Proposition 2.1 provides a topological characterization of network controllability, which is instructive in constructing a controllable graph from a set of controllable sub-graphs and paves a way to controllability-ensured leader selection in the subsequent section. To show how a controllable graph can be constructed, the case of two sub-graphs is first considered in Proposition 2.2, which is then extended to the case of multiple sub-graphs in Proposition 2.3.

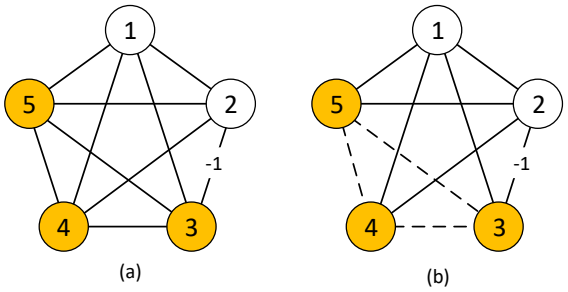

Figure 2-1. (a) Controllable network with the leader set $\{3, 4, 5\}$. (b) Network controllability is invariant with respect to arbitrary removal of leader-to-leader connections (i.e., dashed lines).

First, consider two leader-follower signed graphs $\mathcal{G}_1 = (\mathcal{V}_1, \mathcal{E}_1, \mathcal{A}_1)$ and $\mathcal{G}_2 = (\mathcal{V}_2, \mathcal{E}_2, \mathcal{A}_2)$, where $\mathcal{G}_i$, $i = \{1, 2\}$, has a follower set $\mathcal{V}_{fi} = \{1, \ldots, m_i\}$ and a leader set $\mathcal{V}_{li} = \{m_i + 1, \ldots, n_i\}$ with $\mathcal{V}_{fi} \cup \mathcal{V}_{li} = \mathcal{V}_i$ and $\mathcal{V}_{fi} \cap \mathcal{V}_{li} = \emptyset$, where m_i and n_i denote the cardinality of the follower set and its node set, respectively. The edge set $\mathcal{E}_i$ and weight matrix $\mathcal{A}_i$ indicate the underlying connections among leaders and followers within $\mathcal{G}_i$, $i = \{1, 2\}$.

Proposition 2.2. *Provided that the two signed graphs $\mathcal{G}_1 = (\mathcal{V}_1, \mathcal{E}_1, \mathcal{A}_1)$ and $\mathcal{G}_2 = (\mathcal{V}_2, \mathcal{E}_2, \mathcal{A}_2)$ are controllable and evolve according to (2–1), $\mathcal{G}_0 = (\mathcal{V}_0, \mathcal{E}_0, \mathcal{A}_0)$ remains controllable if $\mathcal{G}_0$ is constructed such that 1) $\mathcal{V}_0 = \mathcal{V}_1 \cup \mathcal{V}_2$ with the follower set $\mathcal{V}_{f0} = \{1, \ldots, m_1 + m_2\}$ and the leader set $\mathcal{V}_{l0} = \{m_1 + m_2 + 1, \ldots, n_1 + n_2\}$, where the nodes are re-indexed, without loss of generality, as the first $m_1 + m_2$ nodes are followers and the rest nodes are leaders, 2) $\mathcal{E}_0 = \mathcal{E}_1 \cup \mathcal{E}_2 \cup \mathcal{E}'$ where $\mathcal{E}' \subset \mathcal{V}_{l1} \times \mathcal{V}_{l2}$, and 3) $\mathcal{A}_0 = \begin{bmatrix} \mathcal{A}_1 & \bar{\mathcal{A}} \\ \bar{\mathcal{A}}^T & \mathcal{A}_2 \end{bmatrix} \in \mathbb{R}^{(n_1+n_2)\times(n_1+n_2)}$, where $\bar{\mathcal{A}}$ indicates the weights associated with the edges in $\mathcal{E}'$.*

Proof. Let $x_{fi} \in \mathbb{R}^{m_i}$ and $u_i \in \mathbb{R}^{n_i - m_i}$, $i = \{1, 2\}$, be the stacked followers' states and the exogenous input by the leaders in $\mathcal{G}_i$, respectively, which evolve according to the following dynamics

$$\begin{aligned} \mathcal{G}_1 &: \dot{x}_{f1}(t) = -\mathcal{L}_{f1}(\mathcal{G}_1) x_{f1} - \mathcal{L}_{fl1}(\mathcal{G}_1) u_1(t) \\ \mathcal{G}_2 &: \dot{x}_{f2}(t) = -\mathcal{L}_{f2}(\mathcal{G}_2) x_{f2} - \mathcal{L}_{fl2}(\mathcal{G}_2) u_2(t) \end{aligned},$$

where $\mathcal{L}_{f1} \in \mathbb{R}^{m_1 \times m_1}$, $\mathcal{L}_{fl1} \in \mathbb{R}^{m_1 \times (n_1 - m_1)}$, $\mathcal{L}_{f2} \in \mathbb{R}^{m_2 \times m_2}$, and $\mathcal{L}_{fl2} \in \mathbb{R}^{m_2 \times (n_2 - m_2)}$ are obtained following similar partitions in (2–2) from $\mathcal{L}_1(\mathcal{G}_1)$ and $\mathcal{L}_2(\mathcal{G}_2)$. Let $E(\mathcal{L}_{f1})$ and $E(\mathcal{L}_{f2})$ be the sets of left eigenvectors of $\mathcal{L}_{f1}$ and $\mathcal{L}_{f2}$, respectively. Since $\mathcal{G}_1$ and $\mathcal{G}_2$ are controllable, based on Lemma 2.1, no eigenvector $\nu \in E(\mathcal{L}_{f1})$ and $\vartheta \in E(\mathcal{L}_{f2})$ are orthogonal to $\mathcal{L}_{fl1}$ and $\mathcal{L}_{fl2}$, respectively.

Let $x_{f0} = \left[x_{f1}^T, x_{f2}^T\right]^T$ and $u_0 = \left[u_1^T, u_2^T\right]^T$ denote the followers' states and the exogenous input by the leaders in $\mathcal{G}_0$. Based on the definition, $\mathcal{G}_0$ is constructed by connecting $\mathcal{G}_1$ and $\mathcal{G}_2$ in a way that its node set $\mathcal{V}_0$ is formed by the union of $\mathcal{V}_1$ and $\mathcal{V}_2$, and its edge set $\mathcal{E}_0$ keeps $\mathcal{E}_1$ and $\mathcal{E}_2$ while including a new subset $\mathcal{E}'$. Since $\mathcal{E}' \subset \mathcal{V}_{l1} \times \mathcal{V}_{l2}$, the additional edges $\mathcal{E}'$ are restricted to leader-to-leader connections within $\mathcal{V}_{l1}$ and $\mathcal{V}_{l2}$, which only affect the structure of $\mathcal{L}_l(\mathcal{G}_0)$ in $\mathcal{L}(\mathcal{G}_0)$. Therefore, the followers' state x_{f0} evolves according to

$$\dot{x}_{f0}(t) = -\mathcal{L}_{f0}(\mathcal{G}_0)\, x_{f0} - \mathcal{L}_{fl0}(\mathcal{G}_0)\, u_0(t),$$

where

$$\mathcal{L}_{f0} = \begin{bmatrix} \mathcal{L}_{f1} & 0_{m_1 \times m_2} \\ 0_{m_2 \times m_1} & \mathcal{L}_{f2} \end{bmatrix}$$

and

$$\mathcal{L}_{fl0} = \begin{bmatrix} \mathcal{L}_{fl1} & 0_{m_1 \times (n_2 - m_2)} \\ 0_{m_2 \times (n_1 - m_1)} & \mathcal{L}_{fl2} \end{bmatrix}.$$

Clearly, for any eigenvector $\nu \in E(\mathcal{L}_{f1})$ and $\vartheta \in E(\mathcal{L}_{f2})$, the vectors $\begin{bmatrix} \nu^T & 0_{m_2}^T \end{bmatrix}^T$ and $\begin{bmatrix} 0_{m_1}^T & \vartheta^T \end{bmatrix}^T$ are the eigenvectors of $\mathcal{L}_{f0}$. Since

$$\begin{bmatrix} \nu^T\, 0_{m_2}^T \end{bmatrix} \begin{bmatrix} \mathcal{L}_{fl1} & 0_{m_1 \times (n_2 - m_2)} \\ 0_{m_2 \times (n_1 - m_1)} & \mathcal{L}_{fl2} \end{bmatrix} = \begin{bmatrix} \nu^T \mathcal{L}_{fl1} & 0_{m_2}^T \end{bmatrix}$$

$$\neq 0_{m_1 + (n_2 - m_2)}$$

and

$$\begin{bmatrix} 0_{m_1}^T & \vartheta^T \end{bmatrix} \begin{bmatrix} \mathcal{L}_{fl1} & 0_{m_1\times(n_2-m_2)} \\ 0_{m_2\times(n_1-m_1)} & \mathcal{L}_{fl2} \end{bmatrix} = \begin{bmatrix} 0_{m_1}^T & \vartheta^T\mathcal{L}_{fl2} \end{bmatrix},$$
$$\neq 0_{(n_1-m_1)+m_2}$$

according to Lemma 2.1, $\mathcal{G}_0$ remains controllable. □

To extend Proposition 2.2 to the case of multiple sub-graphs, consider a set of signed graphs $\mathcal{G}_i = (\mathcal{V}_i, \mathcal{E}_i, \mathcal{A}_i)$, $i = \{1, \ldots, n\}$, where each has a follower set $\mathcal{V}_{fi} = \{1, \ldots, m_i\}$ and a leader set $\mathcal{V}_{li} = \{m_i + 1, \ldots, n_i\}$ with m_i and n_i indicating cardinality of the follower set and its node set, respectively.

Proposition 2.3. *Provided a set of controllable signed graphs $\mathcal{G}_i$, $i = \{1, \ldots, n\}$, evolving according to (2–1), $\mathcal{G}_0 = (\mathcal{V}_0, \mathcal{E}_0, \mathcal{W}_0)$ remains controllable if $\mathcal{G}_0$ is constructed such that 1) $\mathcal{V}_0 = \bigcup_{i=1}^n \mathcal{V}_i$, 2) $\mathcal{E}_0 = \bigcup_{i=1}^n \mathcal{E}_i \cup \mathcal{E}'$ where $\mathcal{E}' \subset \prod_{i=1}^n \mathcal{V}_{li}$, indicating the additional edges $\mathcal{E}'$ are restricted to leader-to-leader connections within the leader sets $\mathcal{V}_{li}$, and 3) $\mathcal{A}_0$ indicates the the weights associated with the edges in $\mathcal{E}_0$.*

The proof of Proposition 2.3 is omitted here, since it can be easily verified by following similar procedure as in the proof of Proposition 2.2.

Remark 2.2. Proposition 2.3 provides a constructive topological design approach in generating a combined graph that preserves network controllability from a set of controllable sub-graphs. Besides constructing a controllable graph, Proposition 2.3 also provides insights on leader selection to render network controllability. For instance, if a given graph can be partitioned into a set of connected sub-graphs, as long as the selected leaders ensure controllability for each sub-graph and are connected following the rules in Proposition 2.3, the given graph is guaranteed to be controllable by Proposition 2.3. This idea will be further explored in the subsequent sections. In addition, the results developed in Proposition 2.1-2.3 are generic in the sense that they hold for not only signed graphs but also for unsigned graphs.

Example 2.2. Fig. 2-2 shows how a controllable graph can be constructed from a set of controllable sub-graphs. Fig. 2-2 (a) contains two sub-graphs, which become controllable if

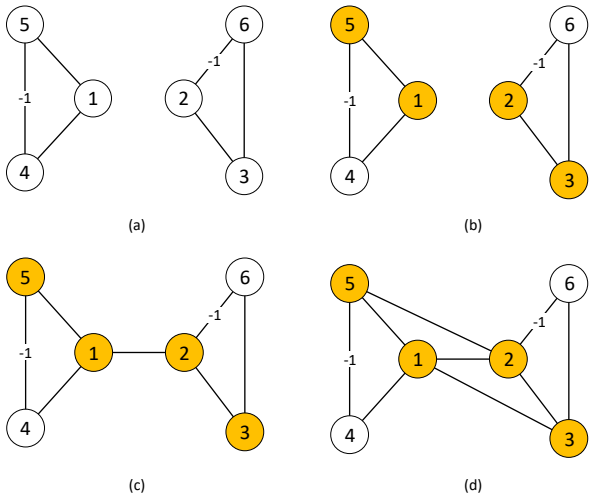

Figure 2-2. Examples of constructing a controllable graph from controllable sub-graphs. (a) Two sub-graphs. (b) Each sub-graph is controllable provided that the nodes $\{1, 5\}$ and $\{2, 3\}$ are selected as leaders, respectively. (c) The combined graph is controllable if a new leader-to-leader connection (i.e., the edge $(1, 2)$) is created. (d) The combined graph remains controllable if new leader-to-leader connections (i.e., the edges $(1, 2)$, $(1, 3)$, and $(5, 2)$) are created.

the nodes $\{1, 5\}$ and $\{2, 3\}$ are selected as leaders, respectively, as shown in Fig. 2-2 (b). The combined graph in Fig. 2-2 (c) is constructed by connecting the two leaders $\{1, 2\}$. It can be verified that the combined graphs in Fig. 2-2 (c) remains controllable, since its construction follows the rules in Proposition 2.2. It is worth pointing out that only sufficient conditions to preserve network controllability are developed in Proposition 2.2. There might exist different ways in connecting graphs to preserve network controllability. As a different construction, the combined graph in Fig. 2-2 (d) is constructed by including three new edges (i.e., $(1, 2)$, $(1, 3)$, and $(5, 2)$), which is also controllable according to Proposition 2.2.

2.3 Leader Selection for Signed Path and Cycle Graphs

Based on the developed topological characterizations of the controllability of signed networks in Section 2.2, this section focuses on developing sufficient conditions on selecting leader nodes for the controllability of signed networks. Specifically, two particular graphs, signed path and cycle graph, are considered first. A path graph is a graph where all internal nodes have degree two except that two end nodes have degree one. A cycle graph is a graph where all

nodes have degree two. Path and cycle graphs are basic building blocks for various sophisticated networks [62]. For instance, grid and lattice networks can be generated by Cartesian products of path graphs [54] while complex circulant networks can be constructed and analyzed based on cycle graphs [95]. Consequently, later in this section, we will show how the developed leader selection rules for path and cycle graphs can be potentially extended to more general signed networks.

As a key tool to study the properties of signed networks, structural balance is introduced.

Definition 2.2 (Structural Balance)**.** A signed graph $\mathcal{G} = (\mathcal{V}, \mathcal{E}, \mathcal{A})$ is structurally balanced if the node set $\mathcal{V}$ can be partitioned into $\mathcal{V}_1$ and $\mathcal{V}_2$ with $\mathcal{V}_1 \cup \mathcal{V}_2 = \mathcal{V}$ and $\mathcal{V}_1 \cap \mathcal{V}_2 = \emptyset$, where $a_{ij} > 0$ if $v_i, v_j \in \mathcal{V}_q$, $q \in \{1, 2\}$, and $a_{ij} < 0$ if $v_i \in \mathcal{V}_q$ and $v_j \in \mathcal{V}_r$, $q \neq r$, and $q, r \in \{1, 2\}$.

Definition 2.2 indicates that v_i and v_j are positive neighbors if they are from the same subset, i.e., either $\mathcal{V}_1$ or $\mathcal{V}_2$, and negative neighbors if v_i and v_j are from different subset. The relation between structural balance and network controllability are first discussed in [59] as follows.

Lemma 2.2. *Consider a structurally balanced signed graph $\mathcal{G}$ with nodes partitioned into $\mathcal{V}_1$ and $\mathcal{V}_2$. If leaders are selected from the same subset (i.e., either $\mathcal{V}_1$ or $\mathcal{V}_2$) and followers evolve according to (2–3), the leader-follower controllability of $\mathcal{G}$ remains the same as its corresponding unsigned graph $\mathcal{G}'$, where $\mathcal{G}' = (\mathcal{V}, \mathcal{E}, \mathcal{A}')$ has the same node and edge set as $\mathcal{G}$ except that $\mathcal{A}' = \mathrm{abs}\,(\mathcal{A})$.*

2.3.1 Signed Path Graph

Let $\mathcal{G}_p = (\mathcal{V}, \mathcal{E}, \mathcal{A})$ denote a signed path graph, where $\mathcal{V} = \{1, \ldots, n\}$ and $\mathcal{E} = \{(i, i+1) | \, i \in \{1, \ldots, n-1\}\}$ represent the node and edge set, respectively, and the weight matrix $\mathcal{A} \in \mathbb{R}^{n \times n}$ indicates associated positive or negative weights in $\mathcal{E}$.

Theorem 2.1. *A signed path graph $\mathcal{G}_p = (\mathcal{V}, \mathcal{E}, \mathcal{A})$ with followers evolving according to (2–3) is controllable if one of the end nodes (i.e., v_1 or v_n) is selected as the leader.*

Proof. As indicated in Corollary 1 in [2], a spanning tree is always structurally balanced. As a particular case of the spanning tree, the path graph $\mathcal{G}_p$ is thus structurally balanced. Since $\mathcal{G}_p$ is

structurally balanced, its node set can be partitioned into $\mathcal{V}_1$ and $\mathcal{V}_2$ as in Definition 2.2. If one leader is considered, the leader must be selected from either $\mathcal{V}_1$ and $\mathcal{V}_2$, i.e., the same subset. Hence, Lemma 2.2 indicates that the controllability of $\mathcal{G}_p$ is equivalent to its corresponding unsigned graph $\mathcal{G}_p' = (\mathcal{V}, \mathcal{E}, \mathcal{A}')$, where $\mathcal{A}'$ consists of non-negative edge weights. Given that an unsigned path graph is controllable if an end node is selected as the leader in [5] and [6], it can be concluded that the signed path graph $\mathcal{G}_p$ is also controllable if an end node is selected as the leader from Lemma 2.2. □

Remark 2.3. As indicated in [6], unsigned path graph is controllable if one of the end nodes is selected as the leader. Although the leader selection approach developed in Theorem 2.1 is similar to that of [6], the inherent analysis is completely different. Specifically, the controllability analysis of unsigned path graph in [6] is based on graph symmetry. Although symmetry with respect to leaders is sufficient to conclude uncontrollability of unsigned graphs, symmetry alone, as indicated in [60], is generally not sufficient to lead to uncontrollability of signed graphs. Therefore, instead of using graph symmetry, structural balance is exploited in Theorem 2.1 to characterize the controllability of signed graphs.

The following theorem extends the result in Theorem 2.1 to multi-leader selection.

Theorem 2.2. *A signed path graph $\mathcal{G}_p$ with followers evolving according to (2–3) is controllable if multiple adjacent nodes in $\mathcal{G}_p$ are selected as leaders.*

Proof. The case of two leaders is first considered in this proof, which will then be extended to include multiple leaders. Suppose that an arbitrary pair of adjacent nodes v_k and v_{k+1}, $\forall k \in \{1, \ldots, n-1\}$, in $\mathcal{G}_p$ are selected as leaders. Let $\mathcal{G}_{p1} = \{\{v_1, v_2\}, \{v_2, v_3\}, \cdots, \{v_{k-1}, v_k\}\}$ denote the sub-graph of $\mathcal{G}_p$ with the leader node v_k and $\mathcal{G}_{p2} = \{\{v_{k+1}, v_{k+2}\}, \cdots, \{v_{n-1}, v_n\}\}$ denote the sub-graph of $\mathcal{G}_p$ with the leader node v_{k+1}, respectively. Based on Theorem 2.1, $\mathcal{G}_{p1}$ and $\mathcal{G}_{p2}$ are both controllable, since v_k and v_{k+1} are the end nodes of the sup-graph $\mathcal{G}_{p1}$ and $\mathcal{G}_{p2}$, respectively. Since $\mathcal{G}_p$ can be constructed by connecting the two leaders in $\mathcal{G}_{p1}$ and $\mathcal{G}_{p2}$ while keeping the rest graph intact, Proposition 2.1 indicates that $\mathcal{G}_p$ will remain controllable.

If n adjacent nodes are selected as leaders, following similar argument above, $\mathcal{G}_p$ can always be partitioned into controllable sub-path graphs. Iteratively invoking Proposition 2.1 indicates $\mathcal{G}_p$ is always controllable if adjacent nodes are selected as leaders. □

Remark 2.4. Theorem 2.2 relaxes the constraint in Lemma 2.2 that leaders have to be selected from the same partitioned subset. Specifically, Theorem 2.2 indicates that, for signed path graphs, leaders are allowed to be selected from different partitioned subsets, as long as they are adjacent nodes in $\mathcal{G}_p$. In addition, the developed leader selection approach in Theorem 2.2 is more convenient in topology design for leader-follower controllability, since no computation for the partitioned subset is required as in Lemma 2.2.

A signed tree is a particular topology where any two vertices are connected by exactly one simple path and the edges admit negative weights. Networks with tree topology have been broadly applied to model multi-agent networks, cyber-physical systems, smart grid, and power networks (cf. [1] and [96] for more applications). Since a tree graph can be naturally partitioned into connected path graphs, the subsequent theorem extends leader selection rules developed in Theorem 2.1 and Theorem 2.2 to signed trees.

Let $\mathcal{G}_t = (\mathcal{V}, \mathcal{E}, \mathcal{A})$ denote a signed tree, where $\mathcal{V}$, $\mathcal{E}$, and $\mathcal{A}$ represent the node set, edge set, and weight matrix, respectively. Since $\mathcal{G}_t$ is a tree with no cycles, it is well known that $|\mathcal{E}| = |\mathcal{V}| - 1$.

Theorem 2.3. *Suppose that a signed tree $\mathcal{G}_t$ can be partitioned into a set of signed path graphs $\{\mathcal{G}_{pi}\}$, $i \in \{1, \ldots, m\}$, with $\mathcal{G}_t = \cup_{i=1}^{m} \mathcal{G}_{pi}$. The tree $\mathcal{G}_t$ is controllable, if selected leaders ensure the controllability of each path graph in $\{\mathcal{G}_{pi}\}$ and $\mathcal{G}_t$ is reconstructed by only connecting leaders from each path graph.*

The proof is omitted here, since Theorem 2.3 is an immediate consequence of Theorem 2.1, Theorem 2.2, and Proposition 2.1. Example 2.3 is provided to illustrate Theorem 2.3.

Example 2.3. Consider a signed tree shown in Fig. 2-3 (a), where the roles (i.e., leaders or followers) are not assigned yet. To determine leaders that ensure leader-follower controllability, the tree can be first partitioned into 5 paths, i.e., $\{5, 10, 14\}$, $\{6, 11\}$, $\{3, 7, 12, 15\}$, $\{8, 13\}$, and

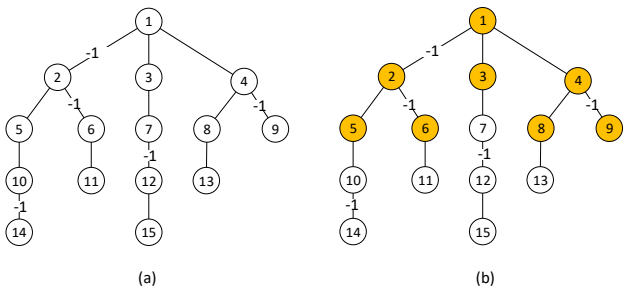

Figure 2-3. (a) A signed tree graph. (b) A controllable signed tree graph with the marked nodes $\{1, 2, 3, 4, 5, 6, 8, 9\}$ selected as leaders.

$\{2, 1, 4, 9\}$. If the leaders are selected as $\{1, 2, 3, 4, 5, 6, 8, 9\}$, then each of the path graphs is controllable by Theorem 2.1. Since the path graphs are connected in a way that only leaders from each path are connected to form the tree, the tree is controllable based on Theorem 2.2 and Proposition 2.1. Therefore, it can be verified that the selected leaders ensure leader-follower controllability of the tree graph.

Remark 2.5. To the best of our knowledge, few existing results consider leader selection from graphical perspective for ensured controllability of signed tree graphs. Theorem 2.1 provides a sufficient condition for selecting control nodes to ensure the controllability of a signed tree graph. In contrast to matrix-theoretical design and analysis approaches in the literature, the developed leader selection approach is graph-inspired, which is more amenable in topology design.

Since the result developed in Theorem 2.1 is based on the partition of a tree graph into path graphs, different partitions could result in different sets of leaders. For instance, Fig. 2-4 considers the same signed tree graph as in Fig. 2-3 (a), where a different set of nodes, i.e., $\{1, 2, 4, 5, 8\}$, is selected as leaders. After reorganizing the nodes, Fig. 2-4 contains three path graphs, i.e., $\{11, 6, 2, 5, 10, 14\}$,$\{1, 3, 7, 12, 15\}$, and $\{9, 4, 8, 13\}$. Based on Theorem 2.2, the three path graphs are controllable with respect to the selected leaders. Since the three path graphs are connected such that only leaders are connected, the combined signed tree graph is controllable by Theorem 2.3.

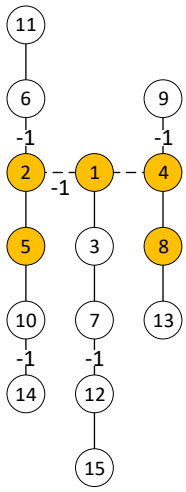

Figure 2-4. The same signed tree graph in Fig. 2-3 (a) is considered, where a different set of nodes are selected as leaders to ensure the network controllability.

2.3.2 Signed Cycle Graph

A cycle graph $\mathcal{G}_c = (\mathcal{V}, \mathcal{E}, \mathcal{A})$ is defined similar to $\mathcal{G}_p$, except that the edge set in $\mathcal{G}_c$ is defined as $\mathcal{E} = \{(i,\ i \mod (n)+1) |\, i \in \{1, \ldots, n\}\}$.

Lemma 2.3. *[12] An unsigned cycle graph is controllable if two adjacent nodes are chosen as leaders.*

This section focuses on extending the leader selection approach for unsigned cycle graphs developed in Lemma 2.3 to signed cycle graphs, where the weight matrix $\mathcal{A}$ can take negative entries.

Lemma 2.4. *Consider a signed cycle graph $\mathcal{G}_c = (\mathcal{V}, \mathcal{E}, \mathcal{A})$, where the followers evolve according to (2–3). The leader-follower controllability of $\mathcal{G}_c$ is equivalent to that of its sign-reversed graph $\bar{\mathcal{G}}_c = (\mathcal{V}, \mathcal{E}, -\mathcal{A})$, where the weight matrix $\mathcal{A}$ in $\mathcal{G}_c$ is replaced by $-\mathcal{A}$ in $\bar{\mathcal{G}}_c$.*

Proof. Since every node in a cycle graph has degree two, the degree matrix $\mathcal{D}$ of a cycle graph is $2I_n$, where I_n represents the n-dimensional identity matrix. Without loss of generality, suppose the first m nodes are followers and the rest $n - m$ nodes are leaders. Graph Laplacian of $\mathcal{G}_c$ can

then be partitioned as

$$\mathcal{L} = \mathcal{D} - \mathcal{A} = \left[\begin{array}{c|c} 2I_m - \mathcal{A}_f & -\mathcal{A}_{fl} \\ \hline -\mathcal{A}_{fl}^T & 2I_{n-m} - \mathcal{A}_l \end{array}\right], \tag{2–6}$$

where $\mathcal{A}_f \in \mathbb{R}^{m\times m}$, $\mathcal{A}_{fl} \in \mathbb{R}^{m\times(n-m)}$, and $\mathcal{A}_l \in \mathbb{R}^{(n-m)\times(n-m)}$. By the dynamics (2–1) and (2–6), the followers evolve according to

$$\dot{x}_f(t) = -\left(2I_m - \mathcal{A}_f\right) x_f - \left(-\mathcal{A}_{fl}\right) u(t)$$

where $x_f \in \mathbb{R}^m$ and $u(t) \in \mathbb{R}^{n-m}$ denote the followers' states and leaders' input, respectively. Hence, based on Def. 2.1, the leader-follower controllability of $\mathcal{G}_c$ is completely determined by $2I_n - \mathcal{A}_f$ and $-\mathcal{A}_{fl}$.

Consider the sign reversed cycle graph $\bar{\mathcal{G}}_c$. Similarly, the leader-follower controllability of $\bar{\mathcal{G}}_c$ is determined by $2I_n + \mathcal{A}_f$ and $\mathcal{A}_{fl}$. Note that the set of eigenvectors of $2I_n - \mathcal{A}_f$ is identical to that of $2I_n + \mathcal{A}_f$. In addition, since $2I_n - \mathcal{A}_f$ and $2I_n + \mathcal{A}_f$ are symmetric matrices, their right and left eigenvectors are equal. Let μ be an eigenvector of $2I_n - \mathcal{A}_f$ (or $2I_n + \mathcal{A}_f$). If $\mu \in \ker\left(-\mathcal{A}_{fl}^T\right)$, it is always true that $\mu \in \ker\left(\mathcal{A}_{fl}^T\right)$. Similarly, if $\mu \notin \ker\left(-\mathcal{A}_{fl}^T\right)$, it will also be true that $\mu \notin \ker\left(\mathcal{A}_{fl}^T\right)$. Therefore, based on Lemma 2.1, the controllability of $\mathcal{G}_c$ is equivalent to that of $\bar{\mathcal{G}}_c$. □

Theorem 2.4. *Provided that all followers evolve according to (2–3), a signed cycle graph $\mathcal{G}_c$ is controllable if any two adjacent nodes in $\mathcal{G}_c$ are selected as leaders.*

Proof. Different from path graphs that are inherently structurally balanced, cycle graphs may not be structurally balanced. In addition, when considering two adjacent nodes as leaders, the sign of inter-leader edge introduces additional challenge to the analysis of leader-follower controllability. Therefore, based on the topological structure of $\mathcal{G}_c$ and the sign of inter-leader edge, four cases are discussed.

Case 1: Structurally balanced $\mathcal{G}_c$ with positive inter-leader edge. Since $\mathcal{G}_c$ is structurally balanced, its node set $\mathcal{V}$ can be partitioned into two subsets $\mathcal{V}_1$ and $\mathcal{V}_2$. Based on Lemma 2.2, the

positive inter-leader edge indicates that the two leaders are from the same subset, i.e., either $\mathcal{V}_1$ or $\mathcal{V}_2$. In addition, there exists an unsigned cycle graph $\mathcal{G}_c^{'} = (\mathcal{V}, \mathcal{E}, |\mathcal{A}|)$, which has the same edge and node set as $\mathcal{G}_c$ except that the edge weights in $\mathcal{G}_c^{'}$ are all positive. Given that leaders are selected from the same subset, Lemma 2.2 indicates that the controllability of $\mathcal{G}_c$ is equivalent to that of $\mathcal{G}_c^{'}$. Since $\mathcal{G}_c^{'}$ is controllable from Lemma 2.3 if two adjacent nodes are selected as leaders, it concludes that $\mathcal{G}_c$ is also controllable with similar leader selection approach from Lemma 2.2.

Case 2: Structurally unbalanced $\mathcal{G}_c$ with negative inter-leader edge. Since $\mathcal{G}_c$ is a structurally unbalanced cycle graph, $\mathcal{G}_c$ is a negative cycle, i.e., the product of edge weights $\mathcal{G}_c$ is negative [2], which implies there exists an odd number of negative edges in $\mathcal{G}_c$. Since graph controllability is invariant to changes of inter-leader edges from Proposition 2.1, the controllability of $\mathcal{G}_c$ with negative inter-leader edge will remain the same if the sign of inter-leader edge flips from negative to positive. After flipping the sign to be positive, $\mathcal{G}_c$ will now contain an even number of negative edges and becomes structurally balanced [2], which implies that $\mathcal{G}_c$ is controllable due to the equivalent to Case 1.

Case 3: Structurally balanced $\mathcal{G}_c$ with negative inter-leader edge. Based on Lemma 2.4, the controllability of $\mathcal{G}_c$ is invariant if all of its signs are flipped. Based on the number of negative edges in $\mathcal{G}_c$, two sub-cases are further discussed. 1) If $\mathcal{G}_c$ in this case has an even number of edges, it must have an even number of negative edges and an even number of positive edges from [2]. After flipping all of its signs, $\mathcal{G}_c$ remains structurally balanced but with positive inter-leader edge, which implies that $\mathcal{G}_c$ in this case is controllable due to the equivalence to Case 1.

2) If $\mathcal{G}_c$ has an odd number of edges, it must have an even number of negative edges and an odd number of positive edges [2]. After flipping all of its signs, $\mathcal{G}_c$ becomes $\mathcal{G}_c^*$, which is structurally unbalanced with positive inter-leader edge and equivalent to Case 4 below. If the sign of any leader-follower edge in $\mathcal{G}_c^*$ is flipped again, $\mathcal{G}_c^*$ becomes $\mathcal{G}_c^\star$, which is structurally balanced with positive inter-leader edge due to the change of negative edges from an odd number of to an even number. Following similar procedure as in the proof of Lemma 2.4, it can be trivially

verified that the change of sign of any leader-follower edge will not affect the controllability of the system. In other words, the controllability of $\mathcal{G}_c^\star$ remains the same as $\mathcal{G}_c^*$, which is then the same as $\mathcal{G}_c$ due to Lemma 2.4. Since $\mathcal{G}_c^\star$ is structurally balanced with positive inter-leader edge, which is the same as Case 1, $\mathcal{G}_c^\star$ is controllable, and hence $\mathcal{G}_c$ is also controllable.

Case 4: Structurally unbalanced $\mathcal{G}_c$ with positive inter-leader edge. Since this case has been discussed in Case 3, $\mathcal{G}_c$ is controllable.

Based on Cases 1-4, $\mathcal{G}_c$ is controllable if adjacent nodes are selected as leaders. □

Remark 2.6. The leader selection approach developed in Theorem 2.4 is valid for all types of signed cycle graphs, no matter it is structurally balanced or not.

The following corollary is an immediate consequence of Theorem 2.4.

Corollary 2.1. *A signed path graph is controllable if two end nodes are selected as leaders.*

Given a controllable signed cycle graph where two adjacent nodes are selected as leaders, if the edge connecting the two leaders is removed, the cycle graph will turn into a path graph with leaders on two ends. Since the removal of leader-to-leader edges will not affect controllability of the system from Proposition 2.1, the path graph is controllable if two end nodes are selected as leaders. In addition to Theorem 2.1-2.3, Corollary 2.1 provides an alternative way to select leaders for ensured controllability.

2.3.3 Extensions and Simulation

This section shows how the leader selection rules developed for signed path and cycle graphs in previous sections can be potentially extended to more general signed networks. Since path and cycle graphs are basic building blocks for general signed graphs, the idea of leader selection in this section is to first partition the general signed graphs into a set of path and cycle graphs, where the results developed in Theorems 2.1-2.4 can be applied.

Motivated by this idea, heuristic leader selection rules are developed in Algorithm 2.1. In Algorithm 2.1, we start from identifying nodes in a given signed graph whose node degree is greater than two. Since nodes in either path and cycle graphs have degree at most two, the reason to identify nodes with degree more than two is to find out those nodes that potentially connect

path or cycle graphs. Those high degree nodes will facilitate the partition of the signed graph into individual path and cycle graphs, where existing graph partition techniques are applicable (e.g., graph partition into paths in [97], cycles in [98], and both paths and cycles in [99]). Once the graph is partitioned into a set of path and cycle graphs, the leader selection rules developed in Theorems 2.1-2.4 and Propositions 2.1-2.3 can be immediately applied to generate a controllable leader-follower network.

Algorithm 2.1 Leader Selection for Signed Graph

procedure INPUT:(Graph $\mathcal{G}(\mathcal{V}, \mathcal{E}, \mathcal{W})$);
    Output: The set of leaders $\mathcal{V}_l$
  Calculate the node degree d_i for each node $v_i \in \mathcal{V}$;
  Select nodes v_i with $d_i > 2$ to form $\mathcal{V}_l$;
  Use graph partition techniques (e.g., [97–99]) to partition $\mathcal{G}$ into cycles and paths based on the selected high degree nodes in $\mathcal{V}_l$;
  for Each cycle or path **do**
    if the cycle or path is controllable **then**
      Keep the selected leaders in $\mathcal{V}_l$;
    else
      Apply Theorems 2.1-2.4 to select appropriate nodes as leaders and update $\mathcal{V}_l$;
    end if
  end for
  Update $\mathcal{V}_l$ based on Propositions 2.1-2.3 to ensure the network controllability;
  Output $\mathcal{V}_l$;
end procedure

To illustrate Algorithm 2.1, Example 2.4 is provided.

Example 2.4. Consider the signed graph in Fig. 2-5 (a) where the objective is to select a set of leaders such that the leader-follower network is controllable. Following rules in Algorithm 2.1, the leader nodes (i.e., high degree nodes $\{8, 9, 11, 13, 15, 21, 22, 25, 29\}$) are first identified in Fig. 2-5 (b). Based on the selected leader nodes and graph partition techniques in [97–99], the signed graph is partitioned into a set of path and cycle graphs, which are shown in dashed lines. The leader selection rules developed in Theorem 2.1-2.4 are then applied to ensure that each path and cycle graph are controllable. For instance, the selected nodes $\{8, 9\}$ ensure the controllability of the cycle graph formed by $\{1, 2, 3, 4, 8, 9\}$. The leader set is then updated to include more nodes (i.e., addition leaders $\{10, 14\}$) whenever necessary such that the individual path and cycle graphs are connected satisfying Propositions 2.1-2.3, which ensues the controllability of the original signed graph.

Remark 2.7. Note that Algorithm 2.1 is based on partitioning a general signed graph into a set of path and cycle graphs. As indicated in [97–99], particular classes of graph topologies, such as trees or loosely connected graphs, can be efficiently partitioned into a small number of path and cycle graphs. Other types of graphs, such as densely connected graphs or complete graphs, can be more challenging to be partitioned. Therefore, the developed leader selection rules perform better on graph topologies that are amenable to be partitioned into path and cycle graphs.

Remark 2.8. The leader selection rules developed in Algorithm 2.1 are only sufficient conditions to ensure network controllability. In other words, the selected leader set from Algorithm 2.1 is by no means an optimal set. There may exist other leader group selections that can also ensure network controllability but with fewer leaders. For instance, minimal controllability problems were considered in [25], where a greedy heuristic approach was developed to ensure network controllability while minimizing the number of selected leaders. Robust minimal controllability was investigated in [100], where additional constraints were included in the minimal controllability problem. However, only unsigned graphs were considered in [25] and [100]. Nevertheless, the developed optimization approach and the unraveled fundamental relationship between minimal controllability and network topological sparsity can be potentially helpful in developing leader group selection rules for signed graphs. In particular, the solution of the minimal controllability problem in [25] and [100] is heavily dependent on the network topological sparsity. Such topological properties have been extensively studied on path and cycle graphs in the works of [11] and [12]. Since our approach is based on the partition of a general signed graph into a set of path and cycle graphs, additional research will therefore leverage tools from [11, 12, 25, 100] to investigate minimal controllability problems over signed graphs.

2.4 Summary

Leader selection on signed multi-agent networks for ensured controllability is considered in this Chapter. Graph-inspired topological characterizations of the controllability of signed networks is studied, based on which leader selection methods are developed for signed path and cycle graphs. Heuristic algorithms are also developed showing how leader selection

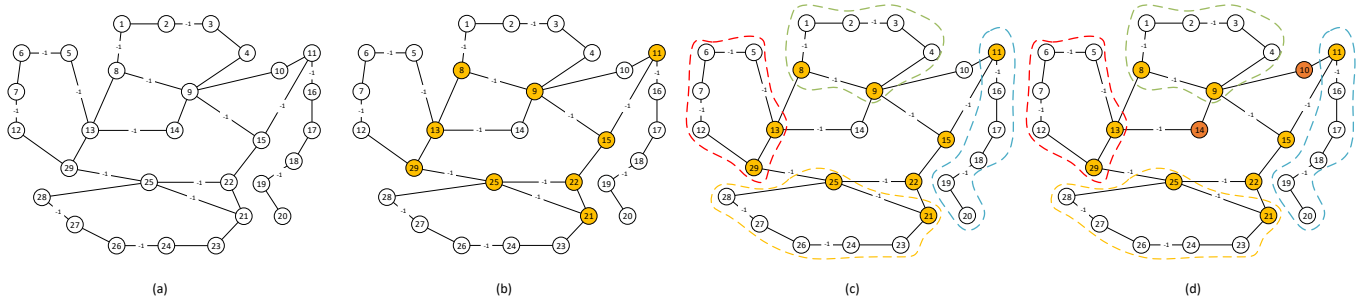

Figure 2-5. (a) A signed graph with 29 nodes. (b) The initial selection of leader nodes (i.e., nodes with degree more than two) are marked. (c) Based on the initially selected leader node, the signed graph is partitioned into a set of path and cycle graphs. (d) Update the leader nodes based on the rules in Theorem 2.1-2.4 to ensure the resulting leader-follower network is controllable.

methods developed for path and cycle graphs can be potentially extended to more general signed networks. Although the effectiveness of the developed leader selection rules is demonstrated via examples, there might exist different leader sets that are capable of ensuring network controllability with additional constraints (e.g., minimal leader number).

CHAPTER 3
ENERGY-RELATED CONTROLLABILITY OF COMPLEX NETWORKS - CHARACTERIZATION OF CONTROL ENERGY METRICS

This chapter investigates energy-related controllability of complex networks. Specifically, the objective is to establish controllability characteristics on signed complex networks, where the network units interact via neighbor-based Laplacian feedback and the network admits positive and negative edges to capture cooperative and antagonistic interactions among these units. This chapter focuses on characterizing the energy-related controllability in signed networks. To this end, controllability Gramian-based measures are exploited to quantify the difficulty of the control problem on signed networks in terms of the energy-related performance. Fundamental relationships between these measures and network topology are developed via graph Laplacian to characterize energy-related controllability. It is revealed that, for structurally unbalanced signed graphs, the energy-related controllability is closely related to the diagonal entries of the inverse of the graph Laplacian. It is also discovered that structurally balanced signed graphs and their corresponding unsigned graphs have the same energy-related controllability.

3.1 Problem Formulation

Consider a complex network represented by an undirected signed graph $\mathcal{G} = (\mathcal{V}, \mathcal{E}, \mathcal{A})$, where the node set $\mathcal{V} = \{v_1, \ldots, v_n\}$ and the edge set $\mathcal{E} \subset \mathcal{V} \times \mathcal{V}$ represent the network units and their interactions, respectively. The network-wide interactions are captured by the adjacency matrix $\mathcal{A} = [a_{ij}] \in \mathbb{R}^{n\times n}$, where $a_{ij} \neq 0$ if $(v_i, v_j) \in \mathcal{E}$ and $a_{ij} = 0$ otherwise. No self-loop is considered, i.e., $a_{ii} = 0\ \forall i = 1, \ldots, n$. Different from unsigned graphs that exclusively contain non-negative adjacency matrices, $a_{ij} : \mathcal{E} \to \mathbb{R}$ in this work is allowed to admit positive or negative weights to capture collaborative or antagonistic interactions between network units, thus resulting in a signed graph $\mathcal{G}$. Let $d_i = \sum_{j\in\mathcal{N}_i} |a_{ij}|$, where $\mathcal{N}_i = \{\, v_j |\, (v_i, v_j) \in \mathcal{E}\}$ denotes the neighbor set of v_i and $|a_{ij}|$ denotes the absolute value of a_{ij}. The graph Laplacian of $\mathcal{G}$ is defined as $\mathcal{L}(\mathcal{G}) \triangleq \mathcal{D} - \mathcal{A}$, where $\mathcal{D} \triangleq diag\{d_1, \ldots, d_n\}$ is a diagonal matrix. Since $\mathcal{G}$ is undirected, the graph Laplacian $\mathcal{L}(\mathcal{G})$ is symmetric.

Let $x(t) = [x_1(t), \ldots, x_n(t)]^T \in \mathbb{R}^n$ denote the stacked system states, where each entry $x_i(t) \in \mathbb{R}$ represents the state of node v_i. Suppose the system states evolve according to the following Laplacian dynamics,

$$\dot{x}(t) = -\mathcal{L}(\mathcal{G})\, x(t), \tag{3–1}$$

where the graph Laplacian $\mathcal{L}(\mathcal{G})$ indicates that each node updates its state taking into account the states of its neighboring nodes.

It is assumed that a set $\mathcal{K} = \{v_{k_1}, \ldots, v_{k_m}\} \subseteq \mathcal{V}$, $|\mathcal{K}| = m \geq 1$, of nodes, referred as leaders in the network, can be endowed with external controls. With external inputs, the system dynamics in (3–1) can be rewritten as

$$\dot{x}(t) = -\mathcal{L}(\mathcal{G})\, x(t) + B_{\mathcal{K}} u(t), \tag{3–2}$$

where $B_{\mathcal{K}} = \begin{bmatrix} e_{k_1} & \cdots & e_{k_m} \end{bmatrix} \in \mathbb{R}^{n\times m}$ is the input matrix with basis vectors e_i, $i = k_1, \ldots, k_m$, indicating that the ith node is endowed with external controls $u(t) \in \mathbb{R}^m$. The dynamics of (3–2) indicates that the network behavior is not only driven by the graph Laplacian $\mathcal{L}$, but also depends on the input matrix $B_{\mathcal{K}}$ via the leader set $\mathcal{K}$. Different leader sets can result in different $B_{\mathcal{K}}$, leading to drastic differences in the capability of controlling a network. The network model with Laplacian dynamics as in (3–2) has various applications in many engineering systems (cf. [9, 22, 42, 59]).

A network with dynamics in (3–2) is controllable, if the controllability matrix $\mathcal{C}_{\mathcal{K}} = [B_{\mathcal{K}} \; -\mathcal{L}B_{\mathcal{K}} \; \cdots \; (-1)^n \mathcal{L}^n B_{\mathcal{K}}]$ has a full row rank. Hence, in theory, a network can be controllable with appropriate selection of leader nodes (and consequently $B_{\mathcal{K}}$). However, it does not tell how difficult it is to control the network in practice, i.e., how much energy is needed to drive the network to the target state. To provide energy-related quantification of network control, the total control energy over the time interval $[0, t]$ is given by

$$E(t) = \int_0^t \|u(\tau)\|_2^2 \, d\tau, \tag{3–3}$$

where $\|u\|_2$ represents the Euclidean norm of u. Assuming the initial state $x(0) = 0$ and the optimal control $u(t)$ in [101], the minimum control energy required to drive the system in (3–2) from $x(0)$ to a desired target state x_f is

$$E(t) = x_f^T \mathcal{W}_{\mathcal{K}}^{-1}(t)\, x_f, \tag{3–4}$$

where

$$\mathcal{W}_{\mathcal{K}}(t) = \int_0^t e^{-\mathcal{L}\tau} B_{\mathcal{K}} B_{\mathcal{K}}^T e^{-\mathcal{L}^T\tau} d\tau \tag{3–5}$$

is the controllability Gramian at time t, which is positive definite if and only if the system in (3–2) is controllable. In this Chapter, the infinite-horizon Gramian is adopted, i.e., the case when $t \to \infty$ in (3–5), due to asymptotic or exponential convergence/stability of most dynamical systems.

Since the controllability Gramian $\mathcal{W}_{\mathcal{K}}$ provides an energy-related measure of network controllability, various quantitative metrics of controllability were developed based on $\mathcal{W}_{\mathcal{K}}$. Typical control energy metrics include average controllability, volumetric control energy, and average control energy [31], as summarized below.

Average Controllability $\mathrm{tr}(\mathcal{W})$: The average controllability is defined as the trace of the controllability Gramian $\mathcal{W}$, which is inversely related to the control energy. Due to the trace, $\mathrm{tr}(\mathcal{W})$ provides an overall measure of network controllability and energy expenditure in all directions in the state space. The zero eigenvalues of $\mathcal{W}$ imply uncontrollable directions (i.e., requiring infinite control energy) in the state space. Thus, the smaller the eigenvalue of $\mathcal{W}$, the more effort needed to transit system states in the corresponding direction.

Volumetric Control Energy $\log\det\mathcal{W}$: The determinant of $\mathcal{W}$ measures the volume of the ellipsoid containing the target states that can be reached within unit control energy. As indicated in [31], the volume of the ellipsoid is $\frac{\pi^{\frac{n}{2}}}{\Gamma(n/2+1)} \sqrt[n]{\det(\mathcal{W})}$, where Γ is the Gamma function. If a system is uncontrollable, the ellipsoid volume is zero, which implies $\det\mathcal{W} = 0$. Since the logarithm is monotone, $\log\det\mathcal{W}$ implies the associated volume in the controllable subspace.

Average Control Energy $\mathrm{tr}\left(\mathcal{W}^{-1}\right)$: The trace of the inverse of controllability Gramian is proportional to the control energy required, on average, to drive the system within the controllable subspace. If the system is uncontrollable, $\mathcal{W}^{-1}$ does not exist and thus the average control energy $\mathrm{tr}\left(\mathcal{W}^{-1}\right)$ is infinite, which implies there exists at least one direction in which the system is uncontrollable with external input.

The objective of this Chapter is to establish these metrics in the context of signed networks and develop topological characterizations on how these metrics are related to the graph Laplacian in quantifying the energy-related performance in the control of signed networks.

3.2 Energy-Related Controllability of Signed Networks

Based on the topological structures, signed graphs can be classified as either structurally balanced or structurally unbalanced.

Def. 2.2 indicates that for a structurally balanced graph $\mathcal{G}$, nodes v_i and v_j in $\mathcal{G}$ are positive neighbors if they are from the same subset, i.e., either $\mathcal{V}_1$ or $\mathcal{V}_2$, and negative neighbors if v_i and v_j are from different subset. To characterize structural balance, necessary and sufficient conditions are provided below.

Lemma 3.1. *[2] A connected signed graph $\mathcal{G}$ is structurally balanced if and only if any of the following equivalent conditions holds:*

1. *all cycles of $\mathcal{G}$ are positive, i.e., the product of edge weights on any cycle is positive;*
2. *there exists a diagonal matrix $\Phi = diag\left\{\phi_1, \ldots, \phi_n\right\} \in \mathbb{R}^{n\times n}$ with $\phi_i \in \{\pm 1\}$ such that $\Phi\mathcal{A}\Phi \in \mathbb{R}^{n\times n}$ has non-negative entries.;*
3. *0 is an eigenvalue of graph Laplacian $\mathcal{L}\left(\mathcal{G}\right)$.*

Since $\mathcal{G}$ is a signed graph, its graph Laplacian $\mathcal{L}\left(\mathcal{G}\right)$ may have negative off-diagonal entries and its row/column sums are not necessarily zero, which indicates that 0 is no longer a default eigenvalue as in the case of unsigned graphs. Lemma 3.1 (condition 3) further indicates that $\mathcal{L}\left(\mathcal{G}\right)$ of a structurally balanced graph is singular (i.e., contains eigenvalue 0) while $\mathcal{L}\left(\mathcal{G}\right)$ of a structurally unbalanced graph is nonsingular. Therefore, to develop controllability results on

signed graphs, the subsequent development will consider the cases when the graph is structurally unbalanced and balanced.

3.2.1 Structurally Unbalanced Signed Graphs

Controllability Gramian-based metrics are widely used to characterize the energy-related performance in network control. However, the eigen-properties of the Gramian are typically challenging to characterize analytically. In addition, topological characterizations of the energy-related controllability are hard to be extracted from the Gramian matrix. To overcome this issue, inspired by the Gramian-based nodal centrality, e.g., in [31, 32, 42, 43, 45], a notion termed *nodal metric* is introduced to quantify how much each node contributes to the energy-related controllability of structurally unbalanced signed graphs, which is defined based on the signed graph Laplacian.

Definition 3.1 (Nodal Metric)**.** Consider a structurally unbalanced signed network $\mathcal{G} = (\mathcal{V}, \mathcal{E}, \mathcal{A})$ with graph Laplacian $\mathcal{L}(\mathcal{G})$. Let $\mathcal{M}(\cdot) : \mathcal{V} \to \mathbb{R}$ denote a metric associated with node v_i, which is defined as the ith diagonal entry of the inverse of the graph Laplacian $\mathcal{L}(\mathcal{G})$, i.e.,$\mathcal{M}(v_i) = \mathcal{L}_{ii}^{-1}(\mathcal{G})$.

Based on the nodal metric defined in Def. 3.1, the following contents determine how various energy-related controllability measures, i.e., average controllability (Theorem 3.1), average control energy (Theorem 3.2), and volumetric control energy (Theorem 3.3), are related to the total nodal metric of the control nodes (i.e., leaders) via graph Laplacian.

Theorem 3.1 (Average Controllability)**.** *Consider an undirected signed graph $\mathcal{G} = (\mathcal{V}, \mathcal{E}, \mathcal{A})$ evolving according to the dynamics in (3–2) with a leader set $\mathcal{K}$. If $\mathcal{G}$ is structurally unbalanced, the average controllability $tr(\mathcal{W}_{\mathcal{K}})$ with the controllability Gramian $\mathcal{W}_{\mathcal{K}}$ defined in (3–5) can be characterized by the sum of the total $\mathcal{M}$ of the leaders in $\mathcal{K}$ as*

$$\mathrm{tr}(\mathcal{W}_{\mathcal{K}}) = \frac{1}{2}\sum_{i\in\mathcal{K}} \mathcal{M}(v_i).$$

Proof. If $\mathcal{G}$ is structurally unbalanced, i.e., its graph Laplacian $\mathcal{L}(\mathcal{G})$ does not have a zero eigenvalue according to Lemma 3.1, then $\mathcal{L}(\mathcal{G})$ is a symmetric positive definite matrix. Let

$\lambda_j \in \mathbb{R}$ and $p_j = \begin{bmatrix} p_{j1} & \cdots & p_{jn} \end{bmatrix}^T \in \mathbb{R}^n$, $j \in \{1, \ldots, n\}$, be the eigenvalues and the corresponding eigenvectors of $\mathcal{L}(\mathcal{G})$, respectively. Then, the graph Laplacian can be written as $\mathcal{L} = P\Lambda P^T$, where $\Lambda = \operatorname{diag}\{\lambda_1, \ldots, \lambda_n\} \in \mathbb{R}^{n\times n}$ is a diagonal matrix and $P = \begin{bmatrix} p_1 & \cdots & p_n \end{bmatrix} \in \mathbb{R}^{n\times n}$. Using the fact that

$$e^{-\mathcal{L}\tau} = e^{-P\Lambda P^T\tau} = Pe^{-\Lambda\tau}P^T,$$

the infinite-horizon controllability Gramian $\mathcal{W}_\mathcal{K}$ of the system in (3–2) is given by

$$\mathcal{W}_\mathcal{K} = P\left(\int_0^\infty e^{-\Lambda\tau}P^T B_\mathcal{K} B_\mathcal{K}^T P e^{-\Lambda\tau} d\tau\right) P^T. \tag{3–6}$$

Since the trace is invariant under cyclic permutations, the trace of $\mathcal{W}_\mathcal{K}$ is obtained from (3–6) as

$$\begin{aligned} \operatorname{tr}(\mathcal{W}_\mathcal{K}) &= \operatorname{tr}\left(\int_0^\infty e^{-\Lambda\tau}P^T B_\mathcal{K} B_\mathcal{K}^T P e^{-\Lambda\tau} d\tau P^T P\right) \\ &= \operatorname{tr}\left(\int_0^\infty e^{-\Lambda\tau}P^T B_\mathcal{K} B_\mathcal{K}^T P e^{-\Lambda\tau} d\tau\right), \end{aligned} \tag{3–7}$$

where $P^T P = I_n$ is used with I_n denoting an $n \times n$ identity matrix. Substituting P and $B_\mathcal{K}$ into (3–7) yields

$$\operatorname{tr}(\mathcal{W}_\mathcal{K}) = \int_0^\infty e^{-2\lambda_1\tau}\sum_{i\in\mathcal{K}} p_{1i}^2 + \cdots + e^{-2\lambda_n\tau}\sum_{i\in\mathcal{K}} p_{ni}^2 d\tau,$$

which can be reorganized as

$$\operatorname{tr}(\mathcal{W}_\mathcal{K}) = \int_0^\infty \sum_{i=1}^n e^{-2\lambda_i\tau} p_{ik_1}^2 + \cdots + \sum_{i=1}^n e^{-2\lambda_i\tau} p_{ik_m}^2 d\tau, \tag{3–8}$$

where $k_1, \ldots, k_m$ are the leader indices as defined in (3–2). Since $\int_0^\infty e^{-2\lambda_i\tau}d\tau = \frac{1}{2\lambda_i}$, (3–8) can be further simplified into

$$\begin{aligned} \operatorname{tr}(\mathcal{W}_\mathcal{K}) &= \sum_{i=1}^n \frac{1}{2\lambda_i} p_{ik_1}^2 + \cdots + \sum_{i=1}^n \frac{1}{2\lambda_i} p_{ik_m}^2 \\ &= \sum_{j\in\mathcal{K}}\sum_{i=1}^n \frac{1}{2\lambda_i} p_{ij}^2. \end{aligned} \tag{3–9}$$

Since $\mathcal{L}^{-1} = P\Lambda^{-1}P^T$, it is always true that

$$\mathcal{L}^{-1}_{jj} = \sum_{i=1}^{n} \frac{1}{\lambda_i} p_{ij}^2, \tag{3–10}$$

which indicates from (3–9) that $\mathrm{tr}\left(\mathcal{W}_{\mathcal{K}}\right) = \frac{1}{2}\sum_{j\in\mathcal{K}} \mathcal{L}^{-1}_{jj}$, where $\mathcal{L}^{-1}_{jj}$ is the jth diagonal entry of $\mathcal{L}^{-1}$. Therefore, by Def. 3.1, $\mathrm{tr}\left(\mathcal{W}_{\mathcal{K}}\right) = \frac{1}{2}\sum_{i\in\mathcal{K}} \mathcal{M}\left(v_i\right)$. □

As discussed in [31], $\mathrm{tr}\left(\mathcal{W}_{\mathcal{K}}\right)$ can be interpreted as the average controllability, providing an overall measure of the network controllability. If a network with dynamics in (3–2) is uncontrollable in certain direction of its state space, then the eigenvalue of $\mathcal{W}_{\mathcal{K}}$ corresponding to that direction will be zero, resulting in infinite control energy in that direction due to the term $\mathcal{W}_{\mathcal{K}}^{-1}$ in (3–4). Likewise, if the system is controllable in certain direction but with a small eigenvalue, then higher effort may be expected to be required to control the network in that direction. Consequently, as the sum of eigenvalues of $\mathcal{W}_{\mathcal{K}}$, $\mathrm{tr}\left(\mathcal{W}_{\mathcal{K}}\right)$ characterizes the average difficulty of network control in all directions. In addition, $\mathrm{tr}\left(\mathcal{W}_{\mathcal{K}}\right)$ is also closely related to the H_2 norm of a system. It is shown in [102] and [18] that the system robustness to external disturbances can be improved based on optimizing $\mathrm{tr}\left(\mathcal{W}_{\mathcal{K}}\right)$. Theorem 3.1 reveals that the graph Laplacian is a key factor in determining the average controllability of a network with the selected leader group. Specifically, the diagonal entries of the inverse graph Laplacian corresponding to the selected leaders together determine the average difficulty of network control.

Remark 3.1. Although leader selection for traditional network controllability has been studied in the literature, the selection of leaders that jointly considers network controllability and energy-related performance is generally a challenging and computationally hard combinatorial problem [26, 37, 43, 50]. A potential benefit of Theorem 3.1 is that it provides constructive insights, as well as a quantitative method, in selecting leader groups for energy-related network control. For instance, exiting methods (cf. [58] and [40] to name a few) can be first used to identify a set of different leader groups that can render leader-follower controllability. Since a greater value of average controllability generally indicates improved network controllability and better H_2 performance, the candidate groups can be further refined based on Theorem 3.1 by

selecting a leader group $\mathcal{K}$ with a larger value of $\sum_{i\in\mathcal{K}}\mathcal{M}(v_i)$ for network control with better performance, where $\mathcal{M}(v_i)$ can be simply determined from the graph Laplacian.

Theorem 3.2 (Average Control Energy)**.** *Consider an undirected signed graph $\mathcal{G}=(\mathcal{V},\mathcal{E},\mathcal{A})$ evolving according to the dynamics in (3–2). If $\mathcal{G}$ is structurally unbalanced and the system (3–2) under the leader group $\mathcal{K}$ is stable, the average control energy metric $\mathrm{tr}\left(\mathcal{W}_{\mathcal{K}}^{-1}\right)$ can be lower bounded by the total $\mathcal{M}$ of the leaders in $\mathcal{K}$ as*

$$\mathrm{tr}\left(\mathcal{W}_{\mathcal{K}}^{-1}\right)\geq\frac{2n^2}{\sum_{i\in\mathcal{K}}\mathcal{M}(v_i)}.$$

Proof. Let $\gamma_i\in\mathbb{R}$ and $q_i=\begin{bmatrix}q_{i1}&\cdots&q_{in}\end{bmatrix}^T\in\mathbb{R}^n$, $i\in\{1,\ldots,n\}$, be the eigenvalues and the corresponding normalized eigenvectors of $\mathcal{W}_{\mathcal{K}}$, respectively. The trace of $\mathcal{W}_{\mathcal{K}}$ and $\mathcal{W}_{\mathcal{K}}^{-1}$ are $\mathrm{tr}\left(\mathcal{W}_{\mathcal{K}}\right)=\sum_{i=1}^{n}\gamma_i$ and $\mathrm{tr}\left(\mathcal{W}_{\mathcal{K}}^{-1}\right)=\sum_{i=1}^{n}\frac{1}{\gamma_i}$, respectively. Consider that the leader group $\mathcal{K}$ can render the system leader-follower controllable, i.e., $\gamma_i>0,\forall i$. Then, the arithmetic mean will not be less than the harmonic mean, i.e., $\frac{1}{n}\sum_{i=1}^{n}\gamma_i\geq n\left(\sum_{i=1}^{n}\frac{1}{\gamma_i}\right)^{-1}$. Therefore, similar to [32], Theorem 3.1 yields

$$\mathrm{tr}\left(\mathcal{W}_{\mathcal{K}}^{-1}\right)\geq\frac{n^2}{\mathrm{tr}\left(\mathcal{W}_{\mathcal{K}}\right)}=\frac{2n^2}{\sum_{i\in\mathcal{K}}\mathcal{M}(v_i)}.$$

□

Since the control energy $E(t)$ in (3–4) is proportional to $\mathcal{W}_{\mathcal{K}}^{-1}$, $\mathrm{tr}\left(\mathcal{W}_{\mathcal{K}}^{-1}\right)$ measures the average energy needed to control a network to an arbitrary target state. Theorem 3.2 indicates that $\mathrm{tr}\left(\mathcal{W}_{\mathcal{K}}^{-1}\right)$ is inversely proportional to the total $\mathcal{M}$ of the leader group $\mathcal{K}$, i.e., $\sum_{i\in\mathcal{K}}\mathcal{M}(v_i)$. In other words, selecting a leader group with higher total $\mathcal{M}$ could potentially result in less energy expenditure in network control.

Theorem 3.3 (Volumetric Control Energy)**.** *Consider an undirected signed graph $\mathcal{G}=(\mathcal{V},\mathcal{E},\mathcal{A})$ evolving according to the dynamics in (3–2). If $\mathcal{G}$ is structurally unbalanced, the volumetric*

control energy metric $\log(\det \mathcal{W}_{\mathcal{K}})$ *can be upper bounded by the total* $\mathcal{M}$ *of the leaders in* $\mathcal{K}$ *as*

$$\log(\det \mathcal{W}_{\mathcal{K}}) \leq \sum_{i \in \mathcal{K}} n \log\left(\frac{\mathcal{M}(v_i)}{n}\right) + c'_{\Psi},$$

where $c'_{\Psi} \in \mathbb{R}^{+}$ *is a constant determined by the eigenvalues of the graph Laplacian.*

Proof. The proof starts by characterizing $\log(\det \mathcal{W}_{\mathcal{K}})$ for the case of a single leader in the network, which will then be extended to a multi-leader scenario.

Consider the case of a single leader, i.e., $m = 1$, and let the leader's index be k_m. As a result, the input matrix $B_{\mathcal{K}}$ is reduced to a basis vector $e_{k_m} \in \mathbb{R}^n$ where the k_mth entry is one while the others are zeros. The controllability Gramian $\mathcal{W}_{\mathcal{K}}$ for $\mathcal{K} = \{k_m\}$ can be simplified from (3–6) as

$$\mathcal{W}_{\mathcal{K}} = P\left(\int_0^{\infty} e^{-\Lambda\tau} P^T e_{k_m} e_{k_m}^T P e^{-\Lambda\tau} d\tau\right) P^T. \tag{3–11}$$

From the definition of P, $P^T e_{k_m}$ can be written as $P^T e_{k_m} = \begin{bmatrix} p_{1k_m}, & \ldots, & p_{nk_m} \end{bmatrix}^T \in \mathbb{R}^n$. Using the fact that $e^{-\Lambda\tau} \in \mathbb{R}^{n\times n}$ is a diagonal matrix one can obtain

$$e^{-\Lambda\tau} P^T e_{k_m} = P_{k_m} z, \tag{3–12}$$

where $P_{k_m} \triangleq \operatorname{diag}\begin{Bmatrix} p_{1k_m}, & \ldots, & p_{nk_m} \end{Bmatrix} \in \mathbb{R}^{n\times n}$ is a diagonal matrix, and $z = \begin{bmatrix} e^{-\lambda_1\tau}, & \ldots, & e^{-\lambda_n\tau} \end{bmatrix}^T \in \mathbb{R}^n$. Substituting (3–12) in (3–11), $\mathcal{W}_{\mathcal{K}}$ can be rewritten as

$$\begin{aligned} \mathcal{W}_{\mathcal{K}} &= P P_{k_m}\left(\int_0^{\infty} z z^T d\tau\right) P_{k_m}^T P^T \\ &= P P_{k_m} \Psi P_{k_m}^T P^T, \end{aligned} \tag{3–13}$$

where $\Psi = [\Psi_{ij}] \in \mathbb{R}^{n\times n}$ with $\Psi_{ij} = \frac{1}{\lambda_i + \lambda_j}$. Since P, P_{k_m}, and Ψ are all square matrices, the determinant of $\mathcal{W}_{\mathcal{K}}$ is

$$\begin{aligned} \det(\mathcal{W}_{\mathcal{K}}) &= \det P \det P_{k_m} \det \Psi \det P_{k_m}^T \det P^T \\ &= \det\left(P_{k_m} P_{k_m}^T\right) \det(\Psi), \end{aligned} \tag{3–14}$$

where the fact that $\det P \det P^T = 1$ is used since P is an orthogonal matrix. Based on (3–14), the volumetric control energy can be obtained as

$$\log\left(\det \mathcal{W}_{\mathcal{K}}\right) = \log\left(\det\left(P_{k_m} P_{k_m}^T\right)\right) + c_{\Psi}, \tag{3–15}$$

where $c_{\Psi} \triangleq \log\left(\det \Psi\right)$ is a constant determined by the eigenvalues of $\mathcal{L}(\mathcal{G})$, and P_{k_m} is determined by the selection of the leader node $k_m \subseteq \mathcal{V}$. Since P_{k_m} is a diagonal matrix, it follows from (3–15) that

$$\log\left(\det \mathcal{W}_{\mathcal{K}}\right) = \log\left(\prod_{i=1}^{n} p_{ik_m}^2\right) + c_{\Psi}.$$

Multiplying the above expression by $\frac{1}{n}$ on both sides, we get

$$\begin{aligned}\frac{1}{n}\log\left(\det \mathcal{W}_{\mathcal{K}}\right) &= \log\left(\prod_{i=1}^{n} p_{ik_m}^2\right)^{\frac{1}{n}} + \frac{c_{\Psi}}{n} \\ &\leq \log\frac{\sum_{i=1}^{n} p_{ik_m}^2}{n} + \frac{c_{\Psi}}{n},\end{aligned} \tag{3–16}$$

where the fact that $\left(\prod_{i=1}^{n} p_{ik_m}^2\right)^{\frac{1}{n}} \leq \frac{\sum_{i=1}^{n} p_{ik_m}^2}{n}$ is used. Subtracting $\log\left(\lambda_{max}\right)$ on both sides of (3–16) yields

$$\log\left(\det \mathcal{W}_{\mathcal{K}}\right) - n\log\left(\lambda_{max}\right) \leq n\log\frac{\sum_{i=1}^{n} p_{ik_m}^2}{n\lambda_{max}} + c_{\Psi}. \tag{3–17}$$

In (3–17), $\lambda_{max} > 0$ is the largest eigenvalue or spectral radius of $\mathcal{L}(\mathcal{G})$. Further, the expression in (3–10) yields $\sum_{i=1}^{n} \frac{1}{\lambda_{max}} p_{ik_m}^2 \leq \sum_{i=1}^{n} \frac{1}{\lambda_i} p_{ik_m}^2 = \mathcal{L}_{k_m k_m}^{-1}$. Using this expression, the inequality in (3–17) can be written as

$$\log\left(\det \mathcal{W}_{\mathcal{K}}\right) \leq n\log\left(\frac{\mathcal{L}_{k_m k_m}^{-1}}{n}\right) + c_{\Psi}', \tag{3–18}$$

where $c_{\Psi}' \triangleq c_{\Psi} + n\log\left(\lambda_{max}\right)$.

For the multi-leader case (i.e., $m > 1$), let $\log\left(\det \mathcal{W}_{\mathcal{K}_i}\right)$ denote the volumetric control energy associated with the leader $v_i \in \mathcal{K}$. From (3–18), one has

$$\log\left(\det \mathcal{W}_{\mathcal{K}_i}\right) \leq n\log\frac{\mathcal{M}\left(v_i\right)}{n} + c_{\Psi}'.$$

As demonstrated in the Theorem 6 in section D of [31], since $\log\left(\det \mathcal{W}_{\mathcal{K}}\right)$ is a submodular function on the leader set, we have

$$\begin{aligned}\log\left(\det \mathcal{W}_{\mathcal{K}}\right) &\leq \sum_{i\in\mathcal{K}} \log\left(\det \mathcal{W}_{\mathcal{K}_i}\right) \\ &\leq \sum_{i\in\mathcal{K}} \left(n \log \frac{\mathcal{M}\left(v_i\right)}{n} + c'_{\Psi}\right)\end{aligned}$$

where $\log\left(\det \mathcal{W}_{\mathcal{K}}\right)$ denotes total volumetric control energy of system under the leader set $\mathcal{K}$. □

The volumetric control energy metric $\log\left(\det \mathcal{W}_{\mathcal{K}}\right)$ indicates the set of states that can be reached within or less than a unit control input energy. Hence, a higher value of $\log\left(\det \mathcal{W}_{\mathcal{K}}\right)$ usually implies a larger target space that can be reached with the same amount of control energy. Theorem 3.3 further indicates that the leader group with a higher value of $\sum_{i\in\mathcal{K}} \mathcal{M}\left(v_i\right)$ has larger reachability, which, in turn, implies improved energy efficiency in network control.

Remark 3.2. Theorems 3.1-3.3 not only show how various energy measures are related to the nodal metric of the leader group in a network, but also reveal that these measures are closely related to the inverse of the graph Laplacian. As such, these theorems offer a new perspective to design networks from the energy-related performance considerations. For different controllability metrics, i.e., average controllability, average control energy, and volumetric control energy, it is shown that the respective metrics can be improved if the network topology is designed such that the diagonal entries of the inverse graph Laplacian corresponding to the leaders are maximized. In addition, as discussed in the works of [38, 84, 103], the inverse of the graph Laplacian can be interpreted as effective resistances, which play important roles in distributed network control and estimation. For instance, effective resistances appear in network control problems in which agents are steered towards a desired formation [103], and also appear in least-squares estimation problems in which global information can be reconstructed from noisy measurements. In the recent work [38], effective resistances were also used to quantify the information centrality. Based on Theorems 3.1-3.3, additional research will consider exploring how controllability

metrics are related to the leader groups via effective resistances on structurally balanced graphs as shown in the next Chapter.

3.2.2 Structurally Balanced Signed Graph

This section considers the case that the signed graph $\mathcal{G}$ is structurally balanced. Lemma 3.1 indicates that, if $\mathcal{G}$ is structurally balanced, there always exists a gauge transformation matrix Φ and a corresponding graph $\bar{\mathcal{G}} = \left(\mathcal{V}, \mathcal{E}, \bar{\mathcal{A}}\right)$ with $\bar{\mathcal{A}} = [\bar{a}_{ij}] \in \mathbb{R}^{n\times n} = \Phi\mathcal{A}\Phi$. Clearly, $\bar{\mathcal{G}}$ is an unsigned correspondence of $\mathcal{G}$, i.e., they share the same node and edge sets except that the edge weights in $\bar{\mathcal{A}}$ are all non-negative, i.e., $\bar{a}_{ij} = |a_{ij}|$. Due to the consideration of a structurally balanced $\mathcal{G}$, its graph Laplacian $\mathcal{L}$ has a 0 eigenvalue, which indicates the Gramian $\mathcal{W}_{\mathcal{K}}$ in (3–5) can be unbounded as $t \to \infty$. To overcome this issue, we consider the Gramian over a finite time interval $[t_0, t_f]$ such that the desired target state x_f can be achieved at t_f under the input u, i.e., $x_f = x\left(t_f\right)$.

Theorem 3.4. *Consider a signed graph $\mathcal{G} = (\mathcal{V}, \mathcal{E}, \mathcal{A})$ and its corresponding unsigned graph $\bar{\mathcal{G}} = \left(\mathcal{V}, \mathcal{E}, \bar{\mathcal{A}}\right)$ with their controllability Gramians $\mathcal{W}_k$ and $\bar{\mathcal{W}}_k$, respectively. Let the nodes in $\mathcal{G}$ and $\bar{\mathcal{G}}$ evolve according to the dynamics in (3–2) but with their respective adjacency matrices $\mathcal{A}$ and $\bar{\mathcal{A}}$. If $\mathcal{G}$ is structurally balanced, then $\mathcal{W}_k$ has the same matrix spectrum as $\bar{\mathcal{W}}_k$.*

Proof. For an unsigned graph $\bar{\mathcal{G}}$, its nodes evolve according to the following dynamics:

$$\dot{x}\left(t\right) = -\mathcal{L}_u\left(\mathcal{G}\right)x\left(t\right) + B_{\mathcal{K}}u\left(t\right), \tag{3–19}$$

where $\mathcal{L}_u = \mathcal{D} - \bar{\mathcal{A}}$ is the graph Laplacian of $\bar{\mathcal{G}}$. From (3–5), the controllability Gramian of (3–19) at time $t \in [t_0, t_f]$ can be obtained as

$$\bar{\mathcal{W}}_k\left(t\right) = \int_{t_0}^{t} e^{-\mathcal{L}_u\tau}B_{\mathcal{K}}B_{\mathcal{K}}^{T}e^{-\mathcal{L}_u^{T}\tau}d\tau.$$

From Lemma 3.1, if $\mathcal{G}$ is structurally balanced then $\mathcal{L}_u = \mathcal{D} - \Phi(\mathcal{A})\Phi = \Phi\mathcal{L}\Phi$. Therefore, $\bar{\mathcal{W}}_k$ becomes

$$\begin{aligned}\bar{\mathcal{W}}_k(t) &= \int_{t_0}^{t} e^{-\Phi\mathcal{L}\Phi} B_{\mathcal{K}} B_{\mathcal{K}}^T e^{-\Phi\mathcal{L}^T\Phi\tau} d\tau \\ &= \int_{t_0}^{t} \Phi e^{-\mathcal{L}\tau}\Phi B_{\mathcal{K}} B_{\mathcal{K}}^T \Phi e^{-\mathcal{L}^T\tau}\Phi d\tau \\ &= \Phi\mathcal{W}_k\Phi,\end{aligned} \tag{3–20}$$

where the fact $\Phi B_{\mathcal{K}} B_{\mathcal{K}}^T \Phi = B_{\mathcal{K}} B_{\mathcal{K}}^T$ is used since gauge transformation preserves diagonal matrices, and $\mathcal{W}_{\mathcal{K}}(t) = \int_{t_0}^{t} e^{-\mathcal{L}\tau} B_{\mathcal{K}} B_{\mathcal{K}} e^{-\mathcal{L}\tau} d\tau$ is the controllability Gramian defined in (3–5). Since gauge transformation preserves the matrix spectra [2], the matrix $\Phi\mathcal{W}_k\Phi$ has the same set of eigenvalues as that of $\mathcal{W}_k$. Therefore, it is clear from (3–20) that $\mathcal{W}_k$ has the same matrix spectrum as of $\bar{\mathcal{W}}_k$. □

The energy-related controllability metrics analyzed in Section 3.2.1 (i.e., average controllability $\mathrm{tr}\left(\bar{\mathcal{W}}_k\right)$, average control energy $\mathrm{tr}\left(\bar{\mathcal{W}}^{-1}\right)$, and volumetric control energy $\log\det\left(\bar{\mathcal{W}}_k\right)$ along with other metrics, including the worst-case controllability $\lambda_{\min}\left(\bar{\mathcal{W}}_k\right)$ and the dimension of the controllable subspace $\mathrm{rank}\left(\bar{\mathcal{W}}_k\right)$, can be directly obtained from the eigenvalues of $\bar{\mathcal{W}}_k$. Since $\mathcal{W}_k$ and $\bar{\mathcal{W}}_k$ have the same set of eigenvalues, Theorem 3.4 indicates that the structurally balanced signed graph $\mathcal{G}$ and its corresponding unsigned graph $\bar{\mathcal{G}}$ are equivalent in terms of the above controllability metrics. Therefore, Theorem 3.4 provides a means to investigate the energy-related controllability of signed networks by examining its corresponding unsigned graph $\bar{\mathcal{G}}$ using the analysis and design methods developed for unsigned graphs.

Remark 3.3. When considering the case that $t \to \infty$, $\mathcal{W}_k(t)$ grows unboundedly with t due to the existence of the 0 eigenvalue. Since the 0 eigenvalue indicates a consensus manifold, the infinite volume of the determinant of $\mathcal{W}_k(t)$ reflects that network state can be moved along the consensus manifold with arbitrarily small control energy. Therefore, in terms of the control energy required in moving network states, we only need to consider the manifolds corresponding

to nonzero eigenvalues. The eigenvalue decomposition approach in [42] can then be leveraged to obtain a sub-Gramian that only contains non-zero eigenvalues, where similar analysis in Theorem 3.4 can be applied to obtain the equivalence of unsigned graph and signed structurally balanced graphs in terms of energy-related metrics.

Corollary 3.1. *Consider a signed graph $\mathcal{G} = (\mathcal{V}, \mathcal{E}, \mathcal{A})$ and its unsigned correspondence $\bar{\mathcal{G}} = \left(\mathcal{V}, \mathcal{E}, \bar{\mathcal{A}}\right)$. If $\mathcal{G}$ is structurally balanced, then the leader-follower controllability of $\mathcal{G}$ is equivalent to that of $\bar{\mathcal{G}}$ under the the same leader set.*

It is well known that a system is controllable if and only if its controllability Gramian is positive definite. Thus, Corollary 3.1 follows immediately from Theorem 3.4 by the fact that $\mathcal{W}_k$ and $\bar{\mathcal{W}}_k$ share the same set of eigenvalues when $\mathcal{G}$ is structurally balanced.

Remark 3.4. The problem of leader group selection on structurally balanced signed graphs has been partially studied in [59], which requires the leaders to be selected from the same partitioned set (i.e., $\mathcal{V}_1$ or $\mathcal{V}_2$) to ensure network controllability. Corollary 3.1 relaxes this constraint by allowing the leaders to be selected from different partitioned sets, as long as the corresponding unsigned graph is controllable under the selected leader group. Additionally, the discovered equivalence of controllability between $\mathcal{G}$ and $\bar{\mathcal{G}}$ enables the use of existing leader group selection methods developed for unsigned graphs [6, 35, 104].

Corollary 3.2. *If $\mathcal{G} = (\mathcal{V}, \mathcal{E}, \mathcal{A})$ is a signed acyclic graph, then there always exists an unsigned correspondence $\bar{\mathcal{G}} = \left(\mathcal{V}, \mathcal{E}, \bar{\mathcal{A}}\right)$, such that the controllability Gramian $\mathcal{W}_k$ of $\mathcal{G}$ has the same matrix spectrum as that of $\bar{\mathcal{W}}_k$ of $\bar{\mathcal{G}}$.*

Since acyclic graphs, e.g., tree or path graphs, are inherently structurally balanced [2], Corollary 3.2 is an immediate result of Theorem 3.4. Corollary 3.2 states that, instead of investigating the signed acyclic graph $\mathcal{G}$, the unsigned correspondence $\bar{\mathcal{G}}$ of $\mathcal{G}$ can be explored to enable leader group selection using the energy-related controllability metrics based on $\mathcal{W}_k$.

3.3 Summary

In this charpter, the energy-related controllability of signed complex networks is characterized in terms of the graph Laplacian, where contributions of each leader with respect to

energy-related performance are investigated. Graph Laplacian has been shown direct implications on the network topological properties via structural balance. Leader selection jointly considering controllability and control energy metrics will be given in next Chapter.

CHAPTER 4
ENERGY-RELATED CONTROLLABILTY OF COMPLEX NETWORKS - LEADER SELECTION

Followed by Chapter 3, a leader group selection approach that jointly considers network controllability and energy-related performance is investigated. Specifically, networked dynamical systems with signed acyclic topology are considered. To effectively and efficiently control a networked system, leader group selection in this Chapter focuses on energy-related controllability, which jointly considers two primary objectives: 1) network controllability, i.e., identification of a subset of units as leaders that can drive the entire network to a desired state even in the presence of antagonistic interactions, and 2) energy-related performance, which takes into account the system performance incurred by the selected leaders in steering the network to the desired state. To achieve these objectives, graph-inspired characterizations of energy-related controllability are developed based on the interaction between the network topology and dynamics. The developed topological characterizations are exploited to derive heuristic leader selection algorithms on signed acyclic graphs. Illustrative examples are provided to demonstrate the effectiveness of the developed leader group selection methods.

4.1 Problem Formulation

Consider a networked system represented by an undirected signed graph $\mathcal{G} = (\mathcal{V}, \mathcal{E}, \mathcal{A})$, where the node set $\mathcal{V} = \{v_1, \ldots, v_n\}$ and the edge set $\mathcal{E} \subset \mathcal{V} \times \mathcal{V}$ represent the units and their interactions, respectively. The network-wide interactions are captured by the adjacency matrix $\mathcal{A} \in \mathbb{R}^{n \times n}$, where $a_{ij} \neq 0$ if $(v_i, v_j) \in \mathcal{E}$ and $a_{ij} = 0$ otherwise. No self-loop is considered, i.e., $a_{ii} = 0 \; \forall i = 1, \ldots, n$. Without loss of generality, it is assumed that $a_{ij} \colon \mathcal{E} \to \{\pm 1\}$, where $a_{ij} = 1$ if v_i and v_j are positive neighbors with cooperative interactions and $a_{ij} = -1$ if v_i and v_j are negative neighbors with antagonistic interactions. In this Chapter, a particular class of graphs, namely acyclic graphs, which does not have cycles are discussed. Tree or path graphs are typical examples of acyclic graphs.

Graph $\mathcal{G}$ is connected if there exists a path between any pair of nodes in $\mathcal{V}$. The neighbor set of v_i is defined as $\mathcal{N}_i = \{v_j | \, (v_i, v_j) \in \mathcal{E}\}$, and the degree of v_i, denoted as $d_i \in \mathbb{Z}^+$, is defined as

the number of its neighbors, i.e., $d_i = |\mathcal{N}_i|$, where $|\mathcal{N}_i|$ denotes the cardinality of $\mathcal{N}_i$. The signed graph Laplacian of $\mathcal{G}$ is defined as $\mathcal{L}(\mathcal{G}) \triangleq \mathcal{D} - \mathcal{A}$, where $\mathcal{D} \triangleq \operatorname{diag}\{d_1, \ldots, d_n\}$ is a diagonal matrix.

Let $\boldsymbol{x}(t) = [x_1(t), \ldots, x_n(t)]^T \in \mathbb{R}^n$ denote the stacked system states, where each entry $x_i(t) \in \mathbb{R}$ represents the state of node v_i. As in Chapter 3, suppose the system states evolve according to the Laplacian dynamics in (3–1), where the graph Laplacian $\mathcal{L}(\mathcal{G})$ indicates that each node v_i updates its state x_i taking into account the states of its neighboring nodes, i.e., $x_j \in \mathcal{N}_i$. It is assumed that a set $\mathcal{K} = \{k_1, \ldots, k_m\} \subseteq \mathcal{V}$ of nodes, referred as leaders in the networked system, can be endowed with external controls. With external inputs, the system dynamics in (3–1) can be rewritten as (3–2), where $B_{\mathcal{K}} = \begin{bmatrix} e_{k_1} & \cdots & e_{k_m} \end{bmatrix} \in \mathbb{R}^{n \times m}$ is the input matrix with basis vectors e_i, $i = k_1, \ldots, k_m$, indicating that the ith node is endowed with external controls $u(t) \in \mathbb{R}^m$. The dynamics of (3–2) indicates that the network behavior is not only driven by the graph Laplacian $\mathcal{L}$, but also depends on the input matrix $B_{\mathcal{K}}$ via the leader set $\mathcal{K}$. Different leader sets can result in different $B_{\mathcal{K}}$, leading to drastic differences in the capability of controlling a network.

As discussed in Chapter 3, energy-related performance can be captured by the controllability Gramian $\mathcal{W}$. Since the controllability Gramian $\mathcal{W}$ provides an energy-related measure of network control as in (3–4), various energy metrics were developed based on $\mathcal{W}$ [31, 32, 48, 49]. In this Chapter, average controllability [31], is considered. Chapter 3 discusses the meanings of $\operatorname{tr}(\mathcal{W})$, as a way of measuring the average effort to control a system and the system robustness to control input noises. Although various methods have been developed to maximize $\operatorname{tr}(\mathcal{W})$ to improve energy-related performance, the issue with these approaches is that the network controllability is generally not guaranteed, since maximizing $\operatorname{tr}(\mathcal{W})$ can not rule out the possibility of having zero eigenvalues of $\mathcal{W}$. Therefore, the goal of this Chapter is to develop leader group selection approaches such that the resulting leader-follower system has guaranteed network controllability and improved system performance in terms of the average controllability $\operatorname{tr}(\mathcal{W})$.

4.2 Leaders Selection on Signed Acyclic Graphs

Since acyclic graphs, e.g., tree or path graphs, are inherently structurally balanced [2], corollary 3.2 indicates that, instead of investigating a signed acyclic graph $\mathcal{G}$, its unsigned correspondence $\bar{\mathcal{G}}$ can be explored to enable leader group selection for improved energy-related performance in terms of $\mathrm{tr}\,(\mathcal{W})$.

Specifically, let $d_{ij} \in \mathbb{R}^+$ denote the the distance between v_i and v_j in $\mathcal{G}$, i.e., the number of edges of the shortest path connecting v_i and v_j. The total distance of node i to all other nodes, often referred as the closeness of node i, is defined as $\sigma_i = \sum_{j \neq i} d_{ij}$. An important result from [51] reveals that, for unsigned graphs, $\mathrm{tr}\,(\mathcal{W})$ is proportional to the node closeness on acyclic graphs. In other words, selecting nodes with higher closeness values can improve $\mathrm{tr}\,(\mathcal{W})$. However, as discussed in section 4.1, simply selecting leaders that maximizes $\mathrm{tr}\,(\mathcal{W})$ may not guarantee the network controllability. Therefore, based on Chapter 2 and Chapter 3, this section focuses on the development of leader group selection algorithms that jointly consider the leader-follower controllability and the average controllability $\mathrm{tr}\,(\mathcal{W})$.

The leader group selection method developed in this section consists of two steps. The first step is to identify a set of leader group candidates that can render the network controllable. Among these candidates, the energy-related metric $\mathrm{tr}\,(\mathcal{W})$ will be exploited in the second step to refine the initial selection by identifying leaders that ensure better system performance in terms of average controllability. Specifically, based on the result of Chapter 2, that a network is controllable if each sub-graph constructing the network via leader-to-leader connection is controllable, the first step is to partition the graph into a set of sub-graphs, where the sub-graphs are connected via leaders. Further, acyclic graphs generally take the form of a tree structure, which has path graphs as its basic building blocks. Therefore, acyclic signed graphs such as tree graphs can always be partitioned into a set of path graphs using the available partition methods, for example in [97]. The following lemma summarizes the leader group selection rules on signed path graphs developed in Chapter 2.

Lemma 4.1. *Consider a signed path graph $\mathcal{G}_p = (\mathcal{V}, \mathcal{E}, \mathcal{A})$ with the node set $\mathcal{V} = \{1, \ldots, n\}$, the edge set $\mathcal{E} = \{(i, i+1) | \, i \in \{1, \ldots, n-1\}\}$, and the weight matrix $\mathcal{A} \in \mathbb{R}^{n \times n}$ indicating associated positive or negative weights in $\mathcal{E}$. Let the nodes in $\mathcal{G}_p$ evolve according to the dynamics in (3–2). The signed path graph $\mathcal{G}_p$ is controllable if the leader group is selected according to either of the following rules: 1) selecting an end node as the leader, i.e. v_1 or v_n; or 2) selecting any two connected nodes as the leaders, i.e., $v_i, v_j \in \mathcal{V}_l$ with $(v_i, v_j) \in \mathcal{E}$.*

Once the initial selection following Lemma 4.1 is complete, the next step is to refine the initial selection based on $\mathrm{tr}\,(\mathcal{W})$ for improved network performance. Note that other leader group selection approaches originally developed for unsigned path graphs [12] are also applicable due to Corollary 3.2.

Lemma 4.2. *For a signed path graph $\mathcal{G}_p$, the closer the node i to the end node of $\mathcal{G}_p$, the higher its closeness σ_i.*

Lemma 4.2 is an immediate result of the fact that, if a node is closer to the end of the path graph, it has greater total distance to the other nodes, i.e., a higher closeness value. It was proven in [51] that selecting nodes with higher closeness as leaders can improve the average controllability. Although Lemma 4.2 is applicable to path graphs, it is alone insufficient to characterize the energy-related controllability of general acyclic graphs consisting of multiple path graphs.

Example 4.1. Consider a signed acyclic graph $\mathcal{G}_T$ composed of 6 nodes as shown in Fig 4-1, where negative edges are marked with "-". Suppose v_6 is a leader and it can be verified that $\mathcal{G}_T$ is controllable if either v_1 or v_4 is selected as an additional leader. Due to the relationship between node closeness and average controllability, it is desirable to select nodes with larger closeness values. For the sub-path graph $\{v_1, v_2, v_3, v_4\}$, clearly v_1 and v_4 have the same closeness from Lemma 4.2. However, due to the additional sub-path graph $\{v_5, v_6\}$, it can be verified that the closeness of v_1 and v_4 in $\mathcal{G}_T$ are $\sigma_1 = 11$ and $\sigma_4 = 13$, respectively. Thus v_4 should be selected as the additional leader to enhance the network performance in terms of average controllability.

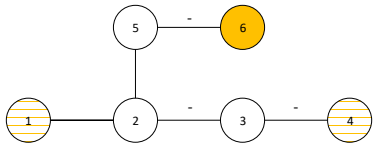

Figure 4-1. Node closeness on the signed acyclic graph.

Motivated by the discussion in Example 4.1, the subsequent lemma quantifies the influence of sub-path graphs on node closeness.

Lemma 4.3. *Consider a sub-path graph* $\mathcal{G}_1 = (\mathcal{V}_1, \mathcal{E}_1, \mathcal{A}_1)$ *and let* $\bar{\sigma}_{ij}$ *be the closeness difference of* v_i *and* v_j *on* $\mathcal{G}_1$*. Suppose* $\mathcal{G}_1$ *is augmented by connecting another sub-path graph* $\mathcal{G}_2 = (\mathcal{V}_2, \mathcal{E}_2, \mathcal{A}_2)$ *with cardinality* $h = |\mathcal{V}_2|$ *via an edge* (v_p, v_q)*, where* $v_p \in \mathcal{V}_1$ and $v_q \in \mathcal{V}_2$*. In the augmented graph, the closeness difference of* v_i *and* v_j*, denoted as* σ_{ij}*, is obtained as*

$$\sigma_{ij} = \bar{\sigma}_{ij} + h\left(d_{ip} - d_{jp}\right), \tag{4–1}$$

where d_{ip} *and* d_{jp} *represent the distance from* v_i *to* v_p *and* v_j *to* v_p*, respectively.*

Proof. From the definition of closeness, $\sigma_i = \sum_{k\in\mathcal{V}_1} d_{ik} + \sum_{l\in\mathcal{V}_2} d_{il}$ and $\sigma_j = \sum_{k\in\mathcal{V}_1} d_{jk} + \sum_{l\in\mathcal{V}_2} d_{jl}$. Therefore, σ_{ij} can be obtained as

$$\sigma_{ij} = \sigma_i - \sigma_j = \bar{\sigma}_{ij} + \left(\sum_{l\in\mathcal{V}_2} d_{il} - \sum_{l\in\mathcal{V}_2} d_{jl}\right). \tag{4–2}$$

Note that, for any node $v_o \in \mathcal{V}_2$ in $\mathcal{G}_2$, one has $d_{io} - d_{jo} = (d_{ip} + d_{po}) - (d_{jp} + d_{po}) = (d_{ip} - d_{jp}) + (d_{po} - d_{po}) = d_{ip} - d_{jp}$. Therefore, (4–2) can be simplified as $\sigma_{ij} = \bar{\sigma}_{ij} + h\left(d_{ip} - d_{jp}\right)$, since $\mathcal{G}_2$ consists of h nodes. □

Lemma 4.3 shows that the closeness difference of any two nodes in a general acyclic graph depends on h, $\bar{\sigma}_{ij}$, and $d_{ip} - d_{jp}$, each of which can easily be obtained from its sub-path graph. For instance, in Example 4.1, the closeness difference of v_1 and v_4 in $\mathcal{G}_T$ can be calculated from the sub-path graph with nodes $\{v_1, v_2, v_3, v_4\}$. According to (4–1), $\sigma_{14} = \bar{\sigma}_{14} + h\left(d_{12} - d_{42}\right)$, where $\bar{\sigma}_{14} = \sum_{k\in\{1,2,3,4\}} d_{1k} - \sum_{k\in\{1,2,3,4\}} d_{4k} = 6 - 6 = 0$, $d_{12} = 1$, $d_{42} = 2$, and $h = 2$ is the cardinality of graph $\{v_5, v_6\}$. Thus, $\sigma_{14} = -2$, which indicates v_4 is a better leader candidate

than v_1 in terms of average controllability. Note that following similar analysis, Lemma 4.3 can be extended to the case of multi-sub-path graphs.

4.3 Algorithm and Simulation

Motivated by the discussion above, Algorithm 4.1 summarizes the heuristic leader selection rules. It starts by identifying nodes in a given acyclic signed graph whose node degree is greater than two. Since the joint nodes in the acyclic graph have degree higher than two, the reason to identify nodes degree more than two is to facilitate the partition of the acyclic graph into paths. Once the graph is partitioned into a set of path graphs, the leader selection rules developed in Lemma 4.1 and Lemma 4.3 can be applied to identify leader groups with ensured network controllability and improved average controllability. The following example is provided to elucidate the approach.

Algorithm 4.1 Leader Selection for Signed Acyclic Graph

procedure INPUT:(Graph $\mathcal{G}(\mathcal{V}, \mathcal{E}, \mathcal{A})$);
  Output: The set of leaders $\mathcal{V}_l$
  Calculate the node degree d_i for each node $v_i \in \mathcal{V}$;
  Select nodes v_i with $d_i > 2$ to form $\mathcal{V}_l$;
  Use graph partition techniques (e.g., [97]) to partition $\mathcal{G}$ into path graphs;
  for Each sub-path graph **do**
    if The path is controllable **then**
      Keep the selected leaders in $\mathcal{V}_l$;
    else
      Update $\mathcal{V}_l$ by including nodes that can render the sub-path graphs controllable (i.e., Lemma 4.1);
      Further update $\mathcal{V}_l$ for improved average controllability (i.e., Lemma 4.3);
    end if
  end for
  Output $\mathcal{V}_l$;
end procedure

Example 4.2. Consider a signed acyclic graph $\mathcal{G}$ in Fig. 4-2 (a) with the objective of selecting a set of leaders with ensured network controllability and improved performance. Based on Algorithm 4.1 the initial leader set is identified as nodes with degrees more than two, i.e., the nodes $\{1, 2, 4, 10, 16\}$ in Fig.4-2 (b). Since a graph can be safely partitioned without affecting the network controllability using leader to leader connections [105], $\mathcal{G}$ is partitioned into two sub-path graphs $\{1, 3, 7, 12, 17\}$ and $\{4, 8, 9, 13\}$, respectively, and a sub-tree with the rest nodes as shown in Fig. 4-2 (c). The next step is to update the leader set ensuring each partitioned graph is controllable. Specifically, the sub-path graph $\{1, 3, 7, 12, 17\}$ is controllable with leader v_1

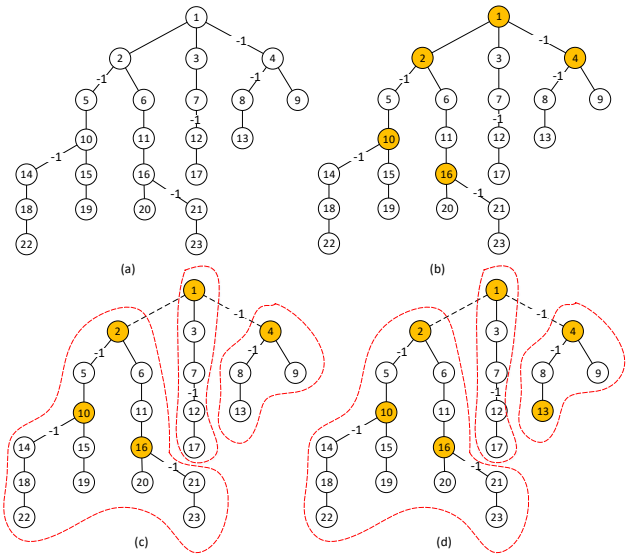

Figure 4-2. (a) A signed tree with 23 nodes. (b) The initial selection of leader nodes (i.e., nodes with degree higher than two) are marked. (c) The signed tree is partitioned into a set of path graphs. (d) Based on Lemma 4.1 and 4.3, the leader set is updated for ensured leader-follower controllability and improved average controllability.

from Lemma 4.1. For the other sub-path graph $\{4, 8, 9, 13\}$, selecting any one node from the set $\{v_8, v_9, v_{13}\}$ along with v_4 can ensure its controllability. According to Lemma 4.3, v_{13} is the best candidate, since it has a higher closeness value than v_8 and v_9, and thus provides better average controllability. Therefore, v_{13} is selected as an additional leader, as shown in Fig.4-2 (d).

Now consider sub-tree of $\mathcal{G}$ in Fig. 4-3 (a), which can be further partitioned into sub-path graphs according to Algorithm 4.1. Suppose that the sub-tree is partitioned into $\{15, 19\}$, $\{20\}$, and a long sub-path graph shown within the dashed region, as shown in Fig. 4-3 (b). According to Lemma 4.1, v_{15} and v_{20} have to be selected as leaders so that the two sub-graphs $\{15, 19\}$ and $\{20\}$ are controllable and the sub-graphs are connected by leaders only. For the sub-path graph within the dashed region, it is observed from Lemma 4.1 that any node except v_{18} from the path can render this sub-path graph controllable. To improve average controllability, the node with the highest closeness value should be selected as the leader. It can be verified from Lemma 4.3 that v_{23} has the highest closeness value, and thus selected as the leader, as shown in Fig. 4-3 (d).

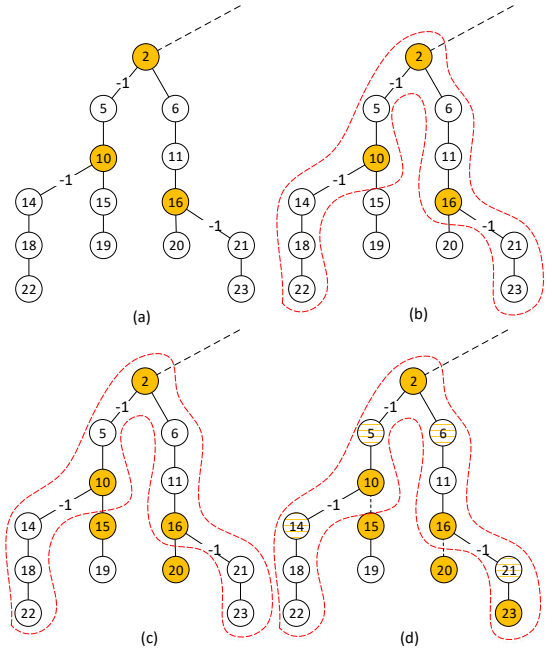

Figure 4-3. (a) The sub-tree of $\mathcal{G}$. (b) Identification of a sub-path graph. In (c) and (d), the leader group is updated based on Algorithm 4.1.

Therefore, the marked nodes in Fig. 4-2 and 4-3 indicate the final selection of leaders that can ensure network controllability with better average controllaiblity.

Remark 4.1. Note that Algorithm 4.1 is based on partitioning an acyclic graph into a set of sub-path graphs. There may exist different ways to partition an acyclic graph, resulting in different leader sets. In addition, the leader selection rules developed in Algorithm 4.1 are only sufficient conditions for network controllability. The selected leader group are by no means the optimal set, in terms of the minimum number of leaders or the best network performance.

4.4 Summary

In this Chapter, leader group selection on networked systems with signed acyclic graphs is investigated. Graph-inspired approaches are developed to facilitate the identification of leaders that can ensure network controllability and better network performance, i.e., better average controllability, required in network control. Since the current work is developed based on acyclic graphs, additional research will focus on extending the developed leader selection approach to general signed graphs.

CHAPTER 5
ENERGY-RELATED CONTROLLABILITY OF COMPLEX NETWORKS - COMPOSITE COMPLEX NETWORKS VIA GRAPH PRODUCT

This Chapter characterizes the energy-related controllability of composite complex networks. A class of composite networks constructed from simple factor networks via graph product are considered, such as Cartesian product, direct product, and strong product. The considered factor networks are leader-follower signed networks with neighbor-based Laplacian dynamics, adopting positive and negative edges to capture cooperative and competitive interactions among network units. Followed by Chapter 3 and Chapter 4, this Chapter investigates the energy-related controllability of composite networks. Specifically, controllability Gramian-based metrics, including average controllability, average control energy, and volumetric control energy, are characterized based on Cartesian graph product, which reveals how the energy-related controllability of a composite network can be inferred from the spectral properties of the local factor systems. These results are then extended to layered control networks, a special, yet widely used, network structure in many man-made systems. Besides Cartesian product, generalizations of the developed results based on direct and strong graph product are proposed. Since structural balance is a key topological property of signed networks, a necessary and sufficient condition to verify the structural balance of composite signed networks is developed, which is applicable to general graph product.

5.1 Preliminaries

5.1.1 Graph Product

Complex networks can be synthesized from a set of smaller size factor graphs via graph product [106]. In this section, typical graph products are introduced, which will be used as a main tool to characterize energy-related controllability of complex networks in the subsequent analysis. Consider two undirected graphs $\mathcal{G}_1 = (\mathcal{V}_1, \mathcal{E}_1, \mathcal{A}_1)$ and $\mathcal{G}_2 = (\mathcal{V}_2, \mathcal{E}_2, \mathcal{A}_2)$. In $\mathcal{G}_1$, $\mathcal{V}_1 = \{v_1^1, \dots v_n^1\}$ represents the set of n nodes, $\mathcal{E}_1 = \mathcal{V}_1 \times \mathcal{V}_1$ represents the edge set, and $\mathcal{A}_1 = \left[a_{ij}^1\right] \in \mathbb{R}^{n\times n}$ is the adjacency matrix with $a_{ij}^1 \neq 0$ if $\left(v_i^1, v_j^1\right) \in \mathcal{E}_1$ and $a_{ij}^1 = 0$ otherwise. The graph $\mathcal{G}_2$ is defined similarly with $\mathcal{V}_2 = \{v_1^2, \dots v_m^2\}$, $\mathcal{E}_2 = \mathcal{V}_2 \times \mathcal{V}_2$, and $\mathcal{A}_2 = \left[a_{ij}^2\right] \in \mathbb{R}^{m\times m}$.

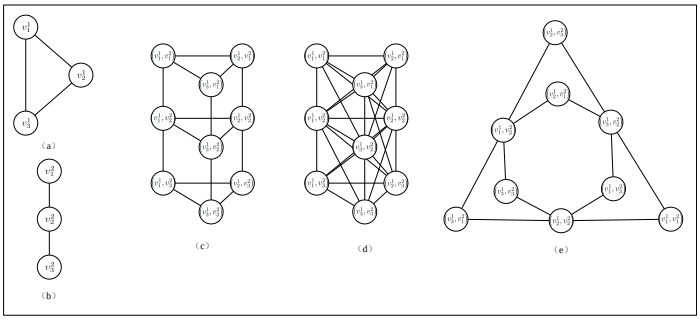

Figure 5-1. Factor graphs (a) and (b), and their product graph (c) $\mathcal{G}_1 \square \mathcal{G}_2$, (d) $\mathcal{G}_1 \times \mathcal{G}_2$, and (e) $\mathcal{G}_1 \boxtimes \mathcal{G}_2$.

Denoted by $\mathcal{G} = (\mathcal{V}, \mathcal{E}, \mathcal{A}) = \mathcal{G}_1 \triangle \mathcal{G}_2$, the composite graph constructed by the graph product of two factor graphs $\mathcal{G}_1$ and $\mathcal{G}_2$, where $\triangle$ denotes the generalized graph product. Among various product graphs, this work considers Cartesian product $\mathcal{G}_1 \square \mathcal{G}_2$, direct product[1] $\mathcal{G}_1 \times \mathcal{G}_2$, and strong product $\mathcal{G}_1 \boxtimes \mathcal{G}_2$, i.e., $\triangle \in \{\square, \times, \boxtimes\}$. Throughout the rest of this work, the general graph product $\triangle$ will be used if the developed result is applicable to any product of $\{\square, \times, \boxtimes\}$, otherwise specific graph product notation will be used. For the composite graph $\mathcal{G}$, the node set is denoted by $\mathcal{V}$ while the edge set $\mathcal{E}$ is defined according to the type of graph product used. Specifically, given two nodes $\left(v_i^1, v_p^2\right)$ and $\left(v_j^1, v_q^2\right)$ in $\mathcal{V}$, $i, j \in \{1, \ldots, n\}$ and $p, q \in \{1, \ldots, m\}$, the edges of different graph product are defined as follows:

-

- Cartesian Product $\mathcal{G}_1 \square \mathcal{G}_2$: $\left(\left(v_i^1, v_p^2\right), \left(v_j^1, v_q^2\right)\right) \in \mathcal{E}$ if and only if either $\left(v_i^1, v_j^1\right) \in \mathcal{E}_1$ and $v_p^2 = v_q^2$, or $\left(v_p^2, v_q^2\right) \in \mathcal{E}_2$ and $v_i^1 = v_j^1$.
- Direct Product $\mathcal{G}_1 \times \mathcal{G}_2$: $\left(\left(v_i^1, v_p^2\right), \left(v_j^1, v_q^2\right)\right) \in \mathcal{E}$ if and only if $\left(v_i^1, v_j^1\right) \in \mathcal{E}_1$ and $\left(v_p^2, v_q^2\right) \in \mathcal{E}_2$.
- Strong Product $\mathcal{G}_1 \boxtimes \mathcal{G}_2$: $\left(\left(v_i^1, v_p^2\right), \left(v_j^1, v_q^2\right)\right) \in \mathcal{E}$ if and only if $\left(v_i^1, v_j^1\right) \in \mathcal{E}_1$ and $v_p^2 = v_q^2$, or $\left(v_p^2, v_q^2\right) \in \mathcal{E}_2$ and $v_i^1 = v_j^1$, or $\left(v_i^1, v_j^1\right) \in \mathcal{E}_1$ and $\left(v_p^2, v_q^2\right) \in \mathcal{E}_2$.

[1] Direct product is also known as Kronecker product, tensor product, categorical product.

The non-zero entry $a_{((i,p),(j,q))}$ in $\mathcal{A} \in \mathbb{R}^{mn \times mn}$ corresponds to the edge $\left(\left(v_i^1, v_p^2\right), \left(v_j^1, v_q^2\right)\right)$ in $\mathcal{G}$, which is defined as

$$a_{((i,p),(j,q))} = \delta_{pq} a_{ij}^1 + \delta_{ij} a_{pq}^2,$$

where $\delta_{uv} = 1$ if $u = v$ and $\delta_{uv} = 0$ otherwise, and a_{ij}^1 and a_{pq}^2 are entries in $\mathcal{A}_1$ and $\mathcal{A}_2$ corresponding to $\left(v_i^1, v_j^1\right)$ and $\left(v_p^2, v_q^2\right)$, respectively. The strong product can be considered as the union of the Cartesian product and the direct product. Examples of Cartesian, direct, strong product are illustrated in Fig. 5-1. Note that these graph products are commutative and associative, i.e., $\mathcal{G}_1 \triangle \mathcal{G}_2$ and $\mathcal{G}_2 \triangle \mathcal{G}_1$ are isomorphic, and $(\mathcal{G}_1 \triangle \mathcal{G}_2) \triangle \mathcal{G}_3$ and $\mathcal{G}_1 \triangle (\mathcal{G}_2 \triangle \mathcal{G}_3)$ are isomorphic for any factor graphs $\mathcal{G}_1$, $\mathcal{G}_2$, $\mathcal{G}_3$.

5.1.2 Kronecker Product and Sum

Consider two matrices $A_1 \in \mathbb{R}^{n \times n}$ and $A_2 \in \mathbb{R}^{m \times m}$. The Kronecker product of A_1 and A_2 is denoted by $A_1 \otimes A_2 \in \mathbb{R}^{nm \times nm}$. Further, the Kronecker sum of of A_1 and A_2 is defined as $A_1 \oplus A_2 = A_1 \otimes I_m + I_n \otimes A_2$, where I_u is a $u \times u$ identity matrix. The Kronecker product has the following properties: $(A_1 \otimes A_2)(A_3 \otimes A_4) = (A_1 A_3) \otimes (A_2 A_4)$ and $e^{A_1 \oplus A_2} = e^{A_1} \otimes e^{A_2}$. The spectrum of matrix A is denoted as $\mathrm{eig}(A)$, i.e., the set of eigenvalues of A. More detailed treatment of Kronecker product and sum can be found in [107].

5.2 Problem formulation

5.2.1 Composite Complex System

This section shows how the leader-follower factor networks can be synthesized to represent a composite complex system. Consider a set of s leader-follower systems $(\mathcal{L}_i, B_i)$ evolving over factor graphs $\mathcal{G}_i$, $i = 1, \ldots, s$, respectively. According to (3–2), the dynamics of the ith factor system is

$$\dot{x}_i(t) = -\mathcal{L}_i x_i(t) + B_i u_i(t), \tag{5–1}$$

where $x_i(t) \in \mathbb{R}^{n_i}$ is the system state, $\mathcal{L}_i = \mathcal{L}(\mathcal{G}_i) \in \mathbb{R}^{n_i \times n_i}$ represents the associated graph Laplacian of $\mathcal{G}_i$, $B_i \in \mathbb{R}^{n_i \times m_i}$ represents the input matrix encoding the leaders, and $u_i(t) \in \mathbb{R}^{m_i}$ is the external input.

Based on the introduced graph product in Sect. 5.1.1, let $\mathcal{G} = \prod_{\triangle} \mathcal{G}_i$, be the composite graph constructed from the factor graphs $\mathcal{G}_i$, $i = 1, \ldots, s$. Provided that each $\mathcal{G}_i$ evolves according to (5–1), the composite dynamics $(\mathcal{L}, B)$ over $\mathcal{G}$ can be written as

$$\begin{aligned} \dot{x}(t) &= -\mathcal{L}\left(\prod_{\triangle} \mathcal{G}_i\right) x(t) + \left(\prod_{\otimes} B_i\right) u(t) \\ &= -\mathcal{L}(\mathcal{G})\, x(t) + Bu(t), \end{aligned} \tag{5–2}$$

where $x(t) \in \mathbb{R}^{\prod_{i=1}^{s} n_i}$ is the system state, $\mathcal{L} \in \mathbb{R}^{\prod_{i=1}^{s} n_i \times \prod_{i=1}^{s} n_i}$ is the graph Laplacian of $\mathcal{G}$, $B \in \mathbb{R}^{\prod_{i=1}^{s} n_i \times \prod_{i=1}^{s} m_i}$ represents the input matrix, and $u(t) \in \mathbb{R}^{\prod_{i=1}^{s} m_i}$ is the external input. The composite system $(\mathcal{L}, B)$ evolves over the composite graph $\mathcal{G}$ with B encoding the leaders inherited from $\mathcal{G}_i$, $i = 1, \ldots, s$. Specifically, given a leader set $\mathcal{K}_i$ in $\mathcal{G}_i$, if $B_i = B(\mathcal{K}_i)$ denotes the input matrix generated from $\mathcal{K}_i$, then the input matrix B of $\mathcal{G}$ can be written as $B = \prod_{\otimes} B(\mathcal{K}_i) = B(\mathcal{K})$, where $\mathcal{K} = \prod_{\times} \mathcal{K}_i$ represents the set of leaders in $\mathcal{G}$ [54].

Direct analysis of the energy-related controllability of a composite network can be challenging, if the composite network is of large size. Hence, the objective is to characterize the energy-related controllability of the composite system by inferring from its factor systems, taking advantage of the smaller size of the factor systems.

As a first attempt to this challenging problem, the subsequent development focuses on a composite system $(\mathcal{L}(\mathcal{G}), B)$ constructed by the graph product of two factor systems $(\mathcal{L}(\mathcal{G}_1), B_1)$ and $(\mathcal{L}(\mathcal{G}_2), B_2)$, where $\mathcal{G}_1$ and $\mathcal{G}_2$ are undirected signed graphs with n and m nodes, respectively. The case of two factor systems is adopted for the simplicity of presentation and is not restrictive, since a general composite system with many factor systems can be realized via sequential composition.

5.3 Energy-Related Controllability of Cartesian Product Graph

This section focuses on the characterizations of energy-related controllability of composite networks that are constructed via Cartesian product. The cases of direct and strong product will be considered in Section 5.5. To better explain the idea, we start from the case that each factor system contains a single leader. Specifically, consider two factor systems $(\mathcal{L}(\mathcal{G}_1), b_1)$

and $(\mathcal{L}(\mathcal{G}_2), b_2)$ with $b_1 = e_{l_1}$ and $b_2 = e_{l_2}$, where the basis vectors e_{l_1} and e_{l_2} indicate that v_{l_1} and v_{l_2} are the leaders in $\mathcal{G}_1$ and $\mathcal{G}_2$, respectively, and $l_1 \in \{1, \ldots, n\}$ and $l_2 \in \{1, \ldots, m\}$. By Cartesian product, the composite graph is constructed as $\mathcal{G} = \mathcal{G}_1 \square \mathcal{G}_2$. Since graph Laplacians belong to the family of symmetry preserving representations[2] , as proved in [54], $\mathcal{L}(\mathcal{G}_1 \square \mathcal{G}_2) = \mathcal{L}(\mathcal{G}_1) \oplus \mathcal{L}(\mathcal{G}_2)$. Hence, the dynamics of the composite system $(\mathcal{L}, b_l)$ can be written as

$$\begin{aligned} \dot{x}(t) &= -\mathcal{L}x(t) + b_l u(t) \\ &= -(\mathcal{L}_1 \oplus \mathcal{L}_2) x(t) + (e_{l_1} \otimes e_{l_2}) u(t), \end{aligned} \tag{5–3}$$

where the input vector $b_l = e_{l_1} \otimes e_{l_2} \in \mathbb{R}^{mn}$ determines the leader v_l in $\mathcal{G}$. Based on (5–3), average controllability, volumetric control energy, and average control energy are explored in the following sections to characterize the energy-related controllability of $(\mathcal{L}, b_l)$ based on its factor systems $(\mathcal{L}_1, b_1)$ and $(\mathcal{L}_2, b_2)$.

Different from unsigned graphs whose graph Laplacian is positive semi-definite by default, when considering signed networks, the graph Laplacian $\mathcal{L}$ can be either positive semi-definite (i.e., $\mathcal{G}$ is structurally balanced) or positive definite (i.e., $\mathcal{G}$ is structurally unbalanced) [2]. To streamline the work, the characterization of the structural balance of the composite graph based on its factor graphs is shown in Section 5.5. The subsequent development will focus on the cases that $\mathcal{G}$ is structurally unbalanced, i.e., $\mathrm{eig}(\mathcal{L})$ contains only positive eigenvalues. If $\mathcal{G}$ is structurally balanced, then, as shown in Chapter 3, a structurally balanced graph can be converted to an unsigned graph under gauge transformation [2], where many existing energy-related characterizations (cf. [108] and [31]) can be immediately applied. In addition, as shown in [38, 42, 109] and Chapter 3, the reduced graph Laplacian can be used, where the row and column associated with the zero eigenvalue are removed from the graph Laplacian, so that

[2] A matrix $\mathcal{L}(\mathcal{G})$ is symmetry preserving if, for all permutation $\sigma \in \mathrm{aut}(\mathcal{G})$, with the corresponding permutation matrix J, $\mathcal{L}(\mathcal{G}) J = J\mathcal{L}(\mathcal{G})$.

a structurally balanced graph can be treated as a structurally unbalanced graph via reduced Laplacian matrix when deriving Gramian-based energy metrics. Therefore, we mainly focus on the energy-related characterizations of structurally unbalanced graphs, which can be extended to balanced graphs logically.

5.3.1 Characterizations of Average Controllability

Before characterizing the average controllability of the composite system $(\mathcal{L}, b_l)$ in (5–3), the following lemma from [110] is introduced.

Lemma 5.1. *Consider two factor graphs $\mathcal{G}_1$ and $\mathcal{G}_2$ with n and m nodes, respectively. Given the Cartesian product graph $\mathcal{G} = \mathcal{G}_1 \square \mathcal{G}_2$, the graph Laplacian $\mathcal{L}(\mathcal{G})$ takes the form of $\mathcal{L} = \mathcal{L}_1 \oplus \mathcal{L}_2 = \mathcal{L}_1 \otimes I_m + I_n \otimes \mathcal{L}_2$, where $\mathcal{L}_1$ and $\mathcal{L}_2$ are the graph Laplacian of $\mathcal{G}_1$ and $\mathcal{G}_2$, respectively. The eigenvalues λ_k and eigenvectors u_k of $\mathcal{L}$ are defined as $\lambda_k = \mu_i + \eta_j$ and $u_k = \vartheta_i \otimes w_j$ for $k = 1, \dots mn$, where (μ_i, ϑ_i), $i = 1, \dots, n$, and (η_j, w_j), $j = 1, \dots m$, represent the eigenpairs of $\mathcal{L}_1$ and $\mathcal{L}_2$, respectively.*

Lemma 5.1 shows how the eigenpairs of $\mathcal{L}$ can be constructed from the eigenpairs of $\mathcal{L}_1$ and $\mathcal{L}_2$. Based on Lemma 5.1, the following theorem characterizes the average controllability of $(\mathcal{L}, b_l)$.

Theorem 5.1. *Provided two factor systems $(\mathcal{L}(\mathcal{G}_1), b_1)$ and $(\mathcal{L}(\mathcal{G}_2), b_2)$, the average controllability of the composite system $(\mathcal{L}(\mathcal{G}_1 \square \mathcal{G}_2), b_l)$ in (5–3) can be characterized as*

$$\operatorname{tr}(\mathcal{W}) = \sum_{i=1}^{n} \sum_{j=1}^{m} \frac{1}{2(\mu_i + \eta_j)} \vartheta_{l_1,i}^2 w_{l_2,j}^2, \tag{5–4}$$

where $\mathcal{W}$ is the controllability Gramian of $(\mathcal{L}, b_l)$, and (μ_i, ϑ_i) for $i = 1, \dots, n$ and (η_j, w_j) for $j = 1, \dots m$ are the eigenpairs of $\mathcal{L}_1$ and $\mathcal{L}_2$, respectively.

Proof. Consider the composite system $(\mathcal{L}, b_l)$. Since $\mathcal{L}$ is symmetric, it can be written as $\mathcal{L} = U \Lambda U^T \in \mathbb{R}^{mn \times mn}$, where $\Lambda = \operatorname{diag}\{\lambda_1, \dots, \lambda_{mn}\} \in \mathbb{R}^{mn \times mn}$ is a diagonal matrix containing the eigenvalues of $\mathcal{L}$ and $U = \begin{bmatrix} u_1 & \cdots & u_{mn} \end{bmatrix} \in \mathbb{R}^{mn \times mn}$ is the orthogonal eigenvector matrix of $\mathcal{L}$. Based on (5–3) and using the fact that $e^{-\mathcal{L}\tau} = e^{-U\Lambda U^T \tau} = U e^{-\Lambda \tau} U^T$,

the controllability Gramian can be written as

$$\mathcal{W} = \int_0^\infty e^{-\mathcal{L}\tau} b_l b_l^T e^{-\mathcal{L}\tau} d\tau = U \Gamma U^T, \tag{5–5}$$

where

$$\Gamma = \int_0^\infty e^{-\Lambda\tau} U^T b_l b_l^T U e^{-\Lambda\tau} d\tau. \tag{5–6}$$

From (5–6), the ijth entry of Γ is

$$\Gamma_{i,j} = \int_0^\infty e^{-\lambda_i\tau - \lambda_j\tau} u_{l,i} u_{l,j} d\tau = \frac{1}{\lambda_i + \lambda_j} u_{l,i} u_{l,j}, \tag{5–7}$$

where $u_{l,i}$ and $u_{l,j}$ are the lith and ljth entries of U, respectively.

Since the trace is invariant under cyclic permutations, from (5–5), the average controllability of $(\mathcal{L}, b_l)$ is

$$\mathrm{tr}\left(\mathcal{W}\right) = \mathrm{tr}\left(U\Gamma U^T\right) = \mathrm{tr}\left(\Gamma U^T U\right). \tag{5–8}$$

Substituting (5–7) into (5–8) and using Lemma 5.1,

$$\begin{aligned} \mathrm{tr}\left(\mathcal{W}\right) &= \mathrm{tr}\left(\Gamma\right) \\ &= \sum_{k=1}^{mn} \frac{1}{2\lambda_k} u_{l,k}^2 \\ &= \sum_{i=1}^{n} \sum_{j=1}^{m} \frac{1}{2\left(\mu_i + \eta_j\right)} \vartheta_{l_1,i}^2 w_{l_2,j}^2, \end{aligned} \tag{5–9}$$

where ϑ_{l_1} and w_{l_2} are the l_1th and l_2th rows of the eigenvector matrices of $\mathcal{G}_1$ and $\mathcal{G}_2$, respectively, corresponding to the leader node v_{l_1} and v_{l_2}. □

A key observation from Theorem 5.1 is that, for a Cartesian product composite graph with a single leader, the average controllability can be inferred from the eigenvalues of the factor graph Laplacian and the associated rows of the eigenvector matrices corresponding to the leaders. In other words, the average controllability of a complex large-scale network can be analyzed based on its relatively simple factor systems. To further clarity, suppose a composite graph Laplacian $\mathcal{L}$ has a dimension of $mn \times mn$ with its factor graph Laplacians $\mathcal{L}_1$ and $\mathcal{L}_2$ of size $n \times n$ and $m \times m$.

Instead of analyzing $\mathcal{L}$ of large size mn, Theorem 5.1 provides a practical means to characterize $\mathrm{tr}\left(\mathcal{W}\right)$ only based on the eigenvalues and eigenvectors of $\mathcal{L}_1$ and $\mathcal{L}_2$. Thus, offering a bottom up approach to reveal the properties of a global system from its local systems.

The discovered relationship between the average controllability of the composite system and its factor systems in Theorem 5.1 also paves a way to leader selection problems, specifically, identification of a leader in the given network that improves average controllability of the leader-follower system. For instance, provided a composite system $\left(\mathcal{L}\left(\mathcal{G}\right), b_l\right)$ formed by the Cartesian product of two factor systems $\left(\mathcal{L}\left(\mathcal{G}_1\right), b_1\right)$ and $\left(\mathcal{L}\left(\mathcal{G}_2\right), b_2\right)$, we are interested in identifying a leader node in $\mathcal{G}$ such that the average controllability of $(\mathcal{L}, b_l)$ is maximized. By Theorem 5.1, the average controllability $\mathrm{tr}\left(\mathcal{W}\right)$ in (5–8) depends on the eigenvalues of $\mathcal{L}_1$ and $\mathcal{L}_2$ and the associated rows of the eigenvector matrices corresponding to the selected leaders. Note that the eigenvalues in (5–9) are determined by the topological structures of $\mathcal{G}_1$ and $\mathcal{G}_2$, and are independent of the leader selection process. Therefore, we can individually select leaders in $\mathcal{G}_1$ and $\mathcal{G}_2$ such that their corresponding entries of the eigenvector matrices yield the maximum $\mathrm{tr}\left(\mathcal{W}\right)$.

Based on the discussion above, the following corollary is an immediate result of Theorem 5.1.

Corollary 5.1. *Consider a composite system $\left(\mathcal{L}\left(\mathcal{G}_1 \square \mathcal{G}_2\right), b_l\right)$ constructed by two factor systems $\left(\mathcal{L}\left(\mathcal{G}_1\right), b_1\right)$ and $\left(\mathcal{L}\left(\mathcal{G}_2\right), b_2\right)$. Determining b_l (i.e., selecting a leader node v_l in $\mathcal{G}$) to maximize the average controllability of $(\mathcal{L}, b_l)$ is equivalent to determining b_1 and b_2 (i.e., selecting the leaders v_{l_1} and v_{l_2} in $\mathcal{G}_1$ and $\mathcal{G}_2$, respectively) such that the average controllability of $(\mathcal{L}_1, b_1)$ and $(\mathcal{L}_2, b_2)$ are individually maximized.*

Based on the single leader case in Theorem 5.1, the following theorem considers multi-leader cases.

Theorem 5.2. *Consider two factor systems $\left(\mathcal{L}\left(\mathcal{G}_1\right), B_1\right)$ and $\left(\mathcal{L}\left(\mathcal{G}_2\right), B_2\right)$, where $\mathcal{G}_1$ has n nodes with p leaders and $\mathcal{G}_2$ has m nodes with q leaders, i.e., $B_1 = \begin{bmatrix} e_{l_1^1} & \cdots & e_{l_p^1} \end{bmatrix} \in \mathbb{R}^{n\times p}$ and $B_2 = \begin{bmatrix} e_{l_1^2} & \cdots & e_{l_q^2} \end{bmatrix} \in \mathbb{R}^{m\times q}$ where the basis vector e_i, $i \in \left\{l_1^1, \ldots, l_p^1\right\}$, and e_j,*

$j \in \{l_1^2, \ldots, l_q^2\}$, *indicate the leader nodes* v_i *and* v_j *in* $\mathcal{G}_1$ *and* $\mathcal{G}_2$*, respectively. The average controllability of the composite system* $(\mathcal{L}(\mathcal{G}_1 \square \mathcal{G}_2), B)$ *can be characterized as in (5–12).*

Proof. From (5–2), $B = B_1 \otimes B_2 = \begin{bmatrix} e_{l_1} & \cdots & e_{l_{pq}} \end{bmatrix} \in \mathbb{R}^{nm \times pq}$. Let $\mathcal{K} = \{l_1, \ldots, l_{pq}\}$ be the leader indices of $\mathcal{G}$. Replacing b_l in (5–5) by B, the controllability Gramian of $(\mathcal{L}(\mathcal{G}), B)$ is given by

$$\mathcal{W} = \int_0^\infty e^{-\mathcal{L}\tau} B B^T e^{-\mathcal{L}\tau} d\tau = U \Gamma U^T, \tag{5–10}$$

where $\Gamma = \int_0^\infty e^{-\Lambda\tau} U^T B B^T U e^{-\Lambda\tau} d\tau$ with $\Gamma \in \mathbb{R}^{mn \times mn}$ and $U \in \mathbb{R}^{mn \times mn}$ as defined in (5–6). From (5–8) and (5–10), the average controllability of $(\mathcal{L}(\mathcal{G}), B)$ can be written as

$$\begin{aligned} \operatorname{tr}(\mathcal{W}) &= \operatorname{tr}(\Gamma) \\ &= \int_0^\infty e^{-2\lambda_1 \tau} \sum_{k \in \mathcal{K}} u_{k,1}^2 + \cdots + e^{-2\lambda_{mn}\tau} \sum_{k \in \mathcal{K}} u_{k,mn}^2 d\tau \end{aligned} \tag{5–11}$$

where $u_{i,j}$ represents the ijth entry of U. Since $\int_0^\infty e^{-2\lambda_i \tau} d\tau = \frac{1}{2\lambda_i}$, (5–11) can be further simplified into

$$\operatorname{tr}(\mathcal{W}) = \sum_{k \in \mathcal{K}} \sum_{i=1}^{mn} \frac{1}{2\lambda_i} u_{k,i}^2.$$

Using Lemma 5.1,

$$\operatorname{tr}(\mathcal{W}) = \sum_{k=1}^{p} \sum_{l=1}^{q} \sum_{i=1}^{n} \sum_{j=1}^{m} \frac{1}{2(\mu_i + \eta_j)} \vartheta_{l_k^1, i}^2 w_{l_l^2, j}^2. \tag{5–12}$$

where $\vartheta_{l_k^1}$ and $w_{l_l^2}$ are the l_k^1th and l_l^2th rows of the eigenvector matrices of $\mathcal{G}_1$ and $\mathcal{G}_2$, respectively, corresponding to the leader node $v_{l_k^1}$ and $v_{l_l^2}$. □

Following similar discussion, Theorem 5.2 indicates that, for a Cartesian product composite system with multiple leaders, its average controllability can also be inferred from the eigenvalues of the factor graph Laplacians and the associated rows of the eigenvector matrices corresponding to the leaders.

5.3.2 Characterizations of Volumetric Control Energy

This section characterizes the volumetric control energy of the composite system $(\mathcal{L}, b_l)$ based on its factor systems $(\mathcal{L}_1, b_1)$ and $(\mathcal{L}_2, b_2)$.

Theorem 5.3. *Consider two factor systems* $(\mathcal{L}(\mathcal{G}_1), b_1)$ *and* $(\mathcal{L}(\mathcal{G}_2), b_2)$ *and its corresponding composite system* $(\mathcal{L}(\mathcal{G}_1 \square \mathcal{G}_2), b_l)$ *in (5–3), where* $\mathcal{G}_1$ *has* n *nodes and* $\mathcal{G}_2$ *has* m *nodes. The volumetric control energy* $\log\det\mathcal{W}$ *of the composite system can be characterized as*

$$\log\det\mathcal{W} = m\log\det\mathcal{W}_1 + n\log\det\mathcal{W}_2 + c,$$

where $\mathcal{W}$*,* $\mathcal{W}_1$*, and* $\mathcal{W}_2$ *are controllability Gramians of the systems* $(\mathcal{L}, b_l)$*,* $(\mathcal{L}_1, b_1)$*, and* $(\mathcal{L}_2, b_2)$*, respectively, and* $c = \log\det\overline{\Gamma} - m\log\det\overline{\Gamma}_1 - n\log\det\overline{\Gamma}_2$ *is a constant determined by* $\mathrm{eig}(\mathcal{L}_1)$ *and* $\mathrm{eig}(\mathcal{L}_2)$*.*

Proof. From (5–5), the volumetric control energy of $(\mathcal{L}, b_l)$ can be written as

$$\begin{aligned}\log\det\mathcal{W} &= \log\left(\det U\det\Gamma\det U^T\right)\\ &= \log\det\Gamma,\end{aligned} \tag{5–13}$$

where $\det U\det U^T = 1$ is used since U is an orthogonal matrix. From (5–7), Γ can be rewritten as $\Gamma = \overline{U\Gamma U}$, where $\overline{U} = \mathrm{diag}\{u_{l,1}, u_{l,2}, \ldots, u_{l,mn}\}$ and $\overline{\Gamma} = \left[\overline{\Gamma}_{ij}\right] \in \mathbb{R}^{mn\times mn}$ with $\overline{\Gamma}_{ij} = \frac{1}{\lambda_i+\lambda_j}$. Based on $\overline{\Gamma}$, $\overline{U}$, and (5–13),

$$\begin{aligned}\log\det\mathcal{W} &= \log\left(\det\overline{U}\det\overline{\Gamma}\det\overline{U}\right)\\ &= 2\sum_{i=1}^{mn}\log u_{l,i} + \log\det\overline{\Gamma}.\end{aligned} \tag{5–14}$$

Expressions, similar to (5–14), can be obtained for factor systems $(\mathcal{L}_1, b_1)$ and $(\mathcal{L}_2, b_2)$ as

$$\log\det\mathcal{W}_1 = \log\det\left(\overline{V}\overline{\Gamma}_1\overline{V}\right) = 2\sum_{i=1}^{n}\log\vartheta_{l_1,i} + \log\det\overline{\Gamma}_1$$

and

$$\log\det\mathcal{W}_2 = \log\det\left(\overline{W}\overline{\Gamma}_2\overline{W}\right) = 2\sum_{i=1}^{m}\log w_{l_2,i} + \log\det\overline{\Gamma}_2,$$

where $\overline{V} = \mathrm{diag}\{\vartheta_{l_1,1}, \vartheta_{l_1,2}, \ldots, \vartheta_{l_1,n}\}$, $\overline{\Gamma}_1 \in \mathbb{R}^{n\times n}$ with the ijth entry $\left(\overline{\Gamma}_1\right)_{ij} = \frac{1}{\mu_i+\mu_j}$ for $i, j \in \{1, \ldots, n\}$, $\overline{W} = \mathrm{diag}\{w_{l_2,1}, w_{l_2,2}, \ldots, w_{l_2,m}\}$, and $\overline{\Gamma}_2 \in \mathbb{R}^{m\times m}$ with the ijth entry $\left(\overline{\Gamma}_2\right)_{ij} = \frac{1}{\eta_i+\eta_j}$ for $i, j \in \{1, \ldots, m\}$.

By Lemma 5.1, $\overline{U} = \overline{V} \otimes \overline{W}$, and the fact that $\det\left(\overline{V} \otimes \overline{W}\right) = \left(\det \overline{V}\right)^m \left(\det \overline{W}\right)^n$, $\log\det \mathcal{W}$ in (5–14) can be written in terms of $\log\det \mathcal{W}_1$ and $\log\det \mathcal{W}_2$ as

$$\begin{aligned}
\log\det \mathcal{W} =& \log\left(\det\left(\overline{V} \otimes \overline{W}\right) \det \overline{\Gamma} \det\left(\overline{V} \otimes \overline{W}\right)\right) \\
=& \log\left(\det \overline{V}\right)^{2m} + \log\left(\det \overline{W}\right)^{2n} + \log\det \overline{\Gamma} \\
=& 2m \sum_{j=1}^{n} \log \vartheta_{l_1,j} + 2n \sum_{k=1}^{m} \log w_{l_2,k} + \log\det \overline{\Gamma} \\
=& m \log\det \mathcal{W}_1 - m \log\det \overline{\Gamma}_1 \\
&+ n \log\det \mathcal{W}_2 - n \log\det \overline{\Gamma}_2 + \log\det \overline{\Gamma},
\end{aligned}$$

which completes the proof. □

Theorem 5.3 indicates that the volumetric control energy of a composite system $(\mathcal{L}, b_l)$ can be inferred from that of its factor systems, i.e., $\log\det \mathcal{W}_1$ and $\log\det \mathcal{W}_2$, and a constant c. Note that $\overline{\Gamma}_1$ and $\overline{\Gamma}_2$ are defined based on $\mathrm{eig}\left(\mathcal{L}_1\right)$ and $\mathrm{eig}\left(\mathcal{L}_2\right)$, respectively, and, by Lemma 5.1, $\overline{\Gamma}$ also depends on $\mathrm{eig}\left(\mathcal{L}_1\right)$ and $\mathrm{eig}\left(\mathcal{L}_2\right)$. As a result, c is a constant determined by $\mathcal{L}_1$ and $\mathcal{L}_2$. In addition, since the selection of leader nodes (i.e., design of b_1 and b_2) does not affect $\mathcal{L}_1$ and $\mathcal{L}_2$, Theorem 5.3 implies that, if the volumetric control energy of the factor systems is individually maximized then the volumetric control energy of the composite system is maximum. In addition, any change in the volumetric control energy of the composite system can be computed precisely from the change in the volumetric control energy of factor systems. This provides a means for network design, where local factor systems can be individually designed for improved volumetric control energy of the composite system.

Theorem 5.3 can be extended for a multi-leader case. Suppose that $\mathcal{G}_1$ has p leaders and $\mathcal{G}_2$ has q leaders, i.e., $B_1 = \begin{bmatrix} e_{l_1^1} & \cdots & e_{l_p^1} \end{bmatrix} \in \mathbb{R}^{n\times p}$ and $B_2 = \begin{bmatrix} e_{l_1^2} & \cdots & e_{l_q^2} \end{bmatrix} \in \mathbb{R}^{m\times q}$. Let $\left(\mathcal{L}\left(\mathcal{G}\right), B\right)$ be the composite system formed by the Cartesian product of $\left(\mathcal{L}\left(\mathcal{G}_1\right), B_1\right)$ and $\left(\mathcal{L}\left(\mathcal{G}_2\right), B_2\right)$, where $B = B_1 \otimes B_2 = \begin{bmatrix} e_{l_1} & \cdots & e_{l_{pq}} \end{bmatrix} \in \mathbb{R}^{nm\times pq}$. Denote by $\mathcal{K} = \{l_1, \ldots, l_{pq}\}$ the leader indices of $\mathcal{G}$. Following similar analysis as in the proof of Theorem 5.2, one has $\log\det \mathcal{W} = \log\det\left(U\Gamma U^T\right) = \log\det \Gamma$, where $\Gamma = \int_0^\infty e^{-\Lambda\tau} U^T B B^T U e^{-\Lambda\tau} d\tau$ with

$\Lambda = \operatorname{diag}\{\lambda_1, \ldots, \lambda_{mn}\} \in \mathbb{R}^{mn\times mn}$ and $U = \begin{bmatrix} u_1 & \cdots & u_{mn} \end{bmatrix} \in \mathbb{R}^{mn\times mn}$ being the eigenvalue and eigenvector matrix of $\mathcal{L}(\mathcal{G})$, respectively. Substituting B into (5–6), the ijth entry of Γ can be written as

$$\Gamma_{ij} = \frac{\sum_{k\in\mathcal{K}} u_{k,i}u_{k,j}}{\lambda_i + \lambda_j}, . \tag{5–15}$$

where u_k, $k \in \mathcal{K}$, represents the eigenvector of $\mathcal{L}$ corresponding to the leaders. Since any eigenpair (λ_i, u_i) in (5–15) can be replaced by the eigenpairs of $\mathcal{L}_1$ and $\mathcal{L}_2$ using Lemma 5.1, it is evident that the volumetric control energy $\log\det\mathcal{W}$ of $(\mathcal{L}(\mathcal{G}), B)$ with multiple leaders can be inferred from its factor systems (i.e., the eigenvalues and the eigenvectors corresponding to the leaders of $\mathcal{L}_1$ and $\mathcal{L}_2$, respectively). However, unlike Theorem 5.3, derivation of volumetric control energy in terms of eigenvalues and eigenvectors of $\mathcal{L}_1$ and $\mathcal{L}_2$ is more involved when considering a multi-leader case. Ongoing research aims to characterize how factor systems individually contribute to the volumetric control energy of the composite system.

In leader selection problems, it is generally assumed that the underlying topology is fixed and we can only select leaders such that the resulting leader-follower network has certain desired properties (e.g., controllability). However, the network properties can be further improved by designing the network's topological structure (i.e., the graph Laplacian). To this end, we provide insights into how the network topology can be modified for improved volumetric control energy. The subsequent development is based on the following assumption that the graph Laplacian $\mathcal{L}$ of the composite graph $\mathcal{G}$ has distinct eigenvalues.

Theorem 5.4. *Consider two factor systems $(\mathcal{L}_1, b_1)$ and $(\mathcal{L}_2, b_2)$ and its corresponding composite system $(\mathcal{L}, b_l)$ in (5–3). If Assumption* **??** *is satisfied, the volumetric control energy $\log\det\mathcal{W}$ of $(\mathcal{L}, b_l)$ can be characterized as in (5–18).*

Proof. From (5–14), $\log\det\mathcal{W}$ depends on $\sum_{i=1}^{mn}\log u_{l,i}$ and $\log\det\overline{\Gamma}$. Since $\mathcal{L}$ has distinct eigenvalues, $\overline{\Gamma}$ is indeed a Cauchy matrix and Γ is a Cauchy-like matrix [111]. The determinant of the Cauchy matrix $\overline{\Gamma}$ is

$$\det\overline{\Gamma} = \frac{\prod_{1\le i_1<i_2\le mn}(\lambda_{i_2} - \lambda_{i_1})^2}{\prod_{1\le i_1,i_2\le mn}(\lambda_{i_1} + \lambda_{i_2})}, \tag{5–16}$$

which indicates

$$\begin{aligned}\log\det\overline{\Gamma} =& 2\sum_{1\le i_1<i_2\le mn}\log|\lambda_{i_1}-\lambda_{i_2}|\\ &-\sum_{1\le i_1,i_2\le mn}\log\left(\lambda_{i_1}+\lambda_{i_2}\right),\end{aligned}\tag{5–17}$$

where λ_{i_1} and λ_{i_2}, $i_i, i_2 \in \{1,\dots,mn\}$, are the eigenvalues of $\mathcal{L}$. Based on (5–14) and (5–17) and using Lemma 5.1, the volumetric control energy of $(\mathcal{L}, b_l)$ can be rewritten as

$$\log\det\mathcal{W} = \Delta - \Theta + 2\sum_{i=1}^{mn}\log u_{l,i}\tag{5–18}$$

where $u_{l,i}$ represents the lith entry of the eigenvector matrix U corresponding to the leader v_l,

$$\Delta = 2\sum_{1\le j_1<j_2\le n}\sum_{1\le k_1<k_2\le m}\log|\mu_{j_1}+\eta_{k_1}-\mu_{j_2}-\eta_{k_2}|,$$

and

$$\Theta = \sum_{1\le j_1,j_2\le n}\sum_{1\le k_1,k_2\le m}\log\left(\mu_{j_1}+\eta_{k_1}+\mu_{j_2}+\eta_{k_2}\right),$$

where μ_{j_1} and μ_{j_2}, $j_1, j_2 \in \{1,\dots,n\}$ are the eigenvalues of $\mathcal{L}_1$, and η_{k_1} and η_{k_2}, $k_1, k_2 \in \{1,\dots,m\}$ are the eigenvalues of $\mathcal{L}_2$. □

Theorem 5.4 indicates that $\log\det\mathcal{W}$ of the composite system are closely related to the spectral distribution of $\mathcal{L}_1$ and $\mathcal{L}_2$. Specifically, the term Δ in (5–18) tends to increase if $\mathrm{eig}\,(\mathcal{L}_1)$ and $\mathrm{eig}\,(\mathcal{L}_2)$ are distributed less centralized such that the difference between $\mu_{j_1}-\mu_{j_2}$ and $\eta_{k_1}-\eta_{k_2}$ is large. The term Θ tends to decrease if the spectral distribution of $\mathcal{L}_1$ and $\mathcal{L}_2$ is close to the origin (i.e., $\mathrm{eig}\,(\mathcal{L}_1)$ and $\mathrm{eig}\,(\mathcal{L}_2)$ have smaller magnitude). Therefore, the volumetric control energy of $\mathcal{G}$ can be improved, if the topology of $\mathcal{G}_1$ and $\mathcal{G}_2$ is designed such that their spectral distribution lead to a large Δ and small Θ. Note that the term $\log u_{l,i}$ in (5–18) depends on the selection of the leader. Once $\mathcal{G}_1$ and $\mathcal{G}_2$ are designed, a leader can be selected to further improve the volumetric control energy.

5.3.3 Characterizations of Average Control Energy

In this section, the properties of Cauchy matrix are utilized to characterize the average control energy of the composite system $(\mathcal{L}, b_l)$ based on its factor systems $(\mathcal{L}_1, b_1)$ and $(\mathcal{L}_2, b_2)$.

Theorem 5.5. *Consider two factor systems* $(\mathcal{L}(\mathcal{G}_1), b_1)$ *and* $(\mathcal{L}(\mathcal{G}_2), b_2)$ *and the corresponding composite system* $(\mathcal{L}(\mathcal{G}), b_l)$ *with* $\mathcal{G} = \mathcal{G}_1 \square \mathcal{G}_2$. *If Assumption* **??** *is satisfied, the average control energy* $\mathrm{tr}(\mathcal{W}^{-1})$ *of the composite system* $(\mathcal{L}, b_l)$ *can be characterized as in (5–20).*

Proof. Based on (5–5), the average control energy $\mathrm{tr}(\mathcal{W}^{-1})$ of $(\mathcal{L}, b_l)$ can be written as

$$\mathrm{tr}\left(\mathcal{W}^{-1}\right) = \mathrm{tr}\left(U\Gamma^{-1}U^T\right) = \mathrm{tr}\left(\Gamma^{-1}\right). \tag{5–19}$$

Since Γ is a Cauchy-like matrix, following [111], the entries of its inverse are

$$\Gamma_{ij}^{-1} = \frac{(\lambda_j + \lambda_i)\prod_{k=1,k\neq i,j}^{mn}(\lambda_j + \lambda_k)(\lambda_k + \lambda_i)}{u_{l,i}u_{l,j}\left(\prod_{k=1,k\neq j}^{mn}(\lambda_j - \lambda_k)\right)\left(\prod_{k=1,k\neq i}^{mn}(\lambda_i - \lambda_k)\right)},$$

which indicates the diagonal entries of Γ^{-1} are

$$\Gamma_{ii}^{-1} = 2\lambda_i \frac{\prod_{j\neq i}(\lambda_i + \lambda_j)^2}{u_{l,i}^2\prod_{j\neq i}(\lambda_i - \lambda_j)^2}.$$

Based on (5–19) and Lemma 5.1,

$$\begin{aligned}\mathrm{tr}\left(\mathcal{W}^{-1}\right) &= \sum_{i=1}^{mn} 2\lambda_i \frac{\prod_{j\neq i}(\lambda_i + \lambda_j)^2}{u_{l,i}^2\prod_{j\neq i}(\lambda_i - \lambda_j)^2} \\ &= \sum_{p=1}^{n}\sum_{k=1}^{m} \frac{2(\mu_p + \eta_k)\prod_{q\neq p, r\neq k}(\mu_p + \mu_q + \eta_k + \eta_r)^2}{(\vartheta_{l_1,p}w_{l_2,k})^2\prod_{q\neq p, r\neq k}(\mu_p - \mu_q + \eta_k - \eta_r)^2},\end{aligned} \tag{5–20}$$

where, by Lemma 5.1, $\lambda_i = \mu_p + \eta_k$, $\lambda_j = \mu_q + \eta_r$ and $u_l = \vartheta_{l_1} \otimes w_{l_2}$ with $p, q = 1, \ldots, n$, $k, r = 1, \ldots, m$, $i, j = 1, \ldots, mn$ are used. □

Similar to Theorem 5.4, Theorem 5.5 also indicates that $\mathrm{tr}(\mathcal{W}^{-1})$ is closely related to the spectral distribution of $\mathcal{L}_1$ and $\mathcal{L}_2$.

Remark 5.1. Theorem 5.4 and 5.5 provide insights into how the spectral distribution of local factor systems can potentially influence the energy-related controllability of the global composite system. However, further research is warranted to help improve understanding of the energy-related controllability of complex composite systems. Specifically, Theorem 5.4 could be extended to characterize the individual contribution of each factor system to the volumetric

control energy of the composite system, and Theorem 5.5 could be further developed to consider multi-leader cases. Nevertheless, Theorem 5.4 and 5.5 open a new door to designing network topological structures for improved energy efficiency by considering the spectral distribution of factor systems, where many existing results can be potentially leveraged. For instance, the work of [49] considered design of network structures based on the spectral distribution of its adjacency matrix, such that the designed network requires minimum control energy. In [33], the average control energy of a network was characterized based on clustering of the eigenvalues of the system matrix in the state space. These results can be leveraged to facilitate the design of factor systems so that they have desired spectral distributions.

5.4 Energy-Related Controllability of Layered Control Networks

Energy-related measures, i.e., average controllability, volumetric control energy, and average control energy, are characterized in Section 5.3. This section extends these characterizations to a special, yet widely used, class of networked systems, namely layered control networks. A layered control network is referred to a class of composite networks constructed by Cartesian graph product, where the composite system has repeated control structure of a factor system. Specifically, consider two factor systems $(\mathcal{L}(\mathcal{G}_1), B_1)$ and $(\mathcal{L}(\mathcal{G}_2), B_2)$, and a composite system $(\mathcal{L}(\mathcal{G} = \mathcal{G}_1 \square \mathcal{G}_2), B)$. If the composite input matrix is $B = I_n \otimes B_2$, the form of the input matrix B_2 is repeated in every $\mathcal{G}_2$ layer of the product graph $\mathcal{G}_1 \square \mathcal{G}_2$. In such networks, each layer shares the same topology of the factor graph $\mathcal{G}_2$ and the layers are connected through the topology of the factor graph $\mathcal{G}_1$. An illustrative example is provided in Fig. 5-2. Many practical applications feature layered control network, such as fault detection [112], quantum computing networks [113], and smart sensor networks [114]. Although layered control networks have been partially investigated in literature, control energy-related properties of layered control networks remains largely unattended, which motivates the research in this section.

Similar to the analysis in Section 5.3, we start with the single leader case. By the definition of layered control network, the dynamics of the composite system $(\mathcal{L}, B)$ is

$$\begin{aligned}\dot{x}(t) =& -\mathcal{L}x(t) + Bu(t) \\ =& -(\mathcal{L}_1 \oplus \mathcal{L}_2)x(t) + (I_n \otimes b_{l_2})u(t),\end{aligned} \tag{5–21}$$

where $(\mathcal{L}_1, I_n)$ and $(\mathcal{L}_2, b_{l_2})$ represent the factor systems over $\mathcal{G}_1$ and $\mathcal{G}_2$, respectively, and b_{l_2} indicates the v_{l_2} in $\mathcal{G}_2$ is the leader. It is worth pointing out that the following development also applies to the composite system $(\mathcal{L}, B)$ constructed by $(\mathcal{L}_1, b_{l_1})$ and $(\mathcal{L}_2, I_n)$ with $B = b_{l_1} \otimes I_n$, due to the permutation equivalence property of the Kronecker product.

Lemma 5.2. *Consider a composite layered control system $(\mathcal{L}(\mathcal{G}), B)$ with $\mathcal{G} = \mathcal{G}_1 \square \mathcal{G}_2$ and $B = I_n \otimes b_{l_2}$, where $\mathcal{G}_1$ and $\mathcal{G}_2$ are the factor graphs and b_{l_2} is the input matrix associated with $\mathcal{G}_2$. The controllability Gramian $\mathcal{W}$ of $(\mathcal{L}, B)$ in (5–21) is*

$$\mathcal{W}(t) = (V \otimes W)\Psi\left(V^T \otimes W^T\right),$$

where $\Psi = \operatorname{diag}\{\Psi_1, \Psi_2, \ldots, \Psi_n\}$ with $(\Psi_k)_{ij} = \frac{w_{l_2,i} w_{l_2,j}}{2\mu_k + \eta_i + \eta_j}$, $k = 1, \ldots, n$, $i, j = 1, \ldots, m$, where μ_k and η_i are the eigenvalues and $V = [\vartheta_{ij}] \in \mathbb{R}^{n\times n}$ and $W = [w_{ij}] \in \mathbb{R}^{m\times m}$ are the eigenvector matrices of $\mathcal{L}_1$ and $\mathcal{L}_2$, respectively.

Proof. Based on (5–5),

$$\begin{aligned}\mathcal{W} =& \int_0^\infty e^{-\mathcal{L}\tau} B B^T e^{-\mathcal{L}\tau} d\tau \\ =& U\left(\int_0^\infty e^{-\Lambda\tau} U^T B B^T U e^{-\Lambda\tau} d\tau\right) U^T d\tau,\end{aligned} \tag{5–22}$$

where U and Λ are the eigenvector and eigenvalue matrices of $\mathcal{L}$, respectively. Since $U = V \otimes W$, (5–22) can be expanded as

$$\begin{aligned}\mathcal{W} =& V \otimes W(\int_0^\infty e^{-\Lambda\tau}\left(V^T \otimes W^T\right)\left(I_n \otimes b_{l_2}\right)\\ &\cdot \left(I_n^T \otimes b_{l_2}^T\right)\left(V \otimes W\right)e^{-\Lambda\tau}d\tau)V^T \otimes W^T\\ =& V \otimes W(\int_0^\infty e^{-\Lambda\tau}\left(V^T I_n I_n^T V\right)\\ &\otimes \left(W^T b_{l_2} b_{l_2}^T W\right)e^{-\Lambda\tau}d\tau)V^T \otimes W^T\\ =& \left(V \otimes W\right)\Psi\left(V^T \otimes W^T\right)\end{aligned}$$

where

$$\Psi = \int_0^\infty e^{-\Lambda\tau} I_n \otimes \left(W^T b_{l_2} b_{l_2}^T W\right) e^{-\Lambda\tau} d\tau.$$

Define $\overline{\Psi} = \operatorname{diag}\left\{\overline{\Psi}_1, \overline{\Psi}_2, \ldots, \overline{\Psi}_n\right\} = I_n \otimes \left(W^T b_{l_2} b_{l_2}^T W\right) \in \mathbb{R}^{mn \times mn}$, which is a block diagonal matrix with $\overline{\Psi}_i = w_{l_2,:}^T w_{l_2,:} \in \mathbb{R}^{m \times m}$ for $i = 1, \ldots, n$, where $w_{l_2,:} \in \mathbb{R}^m$ is the l_2th row of W. Thus, $\Psi = \operatorname{diag}\left\{\Psi_1, \Psi_2, \ldots, \Psi_n\right\} \in \mathbb{R}^{mn \times mn}$ is also a block diagonal matrix with $\Psi_i = \int_0^\infty e^{-\Lambda_i \tau}\overline{\Psi}_i e^{-\Lambda_i \tau} d\tau \in \mathbb{R}^{m \times m}$ for $i = 1, \ldots, n$, where Λ is rewritten as $\Lambda = \operatorname{diag}\left\{\Lambda_1, \Lambda_2, \ldots, \Lambda_n\right\}$ with the diagonal entries of $\Lambda_i \in \mathbb{R}^{m \times m}$ indicating the $((i-1)\,m+1)$th to kmth eigenvalues of $\mathcal{L}$. Let λ_i^k denote the ith diagonal entry of Λ_k. Then, the entries of the kth block Ψ_k can be represented as

$$\left(\Psi_k\right)_{ij} = \frac{w_{l_2,i} w_{l_2,j}}{\lambda_i^k + \lambda_j^k} = \frac{w_{l_2,i} w_{l_2,j}}{2\mu_k + \eta_i + \eta_j}, \tag{5–23}$$

where $\lambda_i^k = \mu_k + \eta_i$ and $\lambda_j^k = \mu_k + \eta_j$ from Lemma 5.1 are used, where μ_k, $k = 1, \ldots n$ is the eigenvalue of $\mathcal{L}_1$ while η_i and η_j for $i, j = 1, \ldots, m$ are the eigenvalues of $\mathcal{L}_2$. □

Based on the controllability Gramian developed in Lemma 5.2, energy-related measures are characterized in the following theorem.

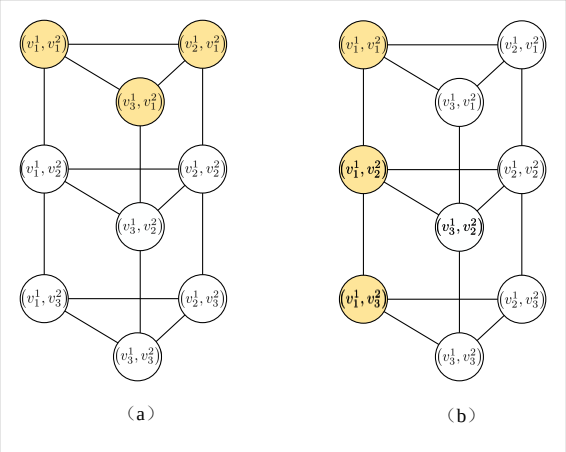

Figure 5-2. An example of layered control network, where leaders are marked in yellow. (a) $\mathcal{G}_1$ with $B_1 = I_3$, (b) $\mathcal{G}_2$ with $B_2 = \begin{bmatrix} 1 & 0 & 0 \end{bmatrix}^T$, (c) $\mathcal{G}_1 \square \mathcal{G}_2$ with $B = I_3 \otimes B_2$.

Theorem 5.6. *Consider a composite layered control system* $(\mathcal{L}(\mathcal{G}_1 \square \mathcal{G}_2), B)$ *with* $B = I_n \otimes b_{l_2}$, *where* $\mathcal{G}_1$ *and* $\mathcal{G}_2$ *are the factor graphs and* b_{l_2} *is the input matrix associated with* $\mathcal{G}_2$ *with* v_{l_2} *being the leader. The average controllability of* $(\mathcal{L}, B)$ *is characterized as in (5–24) and the volumetric control energy of* $(\mathcal{L}, B)$ *is characterized as in (5–25).*

Proof. First consider the average controllability of the composite layered control system $(\mathcal{L}(\mathcal{G}), B)$, where $\mathcal{G} = \mathcal{G}_1 \square \mathcal{G}_2$. Since the trace is invariant under cyclic permutations, based on Lemma 5.2, the average controllability of the system $(\mathcal{L}(\mathcal{G}), B)$ can be represented as

$$\begin{aligned} \operatorname{tr}(\mathcal{W}) &= \operatorname{tr}\left((V \otimes W)\,\Psi\left(V^T \otimes W^T\right)\right) \\ &= \operatorname{tr}(\Psi) \\ &= \sum_{k=1}^{n} \operatorname{tr}(\Psi_k). \end{aligned}$$

Using (5–23) yields the following:

$$\operatorname{tr}(\Psi_k) = \sum_{j=1}^{m} \frac{w_{l_2,j}^2}{2(\mu_k + \eta_j)}.$$

Thus, the average controllability of the composite layered control system $(\mathcal{L}(\mathcal{G}), B)$ is

$$\operatorname{tr}(\mathcal{W}) = \sum_{k=1}^{n} \sum_{j=1}^{m} \frac{w_{l_2,j}^2}{2(\mu_k + \eta_j)}, \tag{5–24}$$

where $w_{l_2,j}$ represents the $l_2 j$th entry of the eigenvector matrix W, μ_k, $k = 1, \ldots n$, is the eigenvalue of $\mathcal{L}_1$, and η_j, $j = 1, \ldots, m$, is the eigenvalue of $\mathcal{L}_2$.

The volumetric control energy of the composite layered system $(\mathcal{L}(\mathcal{G}), B)$, based on Theorem 5.2, is

$$\begin{aligned} \log\det(\mathcal{W}) &= \log\det\left((V \otimes W)\,\Psi\left(V^T \otimes W^T\right)\right) \\ &= \log\det(\Psi) \\ &= \sum_{k=1}^{n} \log\det(\Psi_k), \end{aligned}$$

where Ψ_k is defined in (5–23). Similar to (5–14), one has

$$\begin{aligned} \log\det(\Psi_k) &= \log\det\left(\overline{W}\Gamma_k\overline{W}\right) \\ &= 2\sum_{i=1}^{m} \log w_{l_2,i} + \log\det(\Gamma_k), \end{aligned}$$

where $\overline{W}$ is defined in Theorem 5.3 and $\Gamma_k \in \mathbb{R}^{m\times m}$ with the ijth entry $(\Gamma_k)_{ij} = \frac{1}{2\mu_k+\eta_i+\eta_j}$ for $k = 1, \ldots n$, $i, j = 1, \ldots, m$. Since the term $2\sum_{i=1}^{m} \log w_{l_2,i}$ appears in $\log\det(\Psi_k)$ for each k, using $\log\det\mathcal{W}_2 = 2\sum_{i=1}^{m} \log w_{l_2,i} + \log\det\overline{\Gamma}_2$ from Theorem 5.3 yields

$$\begin{aligned} \log\det(\mathcal{W}) =& 2n\sum_{i=1}^{m} \log w_{l_2,i} + \sum_{k=1}^{n} \log\det(\Gamma_k) \\ =& n\log\det\mathcal{W}_2 + c_1, \end{aligned} \tag{5–25}$$

where $c_1 = -n\log\det\overline{\Gamma}_2 + \sum_{k=1}^{n} \log\det(\Gamma_k)$. □

Theorem 5.6 indicates that the energy-related controllability of the composite layered network can be determined by the eigenvalues of the factor systems (i.e., $\operatorname{eig}(\mathcal{L}_1)$ and $\operatorname{eig}(\mathcal{L}_2)$) and the l_2th row of W corresponding to the leader node v_{l_2} in $\mathcal{G}_2$. If the topology of $\mathcal{G}_1$ and $\mathcal{G}_2$ are fixed, as shown in (5–25), the volumetric control energy $\log\det(\mathcal{W})$ of the composite layered

control network is fully determined by the volumetric control energy of (L_2, b_{l_2}), i.e., $\log\det \mathcal{W}_2$. As discussed before, this provides us not only a way to characterize the energy expenditure of composite layered networks from local factor systems, but also insights into design factor systems such that the composite layered network can have improved energy efficiency.

Theorem 5.6 can be trivially extended to multi-leader cases. To see that, consider a composite layered control system $(\mathcal{L}(\mathcal{G}), B)$ with the input matrix $B = I_n \otimes B_2$, where $B_2 = \begin{bmatrix} e_{l_1^2} & \cdots & e_{l_{m_2}^2} \end{bmatrix} \in \mathbb{R}^{m\times m_2}$ indicates $\mathcal{G}_2$ contains a set of m_2 leaders indexed by l_i^2, $i = 1, \ldots, m_2$. Based on Lemma 5.2, the controllability Gramian of $(\mathcal{L}(\mathcal{G}), B)$ with multiple leaders can be written as

$$\mathcal{W} = (V \otimes W)\, \widetilde{\Psi}\, \left(V^T \otimes W^T\right), \tag{5–26}$$

where $\widetilde{\Psi} = \int_0^\infty e^{-\Lambda\tau} I_n \otimes \left(W^T B_2 B_2^T W\right) e^{-\Lambda\tau} d\tau$. Similar to the proof of Lemma 5.2, $\widetilde{\Psi} = \operatorname{diag}\left\{\widetilde{\Psi}_1, \widetilde{\Psi}_2, \ldots, \widetilde{\Psi}_n\right\}$ is a diagonal matrix with ijth entry of each block $\widetilde{\Psi}_k$, $k = 1, \ldots, n$, defined as

$$\left(\widetilde{\Psi}_k\right)_{ij} = \frac{w_{l_1^2,i} w_{l_1^2,j} + w_{l_2^2,i} w_{l_2^2,j} + \cdots + w_{l_{m_2}^2,i} w_{l_{m_2}^2,j}}{2\mu_k + \eta_i + \eta_j}. \tag{5–27}$$

Since $\operatorname{tr}(\mathcal{W})$ and $\log\det(\mathcal{W})$ are defined based on $\mathcal{W}$ given in (5–26) and (5–27), following similar analysis as in Theorem 5.8, it is straightforward to show that the $\operatorname{tr}(\mathcal{W})$ and $\log\det(\mathcal{W})$ of $(\mathcal{L}(\mathcal{G}), B)$ can be inferred from the eigenvalues and the eigenvector matrices of the factor systems.

5.5 Extensions to More Graph Products

Other than Cartesian product, composite systems can also be constructed based on direct and strong product of factor systems. This section provides a few extensions of the results developed in previous sections. In section 5.5.1, we first develop a necessary and sufficient condition to characterize the structural balance of signed composite networks by its factor networks, which is generally applicable to Cartesian, direct, and strong graph product. In Section 5.5.2, the average controllability of Cartesian product is compared to that of strong product.

5.5.1 Structural Balance of General Product Graphs

This section investigates the structural properties of the general product graph $\mathcal{G} = \mathcal{G}_1 \triangle \mathcal{G}_2$, where $\mathcal{G}_1 = (\mathcal{V}_1, \mathcal{E}_1, \mathcal{A}_1)$ and $\mathcal{G}_2 = (\mathcal{V}_2, \mathcal{E}_2, \mathcal{A}_2)$ are factor graphs as defined in Section 5.1.1.

Def. 2.2 indicates that structural balance of $\mathcal{G}$ can be characterized based on its adjacency matrix $\mathcal{A}$. When considering generalized graph product $\triangle$, as indicated in [57],

$$\begin{aligned} \mathcal{A} &= \mathcal{A}\left(\mathcal{G}_1 \triangle \mathcal{G}_2\right) \\ &= \alpha_1 \mathcal{A}_1 \otimes I_m + \alpha_2 I_n \otimes \mathcal{A}_2 + \alpha_3 \mathcal{A}_1 \otimes \mathcal{A}_2 \end{aligned} \tag{5–28}$$

where $\alpha_1, \alpha_2, \alpha_3 \in \{0, 1\}$. Different graph products can be realized through different combinations of α_i for $i = 1, 2, 3$. For instance, the adjacency matrix $\mathcal{A}$ of Cartesian product $\square$, direct product $\times$, and strong product $\boxtimes$, can be realized if $[\alpha_1, \alpha_2, \alpha_3]$ take the value of $[1, 1, 0]$, $[0, 0, 1]$, and $[1, 1, 1]$, respectively[3] . Although structural balance has proven to be invariant under Cartesian product $\mathcal{G}_1 \square \mathcal{G}_2$ in [56], Theorem 5.7 extends the result in [56] to the generalized product graph $\mathcal{G}_1 \triangle \mathcal{G}_2$ via gauge transformation.

Theorem 5.7. *Consider two signed graphs $\mathcal{G}_1 = (\mathcal{V}_1, \mathcal{E}_1, \mathcal{A}_1)$ and $\mathcal{G}_2 = (\mathcal{V}_2, \mathcal{E}_2, \mathcal{A}_2)$. The generalized product graph $\mathcal{G} = \mathcal{G}_1 \triangle \mathcal{G}_2 = (\mathcal{V}, \mathcal{E}, \mathcal{A})$ is structurally balanced if and only if $\mathcal{G}_1$ and $\mathcal{G}_2$ are structurally balanced.*

Proof. To obtain the necessary condition, suppose $\mathcal{G}_1$ and $\mathcal{G}_2$ are two structurally balanced signed graphs. According to lemma 3.1, there exist gauge transformation matrices Φ_1 and Φ_2 such that

[3] Other product graphs such as skew product and converse skew product can be obtained when the vector takes the value $[0, 1, 1]$ and $[1, 0, 1]$, respectively.

$\Phi_1\mathcal{A}_1\Phi_1$ and $\Phi_2\mathcal{A}_2\Phi_2$ have non-negative entries. Defining a diagonal matrix $\Phi = \Phi_1 \otimes \Phi_2$,

$$\begin{aligned}\Phi\mathcal{A}\Phi =& (\Phi_1 \otimes \Phi_2)(\alpha_1\mathcal{A}_1 \otimes I_m + \alpha_2 I_n \otimes \mathcal{A}_2 \\ &+\alpha_3\mathcal{A}_1 \otimes \mathcal{A}_2)(\Phi_1 \otimes \Phi_2) \\ =&\alpha_1\Phi_1\mathcal{A}_1\Phi_1 \otimes I_m + \alpha_2 I_n \otimes \Phi_2\mathcal{A}_2\Phi_2, \\ &+ \alpha_3(\Phi_1\mathcal{A}_1\Phi_1) \otimes (\Phi_2\mathcal{A}_2\Phi_2),\end{aligned}$$

where the fact that $\Phi_1\Phi_1 = I_n$ and $\Phi_2\Phi_2 = I_m$ are used. Since $\alpha_1, \alpha_2, \alpha_2 \in \{0, 1\}$, it can be shown that $\alpha_1\Phi_1\mathcal{A}_1\Phi_1 \otimes I_m$, $\alpha_2 I_n \otimes \Phi_2\mathcal{A}_2\Phi_2$, and $\alpha_3(\Phi_1\mathcal{A}_1\Phi_1) \otimes (\Phi_2\mathcal{A}_2\Phi_2)$ have non-negative entries. Therefore $\Phi\mathcal{A}\Phi$ is structurally balanced with the gauge transformation matrix Φ by lemma 3.1.

To show the sufficient condition, suppose the product graph $\mathcal{G}$ is structurally balanced. By lemma 3.1, there exists a gauge transformation matrix Φ such that $\Phi\mathcal{A}\Phi$ has non-negative entries. Assuming that $\Phi = \Phi_1 \otimes \Phi_2$ yields

$$\begin{aligned}\Phi\mathcal{A}\Phi =&\alpha_1\Phi\mathcal{A}_1 \otimes I_m\Phi + \alpha_2\Phi I_n \otimes \mathcal{A}_2\Phi + \alpha_3\Phi\mathcal{A}_1 \otimes \mathcal{A}_2\Phi \\ =&\alpha_1\Phi_1\mathcal{A}_1\Phi_1 \otimes I_m + \alpha_2 I_n \otimes \Phi_2\mathcal{A}_2\Phi_2, \\ &+ \alpha_3(\Phi_1\mathcal{A}_1\Phi_1) \otimes (\Phi_2\mathcal{A}_2\Phi_2),\end{aligned}$$

where Φ_1 and Φ_2 are diagonal matrices with with ± 1 as the diagonal entries. It can be verified there is no overlap of non-zero entries among the matrices $\Phi_1\mathcal{A}_1\Phi_1 \otimes I_m$, $I_n \otimes \Phi_2\mathcal{A}_2\Phi_2$, and $(\Phi_1\mathcal{A}_1\Phi_1) \otimes (\Phi_2\mathcal{A}_2\Phi_2)$. If $\Phi\mathcal{A}\Phi$ only has non-negative entries, the entries of $\Phi_1\mathcal{A}_1\Phi_1 \otimes I_m$, $I_n \otimes \Phi_2\mathcal{A}_2\Phi_2$, $(\Phi_1\mathcal{A}_1\Phi_1) \otimes (\Phi_2\mathcal{A}_2\Phi_2)$ must be all non-negative, indicating Φ_1 and Φ_2 are the gauge transformation matrices of $\mathcal{A}_1$ and $\mathcal{A}_2$, respectively. Therefore, both $\mathcal{G}_1$and $\mathcal{G}_2$ are structurally balanced by lemma 3.1. □

Theorem 5.7 indicates that the structural balance of the composite network $\mathcal{G}$ can be efficiently determined by only investigating the structural balance properties of its factor graphs. Although only two factor graphs are considered, Theorem 5.7 can be trivially extended for the

case of multiple factor graphs. That is, $\mathcal{G} = \prod_{\triangle} \mathcal{G}_i$ is structurally balanced if and only if every $\mathcal{G}_i$ is structurally balanced. To see that, we can rewrite $\mathcal{G}$ as $\mathcal{G} = ((\mathcal{G}_1 \triangle \mathcal{G}_2) \triangle \mathcal{G}_3) \triangle \prod_{i \geq 4} \mathcal{G}_i$. By repeatedly invoking Theorem 5.7, it is straightforward to conclude that $\mathcal{G}_1 \triangle \mathcal{G}_2$ is structurally balanced, which leads to $(\mathcal{G}_1 \triangle \mathcal{G}_2) \triangle \mathcal{G}_3$ being structurally balanced, and thus it can be shown that the entire product $\prod_{\triangle} \mathcal{G}_i$ is structurally balanced.

Remark 5.2. In the case of direct product, it is possible that the product graph $\mathcal{G}$ becomes unconnected even if the factor graphs $\mathcal{G}_1$ and $\mathcal{G}_2$ are connected. For such cases, Theorem 5.7 applies to each connected component of $\mathcal{G}$, i.e., each connected component is structurally balanced if and only if the factor graphs $\mathcal{G}_1$ and $\mathcal{G}_2$ are structurally balanced. The proof is straightforward and thus omitted here. In addition, $\Phi \mathcal{A} \Phi$ can be reorganized into a block diagonal matrix via graph automorphism, where the blocks capture individually connected components. Thus, the gauge transformation matrix Φ can be partitioned naturally corresponding to each block, i.e., each connected component is associated with a gauge transformation corresponding to a block matrix in $\mathcal{A}$ to yield structural balance.

5.5.2 Direct and Strong Product

Extensions of the developed results to other types of graph product are discussed in this section. In particular, we will consider the direct and strong product of regular factor graphs[4] with a single leader. The characterizations of the eigenvalues of the direct and strong product from [115] are first introduced.

Lemma 5.3. *Consider a r-regular graph $\mathcal{G}_1$ with n nodes and a s-regular graph $\mathcal{G}_2$ with m nodes. Denote by $\mathcal{L}_{\times}$ and $\mathcal{L}_{\boxtimes}$ the graph Laplacian of $\mathcal{G}_1 \times \mathcal{G}_2$ and $\mathcal{G}_1 \boxtimes \mathcal{G}_2$, respectively. Let (μ_i, ϑ_i), $i = 1, \ldots, n$, and (η_j, w_j), $j = 1, \ldots, m$, represent the eigenpairs of $\mathcal{L}_1$ and $\mathcal{L}_2$, respectively. Then $(r\mu_i + s\eta_j - \mu_i\eta_j, \vartheta_i w_j)$ and $((r+1)\mu_i + (s+1)\eta_j - \mu_i\eta_j, \vartheta_i w_j)$ are the eigenpairs of $\mathcal{L}_{\times}$ and $\mathcal{L}_{\boxtimes}$, respectively.*

[4] A regular graph is a graph where each vertex has the same number of neighbors.

It is worth pointing out that, when considering regular factor graphs with a single leader, most results developed in previous sections for Cartesian product can be extended to the cases of direct and strong graph product by simply using Lemma 5.3, instead of Lemma 5.1, to replace the eigenpairs of $\mathcal{L}$ by that of $\mathcal{L}_1$ and $\mathcal{L}_2$. Besides characterizing the energy-related measures of a composite system formed by different graph product, it is also of interest to compare these measures among different graph products. Due to restricted space, we will take average controllability as an example and compare it between strong and Cartesian graph product.

Theorem 5.8. *Consider a dynamic system $(\mathcal{L}_1, b_{l_1})$ over a r-regular graph $\mathcal{G}_1$ with n nodes and a dynamic system $(\mathcal{L}_2, b_{l_2})$ over a s-regular graph $\mathcal{G}_2$ with m nodes, where b_{l_1} and b_{l_2} indicate the leader v_{l_1} and v_{l_2} in $\mathcal{G}_1$ and $\mathcal{G}_2$, respectively. Denote by $(\mathcal{L}_\boxtimes, b_l)$ the composite system formed by the strong graph product and $(\mathcal{L}_\square, b_l)$ formed by the Cartesian graph product, where $b_l = b_{l_1} \otimes b_{l_2}$ indicates the leader in the composite graph $\mathcal{G}$. Then, the average controllability of $(\mathcal{L}_\boxtimes, b_l)$ is always less than that of $(\mathcal{L}_\square, b_l)$.*

Proof. Let $\mathcal{W}_\square$ and $\mathcal{W}_\boxtimes$ represent the controllability Gramian of $(\mathcal{L}_\square, b_l)$ and $(\mathcal{L}_\boxtimes, b_l)$, respectively. From (5–9), the average controllability of the composite system is

$$\operatorname{tr}(\mathcal{W}) = \sum_{k=1}^{mn} \frac{1}{2\lambda_k} u_{l,k}^2,$$

where λ_k, $k = 1, \ldots, mn$, are the eigenvalues of the graph Laplacian of $\mathcal{G}$ and u_l is the lth row of U. When considering strong product $\mathcal{G} = \mathcal{G}_1 \boxtimes \mathcal{G}_2$, by Lemma 5.3, one has

$$\operatorname{tr}(\mathcal{W}_\boxtimes) = \sum_{i=1}^{n} \sum_{j=1}^{m} \frac{\vartheta_{l,i}^2 w_{l,j}^2}{2\left((r+1)\mu_i + (s+1)\eta_j - \mu_i \eta_j\right)}.$$

Recall from Theorem 5.1 that

$$\operatorname{tr}(\mathcal{W}_\square) = \sum_{i=1}^{n} \sum_{j=1}^{m} \frac{1}{2(\mu_i + \eta_j)} \vartheta_{l,i}^2 w_{l,j}^2.$$

Comparing the ijth entry between $\mathrm{tr}\left(\mathcal{W}_{\boxtimes}\right)$ and $\mathrm{tr}\left(\mathcal{W}_{\square}\right)$, one has

$$\begin{aligned}(r+1)\,\mu_i+(s+1)\,\eta_j-\mu_i\eta_j &= (\mu_i+\eta_j)\\ &\quad+(r\mu_i+s\eta_j-\mu_i\eta_j)\\ &\geq (\mu_i+\eta_j)\,.\end{aligned}$$

The inequality $r\mu_i+s\eta_j-\mu_i\eta_j\geq 0$ is always true, since $r\mu_i+s\eta_j-\mu_i\eta_j$ is an eigenvalue of $\mathcal{L}_{\times}$ and $\mathcal{L}_{\times}$ is at least positive semi-definite by definition[5] . Hence, we have $\mathrm{tr}\left(\mathcal{W}_{\square}\right)\geq\mathrm{tr}\left(\mathcal{W}_{\boxtimes}\right)$. □

Based on Lemma 5.3 and following similar analysis as in the proof of Theorem 5.8, it can also be shown that the average controllability of $(\mathcal{L}_{\boxtimes},b_l)$ is always less than that of $(\mathcal{L}_{\times},b_l)$. The strong product graph $\mathcal{G}_1\boxtimes\mathcal{G}_2$ can be considered as the union of the Cartesian product graph $\mathcal{G}_1\square\mathcal{G}_2$ and the direct product graph $\mathcal{G}_1\times\mathcal{G}_2$, and thus has more edge connections. However, Theorem 5.8 indicates that, when considering regular factor graphs, the average controllability of the composite graph can decrease with more edge connections. In other words, the composite system can become less controllable (i.e., requiring more control energy) even if the composite graph is more connected. A similar research finding was reported in [116], which reveals that increasing edges in a leader-follower network may not necessarily improve network controllability. For instance, consider a complete unsigned graph in which any two nodes are connected. Controlling a complete graph with n nodes requires at least $n-1$ leaders to ensure network controllability. As a complement to the results in [116], Theorem 5.8 provides an energy-related perspective revealing how the network controllability, in terms of energy expenditure, can be influenced with increase in edges.

[5] The graph Laplacian $\mathcal{L}_{\boxtimes}$ is positive semi-definite if $\mathcal{G}=\mathcal{G}_1\boxtimes\mathcal{G}_2$ is structurally balanced, and positive definite if $\mathcal{G}$ is structurally unbalanced.

5.6 Summary

Energy-related controllability measures, i.e., average controllability, average control energy, and volumetric control energy, are characterized via graph product approaches in this work. It is revealed that the energy-related controllability of a composite network can be inferred from the spectral properties of the local factor systems. These results are extended to layered control networks and also to general graph products, including Cartesian, direct, and strong product. Besides the characterizations of the energy-related controllability, a necessary and sufficient condition to verify the structural balance of a signed network is developed, which is applicable to general graph product.

Although the current work provides an energy-related perspective to characterize the controllability of complex composite networks, this work is far from complete. There are many interesting problems demanding further investigation. For instance, the developed results can be potentially used for network design or leader selection for improved energy efficiency. However, the designed network or selected leaders are not guaranteed to ensure classical network controllability. An interesting problem is to consider joint network design considering both energy efficiency and classical network controllability, where the results in [54] can be potentially leveraged. In addition, as discussed in Section 5.3, it is unclear how the volumetric control energy of a composite system with multiple leaders can be characterized in terms of individual factor systems, and how the characterizations of the average control energy can be extended to multi-leader cases. Future research will continue to address these open problems.

CHAPTER 6
HERDABILITY OF COMPLEX NETWORKS - CONTROLLABLE SUBSPACE AND GENERALIZED EQUITABLE PARTITION

Chapter 2-5 focus on developing results to ensure controllability and energy-related controllability of complex networks. Herdability, as a variant of controllability, is an indicator of the ability to drive system states to a specific subset of the state space. This Chapter characterizes the controllable subspace and herdability of signed complex networks. As in Chapter 2-5, a dynamic signed leader-follower network is considered. Motivated by practical applications, the systems states are required to be driven by the leaders to be element-wise above a positive threshold, i.e., a specific subset rather than the entire state space as in classical controllability. Graph equitable partitions are exploited to characterize the controllable subspace of the system, from which sufficient conditions are derived to render the system herdable. It is revealed that the quotient graph can be used to infer the herdability of the original graph, wherein criteria of the herdability of quotient graphs are developed based on positive systems. Examples are provided to illustrate the developed topological characterizations.

6.1 Problem Formulation

Consider a networked system modeled by an undirected signed weighted graph $\mathcal{G} = (\mathcal{V}, \mathcal{E}, \mathcal{A})$, where $\mathcal{V} = \{v_1, \ldots, v_n\}$ denotes the node set and $\mathcal{E} \subset \mathcal{V} \times \mathcal{V}$ denotes the edge set. The interactions between nodes are captured by the weighted adjacency matrix $\mathcal{A} = [a_{ij}] \in \mathbb{R}^{n\times n}$, where $a_{ij} \neq 0$ if $(v_j, v_i) \in \mathcal{E}$ and $a_{ij} = 0$ otherwise. Differing from Chapter 2-5, self-loops are allowed in this work, i.e., $a_{ii} \neq 0$ for some $i \in \mathcal{V}$. The weight $a_{ij} \in \mathbb{R}$ takes real numbers, where $a_{ij} \in \mathbb{R}^+$ and $a_{ij} \in \mathbb{R}^-$ represent cooperative and antagonistic interactions between node v_i and v_j in the network, respectively. Let $\mathcal{A}_{:,i}$ and $\mathcal{A}_{i,:}$ denote the ith column and ith row of $\mathcal{A}$, respectively. The neighbor of node v_i is defined as $\mathcal{N}_i = \{v_j | (v_j, v_i) \in \mathcal{E}\}$ and the node degree of v_i is defined as $\beta_i = \sum_{j\in\mathcal{N}_i} a_{ij}$. The subsequent sections will show that the designed node degree β_i facilitates characterization of the controllable space and herdability of signed graphs.

Let $x(t) = \begin{bmatrix} x_1(t) & \ldots & x_n(t) \end{bmatrix}^T \in \mathbb{R}^n$ denote the stacked system states of the network $\mathcal{G}$, where each entry $x_i(t) \in \mathbb{R}$ represents the state of node v_i. It is assumed that a subset $\mathcal{V}_l \subseteq \mathcal{V}$

of m nodes, referred to as leaders in the network, can be endowed with external controls. The remaining nodes $\mathcal{V}_f = \mathcal{V} \setminus \mathcal{V}_l$ are referred to as followers with $\mathcal{V}_l \cap \mathcal{V}_f = \emptyset$. Without loss of generality, the leaders' and the followers' indices are assumed to be $\mathcal{V}_l = \{1, \dots m\}$ and $\mathcal{V}_f = \{m+1, \dots n\}$. Suppose the system states evolve according to the linear dynamics

$$\dot{x}(t) = \mathcal{A}x(t) + Bu(t), \tag{6–1}$$

where $\mathcal{A} \in \mathbb{R}^{n \times n}$ is the adjacency matrix, $B = \begin{bmatrix} e_1 & \dots & e_m \end{bmatrix} \in \mathbb{R}^{n \times m}$ is the input matrix with basis vectors e_i, $i = 1, \dots, m$, indicating that the ith node is endowed with external controls $u(t) \in \mathbb{R}^m$. Differing from results in Chapter 2-5 that consider Laplacian dynamics, the dynamics (6–1) depends on the adjacency matrix $\mathcal{A}$, indicating a direct influence of the underlying network topology on the system dynamics.

The herdability of the system (6–1) is defined as follows.

Definition 6.1. [72] A networked system with dynamics in (1) is d-herdable if, for any $x(0) \in \mathbb{R}^n$, the system state $x(t)$ can be driven by a control input $u(t)$ to the set $H_d = \left\{ x = [x_1 \dots x_n]^T \in \mathbb{R}^n : x_i \geq d \right\}$ in finite time, where d is an arbitrary positive threshold.

Definition 6.1 implies a network is d-herdable if its states can be driven to a specific subset H_d of the state space. Throughout this Chapter, the herdability of the system (6–1) is particularly referred to as the d-herdability. Recall that the controllability matrix $\mathcal{C} = \begin{bmatrix} B & \mathcal{A}B & \cdots & \mathcal{A}^{n-1}B \end{bmatrix}$ indicates the controllable subspace of a system [117]. Therefore, the system (6–1) is completely controllable, if the controllability matrix $\mathcal{C} = \begin{bmatrix} B & \mathcal{A}B & \cdots & \mathcal{A}^{n-1}B \end{bmatrix}$ has full row rank. Since this work concerns driving $x(t)$ to H_d, the following lemma shows how the herdability of a system relates to the controllability matrix.

Lemma 6.1. *[69] A networked system with dynamics in (6–1) is d-herdable if and only if there exists an element-wise positive vector $k \in \mathrm{img}(\mathcal{C})$, where $\mathrm{img}(\cdot)$ represents the range space of a matrix.*

As indicated in Lemma 6.1, the network herdability depends on the range space of the controllability matrix $\mathcal{C}$, which is closely related to the adjacency matrix $\mathcal{A}$ of the network.

Motivated by this observation, the objective of this work is to develop characterizations of network herdability and its controllable subspace from graph topological perspectives.

6.2 Characterizations of Controllable Subspace

This section presents topological characterizations of controllable subspaces of systems captured by (6–1). Graph partition is used as the primary tool in exploring how network topology influences the herdability of signed networks. Particularly, Section 6.2.1 generalizes the classical definition of equitable partition of unsigned graphs to signed weighted graphs, and Section 6.2.2 characterizes the controllable subspace of system (6–1). Section 6.2.3 discusses the construction of equitable partitions of leader-follower signed weighted graphs.

6.2.1 Generalized Equitable Partition

A graph can be partitioned into a set of cells, where each cell is a subset of the nodes. Let $\pi\colon \mathcal{V} \to \{C_1, C_2, \cdots, C_r\}$ denote a map that partitions the node set $\mathcal{V}$ into a set of distinct cells C_i, $i = 1, \ldots, r$, where $\cup_{i=1}^{r} C_i = \mathcal{V}$ and $C_i \cap C_j = \emptyset$ for $i \neq j$. Let $\beta_\pi(C_j, v_i) = \sum_{k \in \mathcal{N}_i \cap C_j} a_{ik}$ denote the cell-to-node degree of v_i from C_j under the partition π. Based on the partition π, we can construct a quotient graph $\mathcal{G}/\pi = (\mathcal{V}_\pi, \mathcal{E}_\pi, \mathcal{A}_\pi)$, where each cell C_i is treated as a node in $\mathcal{V}_\pi$ and $(C_j, C_i) \in \mathcal{E}_\pi$ represents a directed edge from C_j to C_i. Denote by $\mathcal{A}_\pi = \left[a_{ij}^\pi\right] \in \mathbb{R}^{r \times r}$ the adjacency matrix of the quotient graph $\mathcal{G}/\pi$ where the ijth entry of $\mathcal{A}_\pi$ representing the average edge weights from C_j to C_i is defined as

$$a_{ij}^\pi = \beta_\pi(C_j, C_i) = \frac{\sum_{v_i \in C_i} \beta_\pi(C_j, v_i)}{n_{C_i}}, \tag{6–2}$$

where n_{C_i} represents the number of nodes in C_i. Note that the $\mathcal{G}/\pi$ can be a directed graph, even if $\mathcal{G}$ is an undirected graph. Based on the defined cell-to-node degree, the equitable partition of signed weighted graphs is introduced.

Definition 6.2. Consider an undirected signed weighted graph $\mathcal{G} = (\mathcal{V}, \mathcal{E}, \mathcal{A})$ and let $\pi = \{C_1, C_2, \cdots, C_r\}$ be a partition of $\mathcal{V}$. The partition π is a generalized equitable partition (GEP) if, for any two cells C_i and C_j where i and j are not necessarily distinct, it holds that $\beta_\pi(C_j, v_m) = \beta_\pi(C_j, C_i)$, $\forall v_m \in C_i$.

In the literature, the classical equitable partition is often defined based on the neighborhood of nodes, where an equitable partition indicates that, for any two cells C_i and C_j, all nodes in C_i have the same number of neighbors in C_j. Such a definition is applicable to unweighted unsigned graphs, since the edge weight a_{ij} only takes the value of 1 or 0, and, consequently, only the neighborhood of nodes matters in partitioning a graph. However, when considering signed weighted graphs, as in this Chapter, the classical equitable partition is no longer applicable, since a_{ij} is a real number. Neighborhood of nodes alone are not sufficient to partition a signed weighted graph.

In this Chapter, Def. 6.2 generalizes the classical equitable partition by defining $\beta_\pi(C_j, v_i)$ which takes into account the real edge weights in graph partition. Def. 6.2 implies that, if π is a GEP, every node in C_i has the same cell-to-node degree from C_j. It is worth noting that the classical definition is a particular case of the designed GEP in Def. 6.2, since $\beta_\pi(C_j, v_i)$ reduces to indicate the number of neighbors of v_i in C_j if $a_{ij} \in \{0, 1\}$. In other words, any results developed based on GEP are immediately applicable to unweighted graphs. In addition, it should be noted that any graph $\mathcal{G}$ with n nodes admits a trivial GEP, i.e., $\pi = \{C_1, C_2, \cdots, C_n\}$, where each C_i is a singleton containing only v_i. Given a GEP π, the characteristic matrix of π is an $n \times r$ matrix $P(\pi) = [P_{ij}]$, where $P_{ij} = 1$ if $v_i \in C_j$ and $P_{ij} = 0$ if $v_i \notin C_j$. Clearly, the non-zero entries of the jth column of P indicate the node indices in the cell C_j.

Example 6.1. Fig. 6-1 illustrates the GEP π and the associated quotient graph $\mathcal{G}/\pi$. Fig. 6-1 (a) shows a signed weighted graph $\mathcal{G}$ with 7 nodes and labeled edge weights. Node v_1 is the leader while the remaining nodes are the followers. A non-trivial generalized equitable partition is $\pi = \{C_1, C_2, C_3\}$, where $C_1 = \{v_1\}$, $C_2 = \{v_2, v_3, v_4\}$, $C_3 = \{v_5, v_6, v_7\}$. It can be verified that all nodes within the same cell have the same cell-to-node degree from another connected cell (including itself). Based on the partition π, the quotient graph $\mathcal{G}/\pi$ is shown in Fig. 6-1 (b), where the number associated with the directed edge is the cell degree. Note that self-loop is allowed in Fig. 6-1 (a) and (b). In addition, the graph $\mathcal{G}$ is undirected while the associated quotient graph $\mathcal{G}/\pi$ is directed. The characteristic matrix P of the GEP π and the adjacency

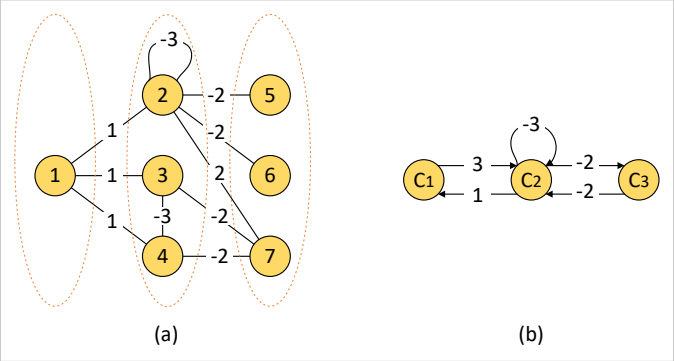

Figure 6-1. (a) A non-trivial generalized equitable partition of $\mathcal{G}$. (b) The associated quotient graph $\mathcal{G}/\pi$.

matrix $\mathcal{A}_\pi$ of the quotient graph $\mathcal{G}/\pi$ are given by

$$P = \begin{bmatrix} 1 & 0 & 0 \\ 0 & 1 & 0 \\ 0 & 1 & 0 \\ 0 & 1 & 0 \\ 0 & 0 & 1 \\ 0 & 0 & 1 \\ 0 & 0 & 1 \end{bmatrix}, \ \mathcal{A}_\pi = \begin{bmatrix} 0 & 3 & 0 \\ 1 & -3 & -2 \\ 0 & -2 & 0 \end{bmatrix}.$$

6.2.2 Controllable Subspace

Based on the defined GEP, this section discusses how the graph partition characterizes the controllable subspace of the system (6–1). Considering a matrix E and a matrix T with appropriate dimensions, the vector space generated by the columns of E is called T-invariant if and only if there exists a matrix F such that $TE = EF$ [62]. That is, T maps any vector from $\mathrm{img}\,(E)$ back to the same space $\mathrm{img}\,(E)$.

Theorem 6.1. *Consider a signed weighted graph $\mathcal{G}$ with the adjacency matrix $\mathcal{A}$. Suppose $\pi = \{C_1, C_2, \cdots, C_r\}$ is a partition of $\mathcal{G}$. Let P and $\mathcal{A}_\pi$ denote the characteristic matrix of π and the adjacency matrix of the quotient graph $\mathcal{G}/\pi$, respectively. The partition π is a GEP of $\mathcal{G}$ if and only if $\mathcal{A}P = P\mathcal{A}_\pi$, i.e., $\mathrm{img}\,(P)$ is $\mathcal{A}$-invariant.*

Proof. To show the necessary condition, suppose π is a GEP of $\mathcal{G}$. Considering a node $v_k \in C_i$, $i \in \{1, \ldots, r\}$, the kth row of $\mathcal{A}P$ is

$$(\mathcal{A}P)_{k,:} = \begin{bmatrix} \sum_{v_l \in C_1 \cap \mathcal{N}_k} a_{kl} & \ldots & \sum_{v_l \in C_r \cap \mathcal{N}_k} a_{kl} \end{bmatrix}, \tag{6–3}$$

where each entry $(\mathcal{A}P)_{k,j}$ indicates the cell-to-node degree $\beta_\pi(C_j, v_k)$ of v_k, i.e., the sum of edge weights from C_j to v_k. If π is a GEP of $\mathcal{G}$, every node in C_i has the same cell-to-node degree from C_j, indicating $\beta_\pi(C_j, v_k) = \beta_\pi(C_j, C_i), \forall v_k \in C_i$, where $\beta_\pi(C_j, C_i)$ is defined in (6–2). Therefore, when π is a GEP of $\mathcal{G}$, (7–1) can be written as

$$(\mathcal{A}P)_{k,:} = \begin{bmatrix} \beta_\pi(C_1, C_i) & \ldots & \beta_\pi(C_r, C_i) \end{bmatrix}.$$

Since the ijth entry of $\mathcal{A}_\pi$ represents the cell degree from C_j to C_i, the kth row of $P\mathcal{A}_\pi$ is $(P\mathcal{A}_\pi)_{k,:} = \begin{bmatrix} \beta_\pi(C_1, C_i) & \ldots & \beta_\pi(C_r, C_i) \end{bmatrix}$, where C_i is the cell to which v_k belongs. Apparently, if π is a GEP of $\mathcal{G}$, $\mathcal{A}P = P\mathcal{A}_\pi$.

To show the sufficient condition, consider an arbitrary node v_k belonging to C_i. If $\mathcal{A}P = P\mathcal{A}_\pi$, the sum of edge weights from C_j to v_k, $\forall v_k \in C_i$ must be equal to the cell degree from C_j to C_i, i.e, $\beta_\pi(C_j, v_k) = \beta_\pi(C_j, C_i), \forall v_k \in C_i$. Since this condition holds for any nodes within the same cell C_i, π is a GEP of $\mathcal{G}$.

In addition, the fact that $\mathcal{A}P = P\mathcal{A}_\pi$ implies $\mathrm{img}(P)$ is $\mathcal{A}$-invariant, due to the existence of $\mathcal{A}_\pi$. Specifically, since the columns of P are linearly independent, $\mathcal{A}_\pi$ can always be constructed by $\mathcal{A}_\pi = P^+\mathcal{A}P$, where $P^+ = \left(P^TP\right)^{-1}P^T$ denotes the left pseudo inverse of P. □

Previous research (cf. [6, 63, 65, 66]) demonstrated that if a graph $\mathcal{G}$ has an almost equitable partition π, the range space of the associated characteristic matrix P is L-invariant, i.e., $LP = PL_\pi$, where L and L_π are the Laplacian matrices of the graph $\mathcal{G}$ and the quotient graph $\mathcal{G}/\pi$, respectively. Many results with respect to network controllability and controllable subspace were developed based on the condition $LP = PL_\pi$. However, such a condition is valid for unsigned graphs. It can be verified that $LP = PL_\pi$ does not in general hold for signed weighted graphs. If a particular signed Laplacian matrix is considered, i.e., the diagonal entries of the Laplacian

matrix are consisting of the sum of all node degrees without considering the absolute value, as shown in [65] and [60], $LP = PL_\pi$ still holds.

To address this challenge, Theorem 6.1 reveals that the range space of P is $\mathcal{A}$-invariant if π is a GEP of $\mathcal{G}$, providing a means to characterize the controllable subspace of system (6–1) over signed graphs. It is well known that the controllable subspace of system (6–1) is

$$\operatorname{img}(\mathcal{C}) = \operatorname{img}(B) + \mathcal{A} \times \operatorname{img}(B) + \cdots + \mathcal{A}^{n-1} \times \operatorname{img}(B), \tag{6–4}$$

which is the smallest $\mathcal{A}$-invariant subspace that contains $\operatorname{img}(B)$, where "+" represents the union of two spaces [117]. Since $\operatorname{img}(P)$ is $\mathcal{A}$-invariant, Lemma 6.2 characterizes the controllable subspace from equitable partitions.

Definition 6.3. A GEP π is called leader-isolated generalized equitable partition (L-GEP) if every leader is a singleton cell in π.

Lemma 6.2. *Suppose π is an L-GEP of the signed weighted graph $\mathcal{G}$. The controllable subspace of system (6–1) satisfies* $\operatorname{img}(\mathcal{C}) \subseteq \operatorname{img}(P)$, *where $\mathcal{C}$ is the controllability matrix and P is the characteristic matrix of π.*

From the definition of the characteristic matrix P of an L-GEP and the input matrix B in (6–1), one has $\operatorname{img}(B) \subseteq \operatorname{img}(P)$. Lemma 6.2 then follows immediately, since

$$\begin{aligned}\operatorname{img}(\mathcal{C}) &= \operatorname{img}(B) + \mathcal{A} \times \operatorname{img}(B) + \cdots + \mathcal{A}^{n-1} \times \operatorname{img}(B) \\ &\subseteq \operatorname{img}(P) + \mathcal{A} \times \operatorname{img}(P) + \cdots + \mathcal{A}^{n-1} \times \operatorname{img}(P) \\ &= \operatorname{img}(P),\end{aligned}$$

where the fact that $\operatorname{img}(P)$ is $\mathcal{A}$-invariant from Theorem 6.1 is used.

Lemma 6.2 provides an upper bound of the controllable subspace of system (6–1), which implies how the controllable subspace is related to the L-GEP of the graph. It should be noted that the L-GEP of $\mathcal{G}$ may not be unique. Let $\Pi = \{\pi_1, \pi_2, \ldots\}$ be the set of L-GEPs of $\mathcal{G}$, which implies that $\operatorname{img}(B) \subseteq \operatorname{img}(P)$ for every $\pi_i \in \Pi$. Consider two L-GEPs $\pi_1, \pi_2 \in \Pi$. The partition π_1 is said to be finer than π_2, denoted as $\pi_1 \leq \pi_2$, if each cell of π_1 is a subset of some

cell of π_2. As demonstrated in [66],

$$\pi_1 \leq \pi_2 \Longleftrightarrow \operatorname{img}(P_2) \subseteq \operatorname{img}(P_1). \tag{6–5}$$

If $\pi_i \leq \pi^*$ for any $\pi_i \in \Pi$, then $\pi^* \in \Pi$ is referred to as the maximal L-GEP. In other words, π^* is the coarsest L-GEP, since the cells of any $\pi_i \in \Pi$ are subsets of the cells of π^*. Clearly, for any $\pi_i \in \Pi$,

$$\operatorname{img}(P(\pi^*)) \subseteq \operatorname{img}(P(\pi_i)) \tag{6–6}$$

obtains from (6–5). From (6–6), Lemma 6.3 is an immediate consequence.

Lemma 6.3. *The controllable subspace of system (6–1) can be upper bounded by* $\operatorname{img}(\mathcal{C}) \subseteq \operatorname{img}(P(\pi^*))$, *where* π^* *is the maximal L-GEP of* $\mathcal{G}$.

Compared with Lemma 6.2, a tighter upper bound of $\mathcal{C}$ derives from Lemma 6.3. For a system evolved with Laplacian dynamics, similar upper bounds of its controllable subspace were developed via almost equitable partition in [59, 63, 66]. As discussed previously, $\operatorname{img}(P)$ is not L-invariant for signed graphs. Therefore, the upper bounds developed in [59, 63, 66] are not applicable in this work.

6.2.3 Construction of π^*

The controllable subspace $\mathcal{C}$ is characterized based on the maximal L-GEP π^*. This section presents an algorithm to identify the maximal L-GEP π^*. The algorithm consists of the following steps:

Step 1: Let $\pi = \{C_1, \ldots, C_m, C_f\}$ be the initial partition, where $C_i = \{v_i\}$, $i = 1, \ldots, m$, indicates that each leader is a singleton cell in π and $C_f = \mathcal{V}_f$ represents the set of followers.

Step 2: For each node $v_i \in C_f$, calculate its node degree $\beta_i = \sum_{j \in \mathcal{N}_i} a_{ij}$, where a_{ij} is the weight associated with $(v_i, v_j) \in \mathcal{E}$. The nodes with the same node degree are then grouped into the same cell, i.e., $C_f = \{C_{m+1}, C_{m+2}, \ldots, C_q\}$. That is, the initial partition is refined by splitting C_f into a set of $q - m$ cells, where the nodes in each cell have the same node degree.

Step 3: For each node v_i in $C_j \in \pi$, $j \in \{m+1, \ldots, q\}$, calculate the cell-to-node degree $\beta_\pi(C_p, v_i) = \sum_{k \in \mathcal{N}_i \cap C_p} a_{ik}$, $p \in \{1, \ldots, q\}$. Nodes with the same cell-to-node degree are grouped into the same cell and C_f is then updated based on the newly created cells such that the nodes in each cell have the same cell-to-node degree.

Step 4: Repeat Step 3 until no cells can be split.

Lemma 6.4. *Provided an undirected signed weighted graph $\mathcal{G} = (\mathcal{V}, \mathcal{E}, \mathcal{A})$, the L-GEP π^* constructed from Step 1-4 is maximal.*

Proof. By Def. 6.2, it is clear that the algorithm yields a generalized equitable partition since all nodes within the same cell have the same cell-to-node degree. The rest of the proof shows that the L-GEP is maximal. If the graph only contains trivial GEP, i.e., each cell only contains one node, the GEP obtained through the algorithm is indeed an L-GEP π^*. Suppose π_1 is a non-trivial L-GEP obtained from the algorithm and there exists another L-GEP π_2 such that π_2 contains π_1. That is, every cell in π_1 is a sub-cell of some cell in π_2. Suppose that two nodes v_p and v_q are in two different cells in π_1 but within the same cell in π_2. Based on Step 3, v_p and v_q are separated in two different cells if and only if there exists a cell C_j, such that $\beta_\pi(C_j, v_p) \neq \beta_\pi(C_j, v_q)$. However, this condition contradicts the fact that v_p and v_q are in the same cell in π_2. Hence, π_1 constructed from the algorithm is guaranteed to be maximum. □

6.3 Characterizations of Network Herdability

Using the characterized controllable subspace, the herdability of system (6–1) is investigated in this section. Section 6.3.1 reveals that the herdability of $\mathcal{G}$ can be verified based on its quotient graph $\mathcal{G}/\pi$. Section 6.3.2 presents the methods for verifying network herdability from positive system's perspectives.

6.3.1 Herdability via Quotient Graphs

Consider a quotient graph $\mathcal{G}/\pi$ constructed from an L-GEP $\pi = \{C_1, \ldots, C_r\}$, where the first m cells are the leader cells with the follower cells indexed from $m+1$ to r. When considering Laplacian dynamics (cf. [64, 67, 68]), due to the consensus properties of graph Laplacian, the average of system states in each cell, i.e., $\bar{x}_i = \sum_{j \in C_i} x_j$, is often used to yield a

compact system representation $\dot{\bar{x}}(t) = L_\pi \bar{x}(t) + B_\pi u_\pi(t)$. Since such a dynamics is no longer valid to represent the evolution of system states when considering adjacency dynamics (6–1), the sum of states in each cell is used instead. Let $\hat{x} = \begin{bmatrix} \hat{x}_1 & \dots & \hat{x}_r \end{bmatrix}^T \in \mathbb{R}^r$ denote the stacked states, where each entry $\hat{x}_i = \sum_{j \in C_i} x_j$ represents the sum of the states in C_i. The system (6–1) can then be rewritten in a compact form of

$$\dot{\hat{x}}(t) = \mathcal{A}_\pi \hat{x}(t) + B_\pi u_\pi(t), \tag{6–7}$$

where $u_\pi \in \mathbb{R}^m$ is the control input reorganized from u in (6–1) based on the L-GEP π, and $B_\pi = \begin{bmatrix} e_1 & \cdots & e_m \end{bmatrix} \in \mathbb{R}^{r \times m}$ is the input matrix with basis vectors e_i indicating the ith cell is the leader cell endowed with external controls u_π. To see that, consider the ith row of (6–7),

$$\begin{aligned} \dot{\hat{x}}_i(t) &= \sum_{j \in \{1,\dots r\}} a^\pi_{ij} \hat{x}_j(t) + B^\pi_{i,:} u_\pi(t) \\ &= \sum_{j \in \{1,\dots r\}} \beta_\pi(C_j, C_i)\, \hat{x}_j(t) + B^\pi_{i,:} u_\pi(t), \end{aligned}$$

where $B^\pi_{i,:}$ represents the ith row of B_π. From (6–1), summing the dynamics of the nodes $v_i \in C_i$, one has

$$\begin{aligned} \sum_{v_i \in C_i} \dot{x}_i &= \sum_{v_i \in C_i} \left(\sum_{v_j \in \mathcal{V}} a_{ij} x_j + B_{i,:} u(t) \right) \\ &= \sum_{v_i \in C_i} \Bigg(\sum_{v_j \in C_1} a_{ij} x_j + \dots + \sum_{v_j \in C_r} a_{ij} x_j \\ &\quad + B_{i,:} u(t) \Bigg), \end{aligned}$$

where $\sum_{v_i \in C_i} \sum_{v_j \in C_j} a_{ij} x_j = \beta_\pi(C_j, C_i)\, \hat{x}_j(t)$ and $\sum_{v_i \in C_i} B_{i,:} u(t) = B^\pi_{i,:} u_\pi(t)$. Therefore, (6–7) is a equivalent representation of the system (6–1).

Theorem 6.2. *Consider a system (6–1) evolving over a signed weighted graph $\mathcal{G}$. Let π be an L-GEP of $\mathcal{G}$, which yields a quotient graph $\mathcal{G}/\pi$ with dynamics (6–7). The system (6–1) over $\mathcal{G}$ is d-herdable if the system (6–7) over $\mathcal{G}/\pi$ is d-herdable.*

Proof. If the system (6–7) over the quotient graph $\mathcal{G}/\pi$ is d-herdable, $\hat{x}$ can be driven by u_π element-wise above an arbitrary positive threshold d. Since each entry $\hat{x}_i$ can be driven above

d, there must exist at least one node $v \in C_i$ whose state is positive. Let $\mathcal{K}$ denote the set of state indices for which $x_i > 0, \forall i \in \mathcal{K}$. Thus, we can construct a vector $k \in \mathrm{img}\,(\mathcal{C})$ such that $k_i > 0, \forall i \in \mathcal{K}$, since v_i is d-herdable [69]. Note that, for each cell in π, there exists at least one node whose corresponding entry in k is positive. According to Lemma 6.2, $k \in \mathrm{img}\,(\mathcal{C})$, $\mathrm{img}\,(\mathcal{C}) \subseteq \mathrm{img}\,(P)$, leading to $k \in \mathrm{img}\,(P)$. Since the columns in P are linearly independent and the non-zero entries are all ones, $k \in \mathrm{img}\,(P)$ indicates that the entries in k corresponding to the nodes in the same cell must all be positive. Therefore, $k \in \mathrm{img}\,(\mathcal{C})$ is an element-wise positive vector. By Lemma 6.1, the system (6–1) evolving over $\mathcal{G}$ is d-herdable. □

Verifying network herdability based on Lemma 6.1 can be challenging, since it needs to check the existence of an element-wise positive vector $k \in \mathrm{img}\,(\mathcal{C})$. Such a method can be significantly challenging, or even prohibitive, when addressing large-scale networks. Theorem 6.2 suggests that, rather than directly verifying the herdability of $\mathcal{G}$, the quotient graph $\mathcal{G}/\pi$ can be exploited. The graph $\mathcal{G}/\pi$ can be viewed as an abstract representation of $\mathcal{G}$ that captures the key topological structure of $\mathcal{G}$ while preserving its certain properties (e.g., herdability). Since $\mathcal{G}/\pi$ is more compact than $\mathcal{G}$ in terms of system dimensions, Theorem 6.2 provides an efficient means to investigate the herdability of $\mathcal{G}$.

6.3.2 Herdability of Positive Systems

Since $\mathcal{G}/\pi$ can be used to verify network herdability, this section presents verification methods based on positive systems.

Definition 6.4. [70] A dynamical system $\dot{x}\,(t) = f\,(x\,(t)\,, t), x \in \mathbb{R}^n$, is a positive system if $x\,(0) \geq 0_n$ implies $x\,(t) \geq 0_n$ for all t.

Def. 6.4 indicates positive systems are a class of systems in which the states remain non-negative during evolution, provided the initial states are non-negative. As indicated in [118], an affine system $\dot{x} = Ax + b$ is a positive system if the system matrix $A \in \mathbb{R}^{n\times n}$ is a Metzler

matrix[1] and $b \in \mathbb{R}^n$ is element-wise positive. Therefore, if system (6–1) evolves on an unsigned graph (i.e., the associated adjacency matrix $\mathcal{A}$ is a Metzler matrix), system (6–1) is positive, since there always exist control inputs u for leaders such that Bu is element-wise positive. Ensuing from [69], Lemma 6.5 characterizes how positive system infers network herdability:

Lemma 6.5. *[69] A positive system is completely d-herdable if and only if it is input connectable, i.e., there exist (directed) paths from leaders to followers.*

However, when evolving on signed graphs, the system matrix $\mathcal{A}$ in (6–1) is no longer a Metzler matrix due to potential negative edge weights. Theorem 6.3 represents how the quotient graph can be exploited to verify network herdability.

Theorem 6.3. *Consider a system (6–1) evolving over an signed weighted graph $\mathcal{G}$. Let π be an L-GEP of $\mathcal{G}$, which yields a quotient graph $\mathcal{G}/\pi$ with dynamics (6–7). The system (6–1) over $\mathcal{G}$ is d-herdable if $\mathcal{G}/\pi$ is input connected (i.e., follower cells are reachable from leader cells) and the cell degree between distinct cells in $\mathcal{G}/\pi$ is non-negative.*

Proof. Consider the quotient graph $\mathcal{G}/\pi$. If the cell degree between distinct cells in $\mathcal{G}/\pi$ is non-negative, the matrix $\mathcal{A}_\pi$ is a Metzler matrix. Note that $\mathcal{A}_\pi$ remains a Metzler matrix if the cell degree with respect to itself is negative (i.e., self-loop with negative weight). Per Def. 6.4, system (6–7) is a positive system since there always exist control inputs u_π for leader cells such that $B_\pi u_\pi$ is element-wise positive. In addition, if $\mathcal{G}/\pi$ is input connected, system (6–7) is d-herdable by Lemma 6.5. Therefore, system (6–1) on $\mathcal{G}$ is also d-herdable by Theorem 6.2. □

Theorem 6.3 indicates that, even if $\mathcal{G}$ is signed with negative edge weights, $\mathcal{G}$ is d-herdable, provided $\mathcal{G}/\pi$ satisfies the conditions stated in Theorem 6.3. In other words, in order to verify the herdability of $\mathcal{G}$, we only need to determine if $\mathcal{G}/\pi$ is input connectable and the cell degree between distinct cells in $\mathcal{G}/\pi$ is non-negative.

[1] A matrix is called a Metzler matrix if all its off-diagonal entries are non-negative.

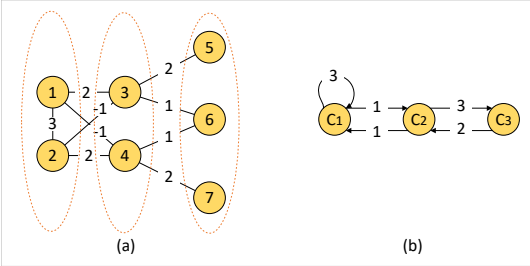

Figure 6-2. (a) A non-trivial generalized equitable partition of $\mathcal{G}$, where $C_1 = \{v_1\}$ and $C_2 = \{v_2\}$ are leader cells, and $C_3 = \{v_3, v_4\}$ and $C_4 = \{v_5, v_6\}$. (b) The system (6–7) evolving on $\mathcal{G}/\pi$ is a positive system.

Example 6.2. To illustrate Theorem 6.3, consider a signed graph $\mathcal{G}$ as shown in Fig. 6-2 (a). The nodes v_1 and v_2 are assumed to be leaders while the remaining nodes as followers. Let $\pi = \{C_1, C_2, C_3, C_4\}$ be an L-GEP of $\mathcal{G}$, where $C_1 = \{v_1\}$, $C_2 = \{v_2\}$, $C_3 = \{v_3, v_4\}$, $C_4 = \{v_5, v_6\}$. The edge weights are as labeled along the edges. Due to the existence of negative edge weights, the adjacency matrix $\mathcal{A}$ is not a Metzler matrix; consequently, it cannot be determined if system (6–1) is a positive system. To verify the herdability of $\mathcal{G}$, the quotient graph $\mathcal{G}/\pi$ is constructed as shown in Fig. 6-2 (b). Since $\mathcal{A}_\pi$ is a Metzler matrix and the leader cell has directed paths to all other cells (i.e., input connectable), system (6–7) is d-herdable, and therefore $\mathcal{G}$ is d-herdable.

6.4 Summary

The herdability of signed weighted graphs is investigated in this Chapter, wherein graph partitions are exploited to characterize topological structures to ascertain network herdability. Generalized equitable partitions are developed to take into account the edge weights of signed graphs. The controllable subspace of such dynamics is then derived based on the generalized equitable partition. It is discovered that the quotient graph can be used to infer the herdability of the original graph, for which criteria for herdability of quotient graphs are developed based on positive systems.

CHAPTER 7
HERDABILITY OF COMPLEX NETWORKS - GRAPH WALKS AND STRUCTURAL BALANCE

To study the herdability of signed leader-follower networks, this Chapter extends the results of Chapter 6 and characterizes topological structures of herdable networks. Note that system dynamics of this Chapter is the same as Chapter 6, while no self-loop is allowed. In particular, graph walks are exploited to develop sufficient conditions ensuring the herdability of signed networks via 1-walks and 2-walks. Leader selection methods on structurally balanced networks to ensure herdability are developed. The leader sets are shown to be refined through graph walks. Examples are provided to illustrate the developed topological methods.

7.1 Preliminary

7.1.1 Graph Walks

Graph walks will be used as main tools to develop topological characterizations of network herdability. Graph walk is defined as an alternating sequence of nodes and edges [62]. Let $\alpha(v_i, v_j)$ denote a walk from v_i to v_j on graph $\mathcal{G}$, i.e., $\alpha(v_i, v_j) = v_i, (v_i, v_m), v_m, \ldots, v_p, (v_p, v_j), v_j$, with nodes and edges belonging to $\mathcal{V}$ and $\mathcal{E}$. Since $\mathcal{G}$ is undirected, $\alpha(v_i, v_j)$ also indicates that v_j is reachable from v_i via the walk. It is worth pointing out that graph walk may have repeated edges, which is different from the path of a graph that comprises only distinct edges [62]. For instance, the path from v_1 to v_2 in Fig. 7-1 is $v_1, (v_1, v_2), v_2$, while a walk from v_1 to v_2 could be $\alpha(v_1, v_2) = v_1, (v_1, v_2), v_2, (v_2, v_1), v_1, (v_1, v_2), v_2$, which includes repetitive edges.

The length of a walk $\alpha(v_i, v_j)$ is defined as its number of edges along the walk, including repetitive edges. Let $\alpha^{(k)}(v_i, v_j)$ denote a k-walk which indicates that there is a walk of length k from v_i to v_j. Let $\eta^{(k)}(v_i, v_j)$ denote the set that contains all k-walks from v_i to v_j. The weight of a k-walk, denoted by $w\left(\alpha^{(k)}(v_i, v_j)\right) \in \mathbb{R}$, is the product of the edge weights in the walk of $\alpha^{(k)}(v_i, v_j)$. Let $\text{sign}\left(w\left(\alpha^{(k)}(v_i, v_j)\right)\right)$ denote the sign of the k-walk from v_i to v_j, where $\text{sign}(\cdot)$ is the sign function. If $\text{sign}\left(w\left(\alpha^{(k)}(v_i, v_j)\right)\right) = 1$, the walk $\alpha^{(k)}(v_i, v_j)$ is called a positive walk, and negative walk otherwise. Denote by $w\left(\eta^{(k)}(v_i, v_j)\right)$ the total weight of a set of k-walks from v_i to v_j, which is defined as the sum of weighted k-walks in the set $\eta^{(k)}(v_i, v_j)$.

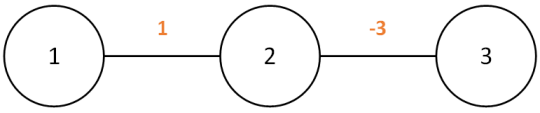

Figure 7-1. Graph walks on a weighted signed graph.

Since a walk $\alpha(v_i, v_j)$ can have repetitive edges, the minimal walk between v_i and v_j is defined as the walk with the smallest k from v_i to v_j.

Example 7.1. To illustrate graph walks, Fig. 7-1 shows a weighted graph $\mathcal{G} = (\mathcal{V}, \mathcal{E}, \mathcal{A})$ with node set $\mathcal{V} = \{v_1, v_2, v_3\}$, edge set $\mathcal{E} = \{(v_1, v_2), (v_2, v_3)\}$. and the weighted adjacency matrix $\mathcal{A} = \begin{bmatrix} 0 & 1 & 0 \\ 1 & 0 & -3 \\ 0 & -3 & 0 \end{bmatrix}$. For example, the set of 3-walks $\eta^{(3)}(v_1, v_2) = \left\{\alpha_1^{(3)}(v_1, v_2), \alpha_2^{(3)}(v_1, v_2)\right\}$ consists of two walks between v_1 and v_2, where

$$\alpha_1^{(3)}(v_1, v_2) = \{v_1, (v_1, v_2), v_2, (v_2, v_3), v_3, (v_3, v_2), v_2\}$$

and

$$\alpha_2^{(3)}(v_1, v_2) = \{v_1, (v_1, v_2), v_2, (v_2, v_1), v_1, (v_1, v_2), v_2\}.$$

The weight of $\eta^{(3)}(v_1, v_2)$ can be computed as

$$\begin{aligned} w\left(\eta^{(3)}(v_1, v_2)\right) &= w\left(\alpha_1^{(3)}(v_1, v_2)\right) + w\left(\alpha_2^{(3)}(v_1, v_2)\right) \\ &= (1)^3 + (1) \times (-3)^2 = 10. \end{aligned}$$

As indicated in Lemma 6.1, network herdability depends on the existence of an element-wise positive vector $k \in \text{range}(\mathcal{C})$, where $\mathcal{C}$ is the controllability matrix of $\mathcal{G}$. The key observation is that the columns of $\mathcal{C}$ are composed of the product of the input matrix B and the matrix $\mathcal{A}^k$, $k = 0, \ldots, n-1$. The following Lemma shows how graph walks relate to the powers of the adjacency matrix $\mathcal{A}$.

Lemma 7.1. *Consider a weighted signed graph $\mathcal{G} = (\mathcal{V}, \mathcal{E}, \mathcal{A})$, where $\mathcal{A}$ is the weighted adjacency matrix. Let $\mathcal{A}^k$ denote the kth power of $\mathcal{A}$. Each entry of $\mathcal{A}^k$ is determined as $\left[\mathcal{A}^k\right]_{ij} = w\left(\eta^{(k)}\left(v_j, v_i\right)\right)$, which is the sum of the weights of all k-walks from v_j to v_i.*

The proof is omitted here since it is a trivial extension of known properties of adjacency matrix [62]. Based on Lemma 7.1, when considering the product $\mathcal{A}^k B$, the entry $\left[\mathcal{A}^k B\right]_{ij}$ indicates the sum of the weights of all k-walks from node v_j to the leader v_i, $i \in \{1, \ldots, m\}$. This observation motivates the use of graph walks to characterize herdability of signed graphs based on the range space of $\mathcal{C}$.

7.2 Herdability and Graph Walks

7.2.1 Herdability on 1-Walk

The following theorem characterizes network herdability via 1-walk, which will then be extended to the case of 2-walk.

Theorem 7.1. *Consider a network $\mathcal{G} = (\mathcal{V}, \mathcal{E}, \mathcal{A})$ evolving according to the dynamics in (6–1). The network $\mathcal{G}$ is herdable by the leader set $\mathcal{V}_l$, if the following two conditions hold: 1) there exists a 1-walk from each follower to at least one leader in $\mathcal{V}_l$, and 2) the 1-walks from followers to the same leader have the same sign.*

Proof. Consider a signed graph $\mathcal{G}$ with the weighted adjacency matrix $\mathcal{A}$ and the input matrix B. Since the first m nodes are assumed as the leaders, $B = \begin{bmatrix} e_1 & \cdots & e_m \end{bmatrix}$ can be rewritten as $B = \begin{bmatrix} I_{m\times m} & 0_{m\times(n-m)} \end{bmatrix}^T$, where $I_{m\times m}$ is an m-dimensional identity matrix and $0_{(n-m)\times m}$ is a zero matrix. The system controllability matrix $\mathcal{C}$ is

$$\begin{aligned} \mathcal{C} &= \left[\begin{array}{c|c|c|c} B & \mathcal{A}B & \cdots & \mathcal{A}^{n-1}B \end{array}\right] \\ &= \left[\begin{array}{c|c|c} I_{m\times m} & *_{m\times m} & \cdots \\ 0_{(n-m)\times m} & \Xi & \cdots \end{array}\right], \end{aligned} \tag{7–1}$$

where $*_{m\times m} \in \mathbb{R}^{m\times m}$ and $\Xi \in \mathbb{R}^{(n-m)\times m}$. Based on Lemma 6.1, the network $\mathcal{G}$ is herdable if and only if there exists an element-wise positive vector $k \in \operatorname{range}(\mathcal{C})$. That is, there exists

a vector $\delta = \begin{bmatrix} \delta_1 & \dots & \delta_{mn} \end{bmatrix}^T \in \mathbb{R}^{mn}$ such that $k = \begin{bmatrix} k_1 & \dots & k_n \end{bmatrix}^T = \mathcal{C}\delta \in \mathbb{R}^n$ is element-wise positive. Note that the vector k is a linear combination of the columns of $\mathcal{C}$, i.e., $k = \sum_{i=1}^{mn} \delta_i \mathcal{C}_{:,i}$, where $\mathcal{C}_{:,i}$ represents the ith column of $\mathcal{C}$. The following proof will show that the first $2m$ columns of $\mathcal{C}$ are sufficient to guarantee the existence of the vector k, provided that the two conditions stated in the theorem are satisfied.

As indicated in (7–1), the first m columns of $\mathcal{C}$ correspond to the input matrix B, where the non-zero entries indicate direct access to the leader set $\mathcal{V}_l$, i.e., the set of nodes with 0-walk to $\mathcal{V}_l$. Due to the identity matrix $I_{m\times m}$, there always exist sufficiently large $\delta_i \in \mathbb{R}^+$, $i = 1, \dots, m$, such that $\delta_i > \sum (\mathcal{C}_{i,i+1:mn})$, where $\sum (\mathcal{C}_{i,i+1:mn})$ represents the sum of the entries from the $(i+1)$th column to the mnth column in the ith row in (7–1). Therefore, the first m entries in k are guaranteed to be positive if δ_i, $i = 1, \dots, m$, are selected sufficiently large.

The second m columns of $\mathcal{C}$ correspond to $\mathcal{A}B$. Based on Lemma 7.1, each non-zero entry Ξ_{ij} indicates there exists a 1-walk from the follower v_{m+i} to the leader $v_j \in \mathcal{V}_l$. If there exists a 1-walk from each follower to at least one leader in $\mathcal{V}_l$, then no row in Ξ is zero. In addition, if the followers connected to the same leader via 1-walk have the same signs, the nonzero entries in each column of Ξ have the same sign (i.e., either all positive or all negative). Then there always exists a proper design of δ_i, $i = m+1, \dots, 2m$, such that the linear combination of the columns of Ξ is element-wise positive.

Based on the analysis above, with proper design of the rest entries of δ as $\delta_i = 0$, $i = 2m+1, \dots mn$, there exists an element-wise positive vector $k \in \text{range}\,(\mathcal{C})$, which indicates the network $\mathcal{G}$ is herdable. □

Theorem 7.1 characterizes a class of herdable networks. For these networks, the analysis above indicates that the herdability of $\mathcal{G}$ depends on the matrix B (i.e., 0-walks to the leader set) and $\mathcal{A}B$ (i.e., 1-walks from the followers to the leader set). In other words, follower-to-follower and leader-to-leader connections will not affect the herdability of the system. That is, a network remains herdable, regardless of the addition and removal of follower-to-follower and leader-to-leader connections, or the change of edge signs.

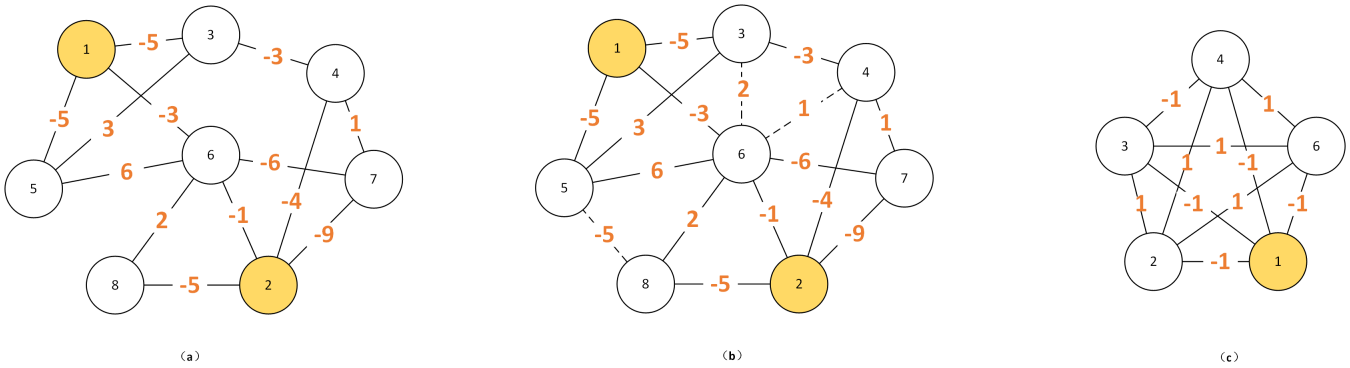

Figure 7-2. Examples of herdable signed graphs.

When considering a single leader, the following corollary is a special case of Theorem 7.1, where the leader set $\mathcal{V}_l$ is a singleton.

Corollary 7.1. *Consider a network $\mathcal{G} = (\mathcal{V}, \mathcal{E}, \mathcal{A})$ evolving according to the dynamics in (6–1). The network $\mathcal{G}$ is herdable by a single leader if there exists a 1-walk from each follower to the leader and leader-follower connections have the same edge signs.*

As demonstrated in [6], a complete graph is not fully controllable under a single leader, due to the topological symmetry with respect to the leader. In contrast, Corollary 7.1 indicates that a complete graph can be herdable, if the leader-follower connections have the same sign. To illustrate Theorem 7.1 and Corollary 7.1, the following examples are provided.

Example 7.2. Fig. 7-2 (a) and (b) consider a weighted signed network $\mathcal{G}$ with the leader set $\mathcal{V}_l = \{v_1, v_2\}$. Based on Theorem 7.1, Fig. 7-2 (a) is herdable, since there exists a 1-walk from each follower to at least one leader in $\mathcal{V}_l$, and the 1-walks from followers to the same leader have the same sign. Fig 7-2 (b) is obtained from Fig. 7-2 (a) by adding new follower-to-follower connections (the dashed lines). It can be verified that Fig 7-2 (b) remains herdable. Figure 7-2 (c) is an example on complete graph, which is not controllable, but herdable by the leader v_1.

7.2.2 Herdability on 2-Walk

This section extends Theorem 7.1 and characterizes the herdability of a class of networks where the followers are reachable from the leader set within 2-walks. Suppose the nodes can be classified into two sets $\mathcal{V}_1$ and $\mathcal{V}_2$ with $\mathcal{V}_1 \cup \mathcal{V}_2 = \mathcal{V}_f$, where the nodes in $\mathcal{V}_1$ and $\mathcal{V}_2$ are reachable

via 1-walks and 2-walks from at least one leader in $\mathcal{V}_l$, respectively. Let $\mathcal{V}_{12}$ denote the set of nodes that are reachable via both 1-walks and 2-walks. Note that $\mathcal{V}_1$ and $\mathcal{V}_2$ are not necessarily mutual exclusive and some followers can be reachable from the leader set via both 1-walk and 2-walk. Let $\mathcal{V}_{12} = \mathcal{V}_1 \cap \mathcal{V}_2$ denote such a set of nodes.

Theorem 7.2. *Consider a network $\mathcal{G} = (\mathcal{V}, \mathcal{E}, \mathcal{A})$ evolving according to the dynamics in (6–1). The network $\mathcal{G}$ is herdable by the leaders $\mathcal{V}_l$, if the following conditions hold: 1) the nodes in $\mathcal{V}_f$ are reachable by at least one leader via either a 1-walk or a 2-walk, i.e.,$\mathcal{V}_1 \cup \mathcal{V}_2 = \mathcal{V}_f$; 2) the 1-walks and the 2-walks from the followers to the same leader in $\mathcal{V}_l$ have the same sign, respectively.*

Proof. Based on the weighted adjacency matrix $\mathcal{A}$ and the input matrix B, the system controllability matrix $\mathcal{C}$ can be written as

$$\begin{aligned} \mathcal{C} &= \left[\begin{array}{c|c|c|c} B & \mathcal{A}B & \mathcal{A}^2B & \cdots \end{array}\right] \\ &= \left[\begin{array}{c|c|c|c} I_{m\times m} & *_{m\times m} & *_{m\times m} & \cdots \\ 0_{(n-m)\times m} & \Psi & \Phi & \cdots \end{array}\right], \end{aligned} \tag{7–2}$$

where $*_{m\times m} \in \mathbb{R}^{m\times m}$ and $\Psi,\ \Phi \in \mathbb{R}^{(n-m)\times m}$. Assume that there are q nodes in $\mathcal{V}_1$, p nodes in $\mathcal{V}_2$, and r nodes in $\mathcal{V}_{12}$ with $p + q \geq n - m$ and $r \leq \min\{p, q\}$. Without loss of generality, the nodes indices are reordered as $v_i \in \mathcal{V}_1$, $i = m+1, \ldots, m+q$ and $v_j \in \mathcal{V}_2$, $j = n-p, \ldots, n$. It is further assumed that the first r nodes in $\mathcal{V}_1$ also belong to $\mathcal{V}_{12}$, i.e., $v_i \in \mathcal{V}_{12}$, $i = m+1, \ldots, m+r$. Based on the defined $\mathcal{V}_1$, $\mathcal{V}_2$, and $\mathcal{V}_{12}$, the matrix Ψ and Φ in (7–2) can be rewritten as

$$\Psi = \begin{bmatrix} \Psi^{(1)}_{q\times m} \\ 0_{(n-m-q)\times m} \end{bmatrix} \text{ and } \Phi = \begin{bmatrix} \Phi^{(12)}_{r\times m} \\ 0_{(n-m-p-r)\times m} \\ \Phi^{(2)}_{p\times m} \end{bmatrix}, \tag{7–3}$$

where the non-zero entry (i, j) in $\Psi^{(1)}_{q\times m}$ indicates that there exists a 1-walk from the follower v_{m+i} to the leader v_j. Similarly, the non-zero entry (i, j) in $\Phi^{(12)}_{r\times m}$ indicates the follower v_{m+i}

are reachable from the leader v_j via both 1-walks and 2-walks, while the non-zero entry (i, j) in $\Phi^{(2)}_{p\times m}$ indicates the follower v_{n-p+i} are reachable from the leader v_j via only 2-walks.

To show that the network $\mathcal{G}$ is herdable by the leader set $\mathcal{V}_l$, based on Lemma 6.1, we need to show there exists a vector $\delta = \begin{bmatrix} \delta_1 & \dots & \delta_{mn} \end{bmatrix}^T \in \mathbb{R}^{mn}$ such that $k = \begin{bmatrix} k_1 & \dots & k_n \end{bmatrix}^T = \mathcal{C}\delta \in \mathbb{R}^n$ is element-wise positive. The vector k is a linear combination of the columns of $\mathcal{C}$ with respect to δ. The following proof will show that the first $3m$ columns of $\mathcal{C}$ are sufficient to guarantee the existence of the vector k, provided that the conditions stated in the theorem are satisfied.

First, following similar analysis as in the proof of Theorem 7.1, it is straightforward to verify that, due to the identity matrix $I_{m\times m}$, there always exist sufficiently large $\delta_i \in \mathbb{R}^+$, $i = 1, \dots, m$, such that the first m entries of the linear combination of the columns in (7–2) are positive. That is, the first m entries in k are guaranteed to be positive if δ_i, $i = 1, \dots, m$, are selected sufficiently large.

The second and third m columns of $\mathcal{C}$ correspond to $\mathcal{A}B$ and $\mathcal{A}^2B$. If the followers connected to the same leader via 1-walks have the same edge signs, the nonzero entries in each column of Ψ have the same sign (i.e., either all positive or all negative). Similar argument indicates that the nonzero entries in each column of Φ also have the same sign. In addition, since each follower is reachable from the leaders via at least one leader, no rows in (7–2) are all zeros. Therefore, there always exists a proper design of δ_i, $i = m + 1, \dots, 2m$, such that the linear combination of the columns of Ψ and Φ is element-wise positive.

Based on the analysis above, with the design of $\delta_i = 0$, $i = 3m + 1, \dots mn$, there exists an element-wise positive vector $k \in \text{range}\,(\mathcal{C})$, which indicates the network $\mathcal{G}$ is herdable. □

Theorem 7.2 extends Theorem 7.1 by characterizing a class of herdable networks that allows followers reachable from the leader set via 1-walks and 2-walks.

7.3 Herdability of Structurally Balanced Networks

Due to the existence of positive and negative weights, structural balance is a topological feature associated with signed graphs. Exploring structural balance has generated fruitful results

regarding the relationships between network controllability and its topological structures, as shown in Chapter 3. Motivated by this topological feature, we focus on developing leader group selection algorithms for the herdability of structurally balanced signed graphs.

Def. 2.2 indicates that, in structurally balanced graphs, v_i and v_j are positive neighbors if they are from the same partitioned set, and negative neighbors if they are from different sets. Based on Def. 2.2, leader group selection from one set (i.e., either $\mathcal{V}_1$ or $\mathcal{V}_2$) and two sets (i.e., $\mathcal{V}_1$ and $\mathcal{V}_2$) are discussed in Sec. 7.3.1 and Sec. 7.3.2, respectively.

7.3.1 Selecting Leaders in One Set

When leaders are all in the same partitioned set, as discussed in [72], systems evolving over structurally balanced graphs have the following properties.

Lemma 7.2. *If the system in (6–1) evolves over a connected signed graph $\mathcal{G} = (\mathcal{V}, \mathcal{E}, \mathcal{A})$ and $\mathcal{G}$ is structurally balanced, its controllability matrix C is sign definite. That is, for any two nodes $v_p \in \mathcal{V}_1$ and $v_q \in \mathcal{V}_2$, the entries of $C_{p,:}$ are all non-negative and the entries of $C_{q,:}$ are all non-positive, given that the leaders are all in $\mathcal{V}_1$.*

Assume $|\mathcal{V}_1| = n_1$ and $|\mathcal{V}_2| = n_2$, with $n_1 + n_2 = n$. An intuitive leader group selection method is presented as follows.

Theorem 7.3. *Consider a leader-follower system in (6–1) evolving over a signed graph $\mathcal{G}$. Suppose $\mathcal{G}$ is connected and structurally balanced with nodes grouped into $\mathcal{V}_1$ and $\mathcal{V}_2$ as in Def. 2.2. If the nodes in either $\mathcal{V}_1$ or $\mathcal{V}_2$ are all selected as leaders, the system in (6–1) is herdable by the selected leaders.*

Proof. Without loss of generality, assume the nodes in $\mathcal{V}_1$ are all selected as leaders, i.e., there are n_1 leaders and n_2 followers. The controllability matrix C of the system in (6–1) can be written as

$$C = \left[\begin{array}{c|ccc} B & \mathcal{A}B & \dots & \mathcal{A}^{n-1}B \end{array}\right] = \left[\begin{array}{c|c} I_{n_1 \times n_1} & * \\ 0_{n_2 \times n_1} & \Xi \end{array}\right], \tag{7–4}$$

where $* \in \mathbb{R}^{n_1 \times (n-1)n_1}$ and $\Xi \in \mathbb{R}^{n_2 \times (n-1)n_1}$. Since $\mathcal{G}$ is connected, any two nodes are connected within $n-1$ walks. As a result, the entries in $*$ and Ξ represent the weights of walks from leaders to leaders and from leaders to followers, respectively.

Based on Lemma 6.1, the system in (6–1) is herdable if and only if there exists an element-wise positive vector $k \in img\,(C)$. That is, there exists a vector $\delta = \begin{bmatrix} \delta_1 & \dots & \delta_{nn_1} \end{bmatrix}^T \in \mathbb{R}^{nn_1}$ such that $k = C\delta \in \mathbb{R}^n$ is element-wise positive. The rest proof is to show the existence of such a vector δ.

Note that Ξ only contains the weights of walks from leaders to followers. By Lemma 7.2, the entries of $*$ are non-negative and the entries of Ξ are non-positive. In addition, since the graph is connected and any follower can be reached by at least one leader within $(n-1)$th walk, no row in Ξ is zero. Therefore, there exists $\delta_i \in \mathbb{R}^-$, $i = n_1+1, \dots, nn_1$, such that the last n_2 entries in k are guaranteed to be positive. Due to the identity matrix $I_{n_1 \times n_1}$, there always exist sufficiently large $\delta_i \in \mathbb{R}^+$, $i = 1, \dots, n_1$, such that $\delta_i > \sum_{j=n_1+1}^{nn_1} C_{i,j}\delta_j$, which indicates the first n_1 entries in k are guaranteed to be positive. Consequently, due to the existence of a vector δ, the system in (6–1) is herdable when the nodes in $\mathcal{V}_1$ are all selected as leaders. □

Theorem 7.3 offers a straightforward way to select leaders for the herdability of structurally balanced networks. This is particularly useful if $|\mathcal{V}_1| << |\mathcal{V}_2|$, since the entire network can be effectively herded by a small set of leaders. However, if the partitioned sets $\mathcal{V}_1$ and $\mathcal{V}_2$ are approximate the same size, Theorem 7.3 can result in a large number of leaders. The following theorem presents how the leader selection algorithm in Theorem 7.3 can be improved by reducing the leader group size. To facilitate the development, the nodes in $\mathcal{V}_1$ with 1-walk neighbors in $\mathcal{V}_2$ are referred to as boundary nodes of $\mathcal{V}_1$.

Theorem 7.4. *Consider a leader-follower system in (6–1) evolving over a connected structurally balanced signed graph $\mathcal{G}$ with nodes grouped into $\mathcal{V}_1$ and $\mathcal{V}_2$. The system in(6–1) remains herdable, if the leaders selected from Theorem 7.3 can be reduced by satisfying all of the following rules: 1) the boundary nodes of $\mathcal{V}_1$ are selected as followers, 2) any boundary node*

is within 1-walk from the reduced leader group, and 3) the non-boundary nodes that are within 1-walk from the reduced leader group are selected as followers.

Proof. Following Theorem 7.3, assume the leaders are only selected from $\mathcal{V}_1$. We further assume that there are m_2 leaders and m_1 followers in $\mathcal{V}_1$, i.e., $m_1 + m_2 = n_1$, where the proposed rules ensure that any follower in $\mathcal{V}_1$ is within 1-walk from the reduced m_2 leaders. The system controllability matrix C is then written as

$$\begin{aligned} C &= \left[\begin{array}{c|c|c|c} B & \mathcal{A}B & \ldots & \mathcal{A}^{n-1}B \end{array}\right] \\ &= \left[\begin{array}{c|c|c} I_{m_2\times m_2} & *_{m_2\times m_2} & * \\ 0_{m_1\times m_2} & \Xi_{m_1\times m_2} & * \\ 0_{n_2\times m_2} & 0_{n_2\times m_2} & \psi_{n_2\times(n-2)m_2} \end{array}\right]. \end{aligned} \tag{7–5}$$

Similar to the proof of Theorem 7.3, to show the system in (6–1) is herdable, we need to show there exists a vector $\delta = \left[\begin{array}{ccc} \delta_1 & \ldots & \delta_{nm_2} \end{array}\right]^T \in \mathbb{R}^{nm_2}$ such that $k = C\delta \in \mathbb{R}^n$ is element-wise positive.

Due to the identity matrix $I_{m_2\times m_2}$, there always exist sufficiently large $\delta_i \in \mathbb{R}^+, i = 1, \ldots, m_2$, such that the first m_2 entries in k are guaranteed to be positive. For the second m_2 columns corresponding to $\mathcal{A}B$, the entries of Ξ represent the weights of 1-walks from leaders to the m_1 followers in $\mathcal{V}_1$. Since the nodes that are 1-walk away from any leader are selected as followers and these m_1 followers are all in $\mathcal{V}_1$, the weights of 1-walks are all non-negative, which indicates the entries in Ξ are all non-negative. Therefore, there always exist sufficiently large $\delta_i \in \mathbb{R}^+, i = m_2 + 1, \ldots, 2m_2$, such that the second m_2 entries in k are guaranteed to be positive. Since the boundary nodes of $\mathcal{V}_1$ are selected as followers, the followers in $\mathcal{V}_2$ are all at least 2-walk away from the leaders, leading to the matrix $0_{n_2\times m_2}$ in the second m_2 columns corresponding to $\mathcal{A}B$.

The entries of ψ represent the weight of walks from leaders to the followers in $\mathcal{V}_2$. If $\mathcal{G}$ is connected, any follower v_k in $\mathcal{V}_2$ can be reached by a leader $v_l \in \mathcal{V}_1$ via a minimum k'-walk containing only one negative edge, since the minimum walk only traverses from $\mathcal{V}_1$ to $\mathcal{V}_2$ once.

As a result, the first non-zero entry in the kth row of C is $\psi_{k,k'm_2+l}$, which is negative and indicates the sum of weights of k'-walks from v_l to v_k. The kth row of (7–5) is in the form of $\begin{bmatrix} \mathbf{0} & \psi_{k,k'm_2+l} & \cdots \end{bmatrix} \in \mathbb{R}^{nm_2}$, where $\mathbf{0}$ is a zero row vector with appropriate dimensions. Therefore, there always exists a sufficiently small $\delta_i \in \mathbb{R}^-$, $i = k'm_2 + l$, such that $\delta_i \psi_{k,k'm_2+l}$ is positive and dominates the sum of rest terms. Following the similar argument for the rest rows of (7–5), it can be shown that there exists proper design of $\delta_i \in \mathbb{R}^-$ such that the last n_2 entries of k are positive.

Based on the analysis above, there exists a vector δ such that $k = C\delta \in \mathbb{R}^n$ is element-wise positive, which indicates the system in (6–1) is herdable. □

To further improve leader selection algorithms, the following method is developed based on graph distances between followers and leaders. Suppose there are $m < n_1$ leaders in $\mathcal{V}_1$ and the rest nodes are followers in $\mathcal{V}_1$ and $\mathcal{V}_2$. Let P^a_{ij}, $i \in \{1, \ldots, m\}$, $j \in \{m+1, \ldots, n\}$, denote the distance (i.e., the minimum walk) from a leader v_i to a follower v_j in $\mathcal{V}_a$, $\{a\} \in \{1, 2\}$. The shortest distance from a follower v_j in $\mathcal{V}_a$ to the leader group is denoted by $\underline{P}^a_j = \min\left\{P^a_{ij}, i \in \{1, \ldots, m\}\right\}$. Similarly, let $\bar{P}^a_j = \max\left\{P^a_{ij}, i \in \{1, \ldots, m\}\right\}$ denote the longest distance from a follower v_j in $\mathcal{V}_a$ to the leader group.

Theorem 7.5. *Consider a leader-follower system in (6–1) evolving over a connected structurally balanced signed graph $\mathcal{G}$ with nodes grouped into $\mathcal{V}_1$ and $\mathcal{V}_2$. Suppose there are $m < n_1$ leaders in $\mathcal{V}_1$. The system in (6–1) is herdable if, for any followers $v_i \in \mathcal{V}_1$ and $v_j \in \mathcal{V}_2$, the selected leaders satisfy $\bar{P}^1_i < \underline{P}^2_j$.*

Proof. Let $\bar{P}^1 = \max\left\{\bar{P}^1_i, i \in \{m+1, \ldots, n_1\}\right\}$ denote the maximum distance (in terms of walks) from followers to the leader group in $\mathcal{V}_1$. Given m leaders in $\mathcal{V}_1$ satisfying the proposed

rule, the system controllability matrix C can be written as

$$
\begin{aligned}
C &= \left[\begin{array}{c|ccc|c|c} B| & \mathcal{A}B & \cdots & \mathcal{A}^{\bar{P}^1}B & \ldots & \mathcal{A}^{n-1}B \end{array}\right] \\
&= \left[\begin{array}{c|c|c} I_{m\times m} & *_{m\times m\bar{P}^1} & \ldots \\ 0_{(n_1-m)\times m} & \Lambda & \ldots \\ 0_{n_2\times m} & 0_{n_2\times m\bar{P}^1} & \Delta \end{array}\right],
\end{aligned} \tag{7–6}
$$

where $\Lambda \in \mathbb{R}^{(n_1-m)\times m\bar{P}^1}$ and $\Delta \in \mathbb{R}^{n_2\times m\left(n-1-\bar{P}^1\right)}$. Similar to the proof of previous theorems, the rest proof is to show the existence of a vector $\delta = \left[\begin{array}{ccc} \delta_1 & \ldots & \delta_{nm} \end{array}\right]^T \in \mathbb{R}^{nm}$ such that $k = C\delta \in \mathbb{R}^n$ is element-wise positive.

First, due to the identity matrix $I_{m\times m}$, there always exist sufficiently large $\delta_i \in \mathbb{R}^+$, $i = 1, \ldots, m$, such that the first m entries in k are guaranteed to be positive. Since the entries of Λ represent the sum of weight within $\bar{P}^1$ walks from leaders to the $n_1 - m$ followers in $\mathcal{V}_1$, these entries are guaranteed to be non-negative, as the nodes in $\mathcal{V}_1$ are positive neighbors. Clearly, there exist sufficiently large $\delta_i \in \mathbb{R}^+$, $i = m+1, \ldots, m\left(\bar{P}^1+1\right)$, such that the corresponding entries in k are guaranteed to be positive. In addition, if the selected leaders satisfy $\bar{P}_i^1 < \underline{P}_j^2$ for any followers $v_i \in \mathcal{V}_1$ and $v_j \in \mathcal{V}_2$, no followers in $\mathcal{V}_2$ are within $\bar{P}^1$ walks to the leader group. As a result, one has the zero matrix $0_{n_2\times m\bar{P}^1}$. In addition, by Lemma 7.2, the entries of Δ are non-positive, since they correspond to the weights of walks from leaders to the followers in $\mathcal{V}_2$. There always exist $\delta_i \in \mathbb{R}^-$, $i = m\left(\bar{P}^1+1\right)+1, \ldots, mn$, such that the last n_2 entries of k are positive. Therefore, due to the existence of a positive element-wise vector $k \in \mathrm{img}\,(C)$, the system is herdable based on Lemma 6.1. □

Theorem 7.5 is more general than Theorem 7.4 in the sense that it only requires the longest distance from the followers in $\mathcal{V}_1$ to the leader group less than the shortest distance from the followers in $\mathcal{V}_2$ to the leader group. Note that the walks among nodes can be computed first using existing algorithms [62]. The leaders can then be selected following the condition in Theorem 7.5. To illustrate the ideas of Theorem 7.3-7.5, the following example is provided.

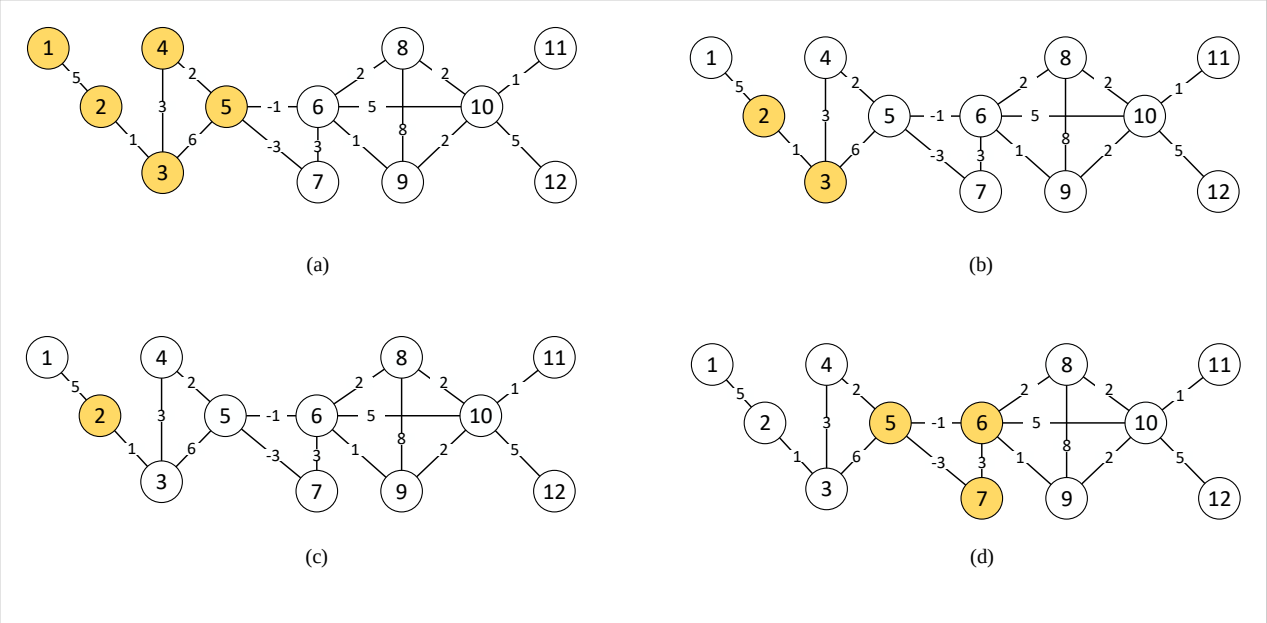

Figure 7-3. Examples of leader group selection in one set for network herdability, where the selected leaders are marked as solid nodes. Figures (a), (b), and (c) follow the developed leader selection algorithms in Theorem 7.3-7.5, respectively.

Example 7.3. Consider a structurally balanced signed network $\mathcal{G}$ with the partitioned sets $\mathcal{V}_1 = \{v_1, v_2, v_3, v_4, v_5\}$ and $\mathcal{V}_2 = \{v_6, v_7, v_8, v_9, v_{10}, v_{11}, v_{12}\}$. Following the leader selection rules in Theorem 7.3, Fig. 7-3 (a) shows a herdable network with all nodes in $\mathcal{V}_1$ selected as the leader group. Fig. 7-3 (b) and (c) illustrate the leader selection rules developed in Theorem 7.4 and Theorem 7.5, respectively.

7.3.2 Selecting Leaders in Two Sets

This section considers selecting leaders from both $\mathcal{V}_1$ and $\mathcal{V}_2$ in a structurally balanced graph.

Theorem 7.6. *Consider a leader-follower system in (6–1) evolving over a connected structurally balanced signed graph $\mathcal{G}$ with nodes grouped into $\mathcal{V}_1$ and $\mathcal{V}_2$. The system in (6–1) is herdable, if the boundary nodes of $\mathcal{V}_1$ and $\mathcal{V}_2$ are all selected as leaders.*

Proof. Suppose there are m boundary nodes. Assume there are m_1 leaders and q_1 followers in $\mathcal{V}_1$, and m_2 leaders and q_2 followers in $\mathcal{V}_2$, where $m_1 + m_2 = m$. The leader and follower group in $\mathcal{V}_1$ and $\mathcal{V}_2$ are represented as $\mathcal{V}_l^1$, $\mathcal{V}_f^1$, $\mathcal{V}_l^2$, and $\mathcal{V}_f^2$, respectively.

To facilitate the analysis, the followers are grouped based on the distance to the leaders within the same partitioned set. Specifically, the followers in $\mathcal{V}_f^1$ that are k walks away from the leader group $\mathcal{V}_l^1$ are grouped as f_k^1, and the group size is $|f_k^1|$ such that $\sum_k |f_k^1| = q_1$. The followers in $\mathcal{V}_f^2$ are defined similarly by f_k^2 and $|f_k^2|$ where $\sum_k |f_k^2| = q_2$. Let p and q be the longest distance from followers to leaders within $\mathcal{V}_1$ and $\mathcal{V}_2$, respectively.

Based on the grouped followers, the system controllability matrix C can be written as

$$
\begin{aligned}
C &= \begin{bmatrix} B & \mathcal{A}B & \dots & \mathcal{A}^{n-1}B \end{bmatrix} \\
&= \begin{bmatrix}
I_{m\times m} & * & * & \cdots & * & * & * \\
\mathbf{0} & \phi_1^1 & * & \cdots & * & * & * \\
\vdots & \mathbf{0} & \phi_1^2 & \cdots & * & * & * \\
\vdots & \vdots & \mathbf{0} & \ddots & * & * & * \\
\vdots & \vdots & \vdots & \cdots & \phi_p^1 & * & * \\
\mathbf{0} & \mathbf{0} & \mathbf{0} & \cdots & \mathbf{0} & \phi_q^2 & *
\end{bmatrix},
\end{aligned}
\tag{7–7}
$$

where $\phi_i^1 \in \mathbb{R}^{|f_i^1|\times m_1}$, $i = 1, \dots, p$, represent the sum of weights of all i-walk from $\mathcal{V}_l^1$ to $\mathcal{V}_f^1$, $\phi_j^2 \in \mathbb{R}^{|f_j^2|\times m_2}$, $j = 1, \dots, q$, represent the sum of weights of j-walk from $\mathcal{V}_l^2$ to $\mathcal{V}_f^2$, $\mathbf{0}$ represent zero matrices with appropriate dimensions, and $*$ represent matrices of no interest. By Lemma 6.1, the rest proof is to show the existence of a vector $\delta = \begin{bmatrix} \delta_1 & \dots & \delta_{nm} \end{bmatrix}^T \in \mathbb{R}^{nm}$ such that $k = C\delta \in \mathbb{R}^n$ is element-wise positive.

First, due to the identity matrix $I_{m\times m}$, there always exist sufficiently large $\delta_i \in \mathbb{R}^+$, $i = 1, \dots, m$, such that the first m entries in k are guaranteed to be positive. The nonzero entries of ϕ_1^1 indicate that the followers in $f_1^1 \subseteq \mathcal{V}_f^1$ can be reached by the leaders in $\mathcal{V}_l^1$ within 1-walk. Since they are in the same $\mathcal{V}_1$, the nonzero entries of ϕ_1^1 are all positive. Note that the followers in f_i^1, $i > 1$, can not be reached by the leaders in $\mathcal{V}_l^1$ within 1-walk, which gives rise the zero matrices. Similarly, the nonzero entries of ϕ_1^2 are positive due to the fact that the followers in $f_1^2 \subseteq \mathcal{V}_f^2$ can be reached by the leaders in $\mathcal{V}_l^2$ within 1-walk and they are in the same $\mathcal{V}_2$. Following similar argument for the rest followers, it can be shown the nonzero entries of ϕ_i^1,

Table 7-1. Nodal Distance from $\mathcal{V}_1$

Node Set	Node numbers	Highest Distance in $\mathcal{V}_1$	Lowest Distance in $\mathcal{V}_2$
$\mathcal{V}_1$	1	3,(v_4, v_8)	3,(v_{11}, v_{12}, v_{13})
	2	3, (v_9)	3,(v_{12}, v_{15})
	3	3,(v_9)	3, (v_{12}, v_{15})
	4	4, (v_9)	13, (v_{13})
	5	3,(v_4, v_8)	3, (v_{14}, v_{15})
	6	2,(v_1, v_4, v_8, v_9)	2,(v_{15})
	7	3,(v_9)	3,(v_{12}, v_{15})
	8	4,(v_9)	3, (v_{13})
	9	4,(v_4, v_8)	1, (v_{12})
	10	3, (v_8)	2, (v_{12}, v_{13})
	11	3,(v_1, v_4)	1,(v_{13})

$i = 2, \ldots, p$, and ϕ_i^2, $i = 2, \ldots, q$, are all positive. Consequently, there always exist proper design $\delta_i \in \mathbb{R}^+, i = m+1, ...mn$, such that k is element-wise positive, which indicates the network $\mathcal{G}$ is herdable. □

Example 7.4. Reconsider the structurally balanced signed graph in Example 7.3. The idea of selecting boundary nodes as leaders is illustrated in Fig. 7-3 (d).

7.3.3 Numerical Example

In this section, an illustrative example on a structurally balanced network is given to show the application of Theorem 7.5. To show the generalization of the developed theorems, consider a signed balanced graph with 20 nodes shown in Fig. 7-4, where the edges with negative signs capture arbitrary negative weights, while the edges without negative signs represent arbitrary positive weights. The example will show how to utilize Theorem 7.5 to select proper leaders to ensure network herdability through graph distance. The graph distances between any pair of nodes are calculated first. Followed by Theorem 7.5, the shortest distance from v_i to v_j ($v_i \in \mathcal{V}_p$, $v_j \in \mathcal{V}_q$, $p \neq q$) and the longest distance from v_i to v_j ($v_i \in \mathcal{V}_p$, $v_j \in \mathcal{V}_q$, $p = q$) are presented in Table 7-1 and Table 7-2, respectively. Based on the results in Table 7-1 and Theorem 7.5, to select any node from the set $\{v_{16}, v_{17}, v_{18}, v_{19}, v_{20}\}$ can ensure the balanced network to be herdable.

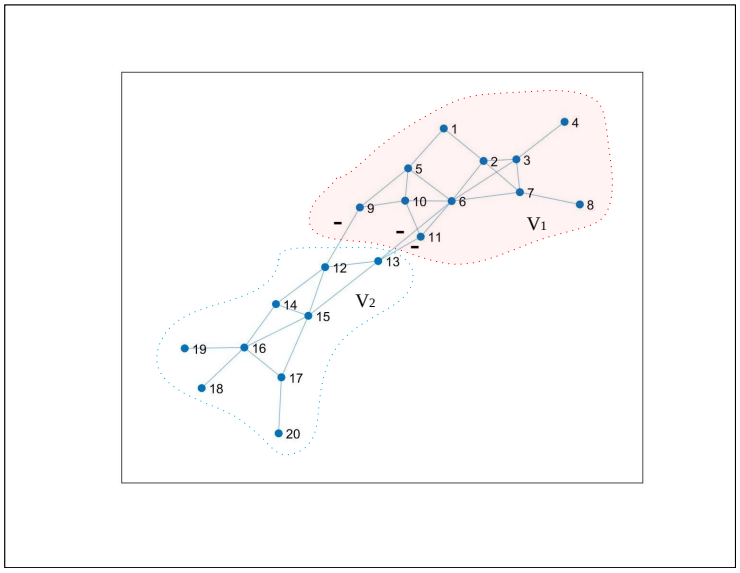

Figure 7-4. A Signed Balanced Graph

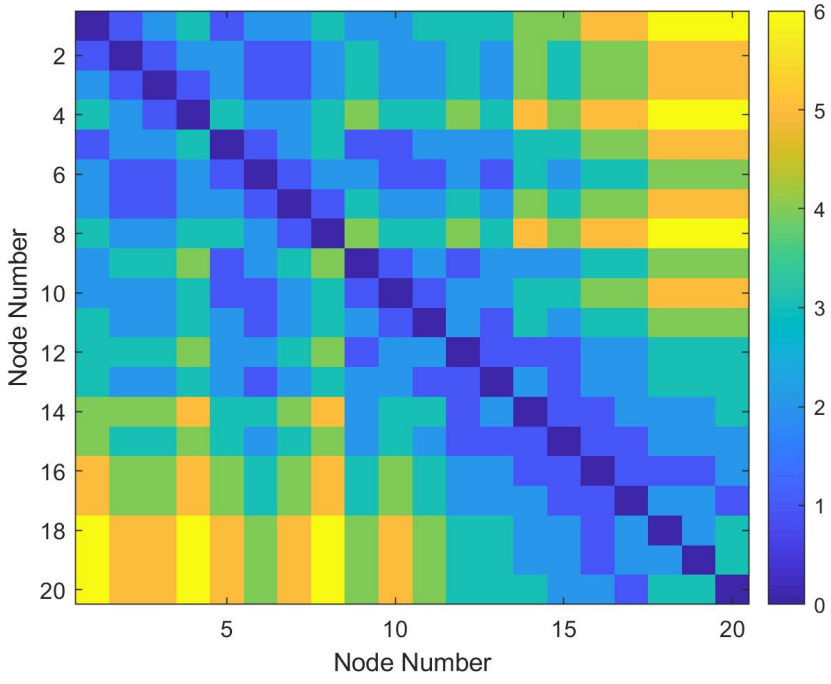

Figure 7-5. Distance Matrix

Table 7-2. Nodal Distance from $\mathcal{V}_2$

Node Set	Node numbers	Highest Distance in $\mathcal{V}_2$	Lowest Distance in $\mathcal{V}_1$
$\mathcal{V}_2$	12	$3(v_{18}, v_{19}, v_{20})$	$1(v_9)$
	13	$3(v_{18}, v_{19}, v_{20})$	$1(v_6, v_{11})$
	14	$3(v_{20})$	$2(v_9)$
	15	$2(v_{18}, v_{19}, v_{20})$	$2(v_9, v_{11})$
	16	$2(v_{12}, v_{13}, v_{20})$	$3(v_6, v_9, v_{11})$
	17	$2(v_{12}, v_{13}, v_{14}, v_{18}, v_{19})$	$3(v_6, v_9, v_{11})$
	18	$3(v_{12}, v_{13}, v_{20})$	$4(v_6, v_9, v_{11})$
	19	$3(v_{12}, v_{13}, v_{20})$	$4(v_6, v_9, v_{11})$
	20	$3(v_{12}, v_{13}, v_{14}, v_{18}, v_{19})$	$4(v_6, v_9, v_{11})$

7.4 Summary

In this Chapter, leader group selection to ensure network herdability is investigated through graph walks on general signed networks and structurally balanced networks. Several graph-theoretic methods are proposed to build the connection between graph structure and network herdability. Future work will extend the concept of network herdability to other cases, such as, to driven system states to a specific set of the controllable subspace, as well as explore novel graph methods to capture network herdability.

CHAPTER 8
ALGEBRAIC TOPOLOGICAL CHARACTERIZATIONS OF STRUCTURAL BALANCE ON COMPLEX NETWORKS

Due to the significance of the structural balance in network performance as explored in Chapter 2-7, Chapter 8 is particularly motivated to investigate the fundamental relationship between the structural balance and the underlying topological structure of signed networks. Different from existing graph-theoretic approaches, simplicial complexes are employed as the primary tool to model the signed graph. The developed topological characterizations reveal the fundamental relationship between the structural balance and the underlying network topology by showing that the structural balance is closely related to the first homology and cohomology of the modeled simplicial complex. In particular, the vanishing first homology and cohomology along with positive 3-node circular subgraphs are found to be sufficient to lead to a structurally balanced network. A necessary and sufficient condition is developed to characterize structure balance on signed networks through the 3-node circular subgraphs and first homology groups of simplicial complex.

8.1 Problem Formulation

Consider a network with cooperative and antagonistic interactions represented by an undirected signed graph $\mathcal{G} = (\mathcal{V}, \mathcal{E}, \mathcal{A})$, where the node set $\mathcal{V} = \{v_1, \ldots, v_n\}$ and the edge set $\mathcal{E} \subset \mathcal{V} \times \mathcal{V}$ represent the individuals and the interactions between pairs of individuals, respectively. Let $a_{ij} \colon \mathcal{E} \to \{\pm 1\}$ denote the weight associated with the edge $(v_i, v_j) \in \mathcal{E}$. If $a_{ij} = 1$, v_i and v_j are called positive neighbors and negative neighbors if $a_{ij} = -1$. Positive neighborhood indicates cooperative interactions while negative neighborhood indicates competitive interactions. The interactions within $\mathcal{G}$ are then captured by the adjacency matrix $\mathcal{A} = [a_{ij}] \in \mathbb{R}^{n \times n}$, where $a_{ij} = 0$ if $(v_i, v_j) \notin \mathcal{E}$. No self-loop is considered, i.e., $a_{ii} = 0$ $\forall i = 1, \ldots, n$.

Def. 2.2 in Chapter 2 indicates that, for a structurally balanced graph, the nodes within the same subgroup (i.e., $\mathcal{V}_1$ or $\mathcal{V}_2$) contain only positive neighbors, while nodes from different subgroups are negative neighbors. Based on Def. 2.2, various graph-theoretic characterizations

of the structural balance were developed in the literature [2, 119–121]. As a complement to the existing results, rather than using traditional graph-theoretic approaches as in [2, 119–121], the objective of this Chapter is to characterize the structural balance of signed graphs based on a new perspective from algebraic topology, and exploits algebraic topological tools to develop topological insights of the structural balance.

8.2 Algebraic Topological Characterizations of Structural Balance

Topological characterizations of the structural balance in signed graphs are developed in this section. To facilitate the development, algebraic topology is briefly reviewed in Section 8.2.1 (cf. [87] for a detailed explanation). Leveraging tools from algebraic topology, topological characterizations of the structural balance are extracted in Section 8.2.2. Examples are provided in Section 8.2.3 to elaborate on the developed topological characterizations.

8.2.1 Background on Simplicial Complex, Homology, and Cohomology

Let $\mathcal{V} = \{v_i\}, i \in \{0, \ldots, n-1\}$, be a finite set of n points. A *k-simplex* σ_k (or a k-dimensional simplex) is a k-dimensional convex polyhedron formed by an unordered set $\{v_0, \ldots, v_k\} \subseteq \mathcal{V}$ with $v_i \neq v_j$ for all $i \neq j$. The faces of the σ_k consist of $(k-1)$-simplices of the form $\{v_0, \ldots, v_{i-1}, v_{i+1}, \ldots, v_k\}$ for $0 \leq i \leq k$. A *simplicial complex* X is then defined as a finite collection of simplices closed with respect to the inclusion of faces. In terms of geometrical realization, a simplicial complex is a combinatorial object composed of simplices, where graphical components (e.g., nodes, edges, and cliques[1]) can be represented by simplices of various dimensions. In addition to binary relations by edges in conventional graphs, a simplicial complex also captures higher-order relations among a set of nodes by simplices of higher dimensions. Simplicial complexes thereby represent a generalization of traditional graphs, providing a global topological characterization of graphs.

Example 8.1. To illustrate the simplicial complex, graphical examples are provided in Fig. 8-1. Fig. 8-1 (a) and (b) show that nodes and edges in graphs are 0-simplices and 1-simplices,

[1] A clique is a complete graph formed by a subset of nodes.

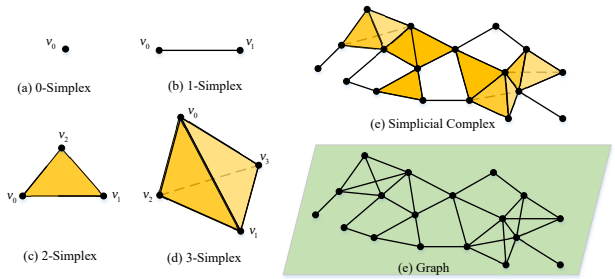

Figure 8-1. The illustration of the simplices and the simplicial complex.

respectively. Fully connected subsets of nodes (i.e., cliques) can be represented by higher-order simplices. For instance, a complete graph of 3 nodes corresponds to a 2-simplex (i.e., a triangle) in Fig. 8-1 (c), while a complete graph of 4 nodes corresponds to a 3-simplex (i.e., a tetrahedron) in Fig. 8-1 (d). Fig. 8-1 (e) shows the construction of a simplicial complex from a conventional graph, where the graph at the bottom can be considered as the projection of the simplicial complex onto a 2D plane, in which all simplices with dimension greater than 1 are neglected. Note that, in Fig. 8-1 (e), the edge connections in the graph at the bottom are preserved in the simplicial complex by the 0-simplices and 1-simplices. No existing relationships are lost when modeling a graph by a simplicial complex. Therefore, any features that can be extracted from graphs are preserved in the corresponding simplicial complex.

An orientation of a k-simplex is induced by an ordering of its vertices, where two orderings are equivalent if and only if one can be obtained from the other by an even permutation. In particular, A *k-simplex* $\{v_0, \ldots, v_k\}$ with an ordering is denoted by $[v_0, \ldots, v_k]$, and a change in the ordering corresponds to a change in the sign of the simplex, i.e., $[v_0, \ldots, v_i, \ldots, v_j, \ldots, v_k] = -[v_0, \ldots, v_j, \ldots, v_i, \ldots, v_k]$. Given an oriented simplicial complex[2] X, for each $k \geq 0$,

[2] Oriented simplicial complexes are used throughout in this Chapter. Please note that oriented simplicial complexes are different from ordered simplicial complexes which are simply simplicial complexes with ordered vertices. For instance, $[a, b, c]$ and $[c, a, b]$ are two different ordered 2-simplexes as the vertices have different orders, while $[a, b, c]$ and $[c, a, b]$ are the same orientated 2-simplexes as $[c, a, b] = -[a, c, b] = [a, b, c]$.

$C_k(X;\mathbb{Z})$ is a free abelian group whose basis is the set of oriented k-simplices $\sigma_k \in X$. The elements of $C_k(X;\mathbb{Z})$ are called *k-chains*, where a k-chain is defined as a sum of the form $\sum_j a_j \sigma_j^{(k)}$ with $a_j \in \mathbb{Z}$ and $\sigma_j^{(k)}$ denoting an oriented k-simplex σ_k. From the definition of k-chains, the vector space $C_k(X;\mathbb{Z})$ is clearly an additive abelian group[3] . It is worth pointing out that other types of abelian groups, such as multiplicative abelian groups, are also applicable. The dimension of X is the maximum dimension of its simplices. If k is larger than the dimension of X, $C_k(X;\mathbb{Z}) = 0$.

The k-th simplicial boundary map is a homomorphism[4] $\partial_k \colon C_k(X;\mathbb{Z}) \to C_{k-1}(X;\mathbb{Z})$ defined as

$$\partial_k [v_0, \ldots, v_k] = \sum_{j=0}^{k} (-1)^j [v_0, \ldots, \hat{v}_j, \ldots, v_k], \tag{8–1}$$

where $\hat{v}_j$ indicates that v_j is removed from the sequence $v_0, \ldots, v_k$. A *chain complex* is a sequence of homomorphism,

$$\cdots \xrightarrow{\partial_{k+2}} C_{k+1} \xrightarrow{\partial_{k+1}} C_k \xrightarrow{\partial_k} C_{k-1} \xrightarrow{\partial_{k-1}} \cdots, \tag{8–2}$$

where the homomorphism ∂_k satisfies $\partial_{k-1} \circ \partial_k = 0$ [87], i.e., the image of ∂_k is included in the kernel of ∂_{k-1}.

Example 8.2. Fig. 8-2 illustrates the boundary maps on oriented simplices. For instance, the oriented 1-simplex $[v_0, v_1]$ corresponds to an edge, where the boundary map in (8–1) yields $\partial_1 [v_0, v_1] = [v_1] - [v_0]$. Similarly, a 2-simplex $[v_0, v_1, v_2]$ corresponds to a triangle with the boundary map $\partial_2 [v_0, v_1, v_2] = [v_1, v_2] - [v_0, v_2] + [v_0, v_1]$, while a 3-simplex $[v_0, v_1, v_2, v_3]$

[3] An additive abelian group $(G, +)$ is a set G together with a binary operation $+ \colon G \times G \to G$ satisfying the following axioms: 1) associativity: $(a + b) + c = a + (b + c)$ for all $a, b, c \in G$; 2) commutativity: $a + b = b + a$ for all $a, b \in G$; 3) identity element is 0 satisfying $a + 0 = a$ for each $a \in G$; and 4) the inverse element $a^{-1} = -a$ for each $a \in G$ such that $a + (-a) = 0$ [122]. Some example additive abelian groups are the set of integers $\mathbb{Z}$, the set of rationals $\mathbb{Q}$, and the set of reals $\mathbb{R}$.

[4] If $(A, \cdot)$ and $(B, *)$ are two abelian groups with operations $\cdot$ and $*$, a homomorphism is a mapping $f \colon A \to B$ satisfying $f(a \cdot b) = f(a) * f(b)$ for all $a, b \in A$ [122].

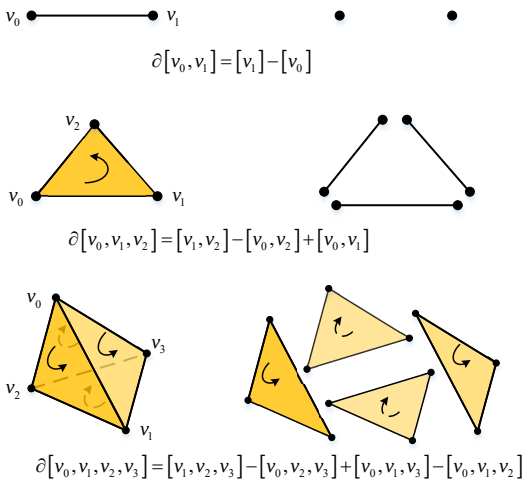

Figure 8-2. The boundary maps of an oriented 1-simplex, 2-simplex, and 3-simplex.

corresponds to a tetrahedron with the boundary map $\partial_3 [v_0, v_1, v_2, v_3] = [v_1, v_2, v_3] - [v_0, v_2, v_3] + [v_0, v_1, v_3] - [v_0, v_1, v_2]$.

As basic building blocks for simplicial homology, the *k-cycles* and the *k-boundaries* are defined as

$$\begin{aligned} k\text{-cycles: } &\ker \partial_k = \{x \in C_k | \, \partial_k x = 0\}, \\ k\text{-boundaries: } &\mathrm{img}\partial_{k+1} = \{x \in C_k | \, \exists y \text{ s.t. } x = \partial_{k+1} y\}. \end{aligned} \tag{8–3}$$

Intuitively, $\ker \partial_k$ indicates a set of k-chains without boundary and therefore represent k-dimensional cycles in the simplicial complex X. Since some of the k-cycles also bound a subcomplex of dimension $k+1$ in X, the k-boundaries in (8–3) particularly indicate a set of k-chains forming boundaries of higher-dimensional chains. Based on the k-cycles and the k-boundaries, the kth simplicial homology is defined as the quotient vector space

$$\mathcal{H}_k(X;\mathbb{Z}) \triangleq \ker \partial_k / \mathrm{img}\partial_{k+1}. \tag{8–4}$$

Consequently, $\mathcal{H}_k$ indicates the k-dimensional cycles that are not the boundaries of higher-dimensional chains, and the dimension of $\mathcal{H}_k$ is the number of "k-dimensional holes" in X. For instance, the uncolored quadrilaterals of the simplicial complex in Fig. 8-1 (e) are elements of the first homology group $\mathcal{H}_1$ indicating 1-dimensional holes, since the edges of the quadrilaterals

form 1-cycles that are not the boundaries of any higher-dimensional simplices. Despite various types, the graphs can be topologically identical in terms of the number of k-dimensional cycles. As a topological invariant, $\mathcal{H}_k$ provides a characterization of topological structures of graphs.

Cohomology groups are constructed by turning chain groups C_k into groups of homomorphisms and boundary operators ∂_k into their dual homomorphisms. Specifically, given a chain group C_k and an abelian group $\mp$, a *k-dimensional cochain* $C^k(X;\mp)$ is defined as a homomorphism $\varphi\colon C_k \to \mp$, which maps elements in C_k to $\mp$. Note that the cochains C^k are also abelian groups. A *cochain complex* is a dual notion to the chain complex in (8–2) as

$$\cdots \xrightarrow{\delta^{k-1}} C^{k-1} \xrightarrow{\delta^{k}} C^{k} \xrightarrow{\delta^{k+1}} C^{k+1} \xrightarrow{\delta^{k+2}} \cdots \tag{8–5}$$

where $\delta^k\colon C^{k-1} \to C^k$ represents the dual homomorphism to ∂_k, satisfying $\delta^{k+1} \circ \delta^k = 0$. The cochain complex in (8–5) represents maps between abelian groups C^k but with reversed arrows. The *k-cocycles* and the *k-coboundaries* are defined as

$$\begin{aligned} k\text{-cocycles: } \ker \delta^{k+1} &= \left\{ x \in C^k \middle| \, \delta^{k+1} x = 0 \right\}, \\ k\text{-coboundaries: } \mathrm{img}\delta^{k} &= \left\{ x \in C^k \middle| \, \exists y \text{ s.t. } x = \delta_k y \right\}. \end{aligned} \tag{8–6}$$

Based on k-cocycles and k-coboundaries, the kth cohomology is then defined as

$$\mathcal{H}^k(X;\mathcal{A}) \triangleq \ker \delta^{k+1} / \mathrm{img}\delta^k. \tag{8–7}$$

8.2.2 Homology and Cohomology Based Characterizations of Structural Balance

To develop homology and cohomology based characterizations, we start from modeling the signed graph $\mathcal{G}$ by a simplicial complex $X_{\mathcal{G}}$, where existing methods in [87–89] can be used to construct $X_{\mathcal{G}}$. Based on the constructed $X_{\mathcal{G}}$, the cohomology-based topological characterization is developed first, followed by an extension to homology-based characterizations. Consider

the group $\mp$ in (8–7) taking the form of a multiplicative abelian group[5] $(\mathbb{Z}_2, \times)$ with the basis $\mathbb{Z}_2 = \{-1, 1\}$ and the multiplication operation "$\times$". The multiplicative abelian group $(\mathbb{Z}_2, \times)$ is particularly motivated by the use of the product of edge weights. Let $\varphi\colon X_{\mathcal{G}} \to \mathbb{Z}_2$ be a group homomorphism mapping simplices in $X_{\mathcal{G}}$ to an element in $\mathbb{Z}_2$, i.e., each simplex is marked as -1 or $+1$. In particular, the homomorphism φ maps each edge (v_i, v_j) in $\mathcal{G}$ to its weight w_{ij}, i.e., $\varphi([v_i, v_j]) = w_{ij}$ where $[v_i, v_j]$ is the corresponding 1-simplex in $X_{\mathcal{G}}$. The cochain group $C^k(X_{\mathcal{G}}; \mathbb{Z}_2)$ is thereby formed by $\varphi(\sigma_k)$, where σ_k denotes oriented k-simplices in $X_{\mathcal{G}}$.

The cochain complex on $X_{\mathcal{G}}$ with the group $(\mathbb{Z}_2, \times)$ is defined as

$$\cdots \xrightarrow{\delta^{k-1}} C^{k-1}(X_{\mathcal{G}}; \mathbb{Z}_2) \xrightarrow{\delta^k} C^k(X_{\mathcal{G}}; \mathbb{Z}_2) \xrightarrow{\delta^{k+1}} \cdots, \tag{8–8}$$

where the coboundary δ^k maps an element in $C^{k-1}(X_{\mathcal{G}}; \mathbb{Z}_2)$ to an element in the group $C^k(X_{\mathcal{G}}; \mathbb{Z}_2)$. Specifically, given an oriented $(k-1)$-simplex $[v_0, \ldots, v_{k-1}]$ and an oriented k-simplex $[v_0, \ldots, v_k]$,

$$\begin{aligned} \delta^k \varphi([v_0, \ldots, v_{k-1}]) &= \varphi([v_0, \ldots, v_k]) \\ &= \prod_{j=0}^{k} \varphi^{(-1)^j}([v_0, \ldots, \hat{v}_j, \ldots, v_k]) \end{aligned} \tag{8–9}$$

where $\hat{v}_j$ indicates that v_j is removed and φ^{-1} denotes the inverse element in $(\mathbb{Z}_2, \times)$. Due to the consideration of a multiplicative abelian group, $\varphi([v_0, \ldots, v_k])$ in (8–9) is written as products, rather than the sums in (8–1) as an additive abelian group. For instance, given a 0-simplex v_0 and a 1-simplex $[v_0, v_1]$ in $X_{\mathcal{G}}$, the coboundary δ^1 mapping $\varphi(v_0) \in C^0(X_{\mathcal{G}}; \mathbb{Z}_2)$ to

[5] A multiplicative abelian group $(G, \times)$ is a set G together with a binary multiplication operation $\times$ that maps the product $c = ab$ to G for any $a, b \in G$. The multiplicative abelian group $(G, \times)$ is associative (i.e., $(ab)c = a(bc)$ for all $a, b, c \in G$) and commutative (i.e., $ab = ba$ for all $a, b \in G$). In addition, for each $a \in G$, there exists an identity element of 1 satisfying $a \times 1 = a$ and an inverse element of a^{-1} such that $aa^{-1} = 1$. For instance, the integers $\mathbb{Z} \setminus \{0\}$, the rationals $\mathbb{Q} \setminus \{0\}$, and the reals $\mathbb{R} \setminus \{0\}$ are all multiplicative abelian groups.

$\varphi([v_0, v_1]) \in C^1(X_{\mathcal{G}}; \mathbb{Z}_2)$ by $\delta^1\varphi(v_0) = \varphi([v_0, v_1]) = \varphi(v_1)\varphi^{-1}(v_0) = \varphi(v_0)\varphi(v_1)$, where the fact that $\varphi^{-1}(v_0)\varphi(v_0) = 1$ in $(\mathbb{Z}_2, \times)$ is used.

Based on the cochain complex in (8–8), the kernel group $\ker \delta^{k+1}$ is defined as

$$\ker \delta^{k+1} = \{x \in C^k(X_{\mathcal{G}}; \mathbb{Z}_2) \mid \delta^{k+1}x = 1\}, \tag{8–10}$$

where $\delta^{k+1}x = 1$ indicates that 1 is the identity element of the multiplicative abelian group. Similar to (8–6) and (8–7), the $\mathrm{img}\delta^k$ of $C^k(X_{\mathcal{G}}; \mathbb{Z}_2)$ and the kth cohomology are defined as

$$\mathrm{img}\delta^k = \left\{ x \in C^k(X_{\mathcal{G}}; \mathbb{Z}_2) \middle| \exists y \text{ s.t. } x = \delta^k y \right\}, \tag{8–11}$$

and

$$\mathcal{H}^k(X_{\mathcal{G}}; \mathbb{Z}_2) \triangleq \ker \delta^{k+1}/\mathrm{img}\delta^k, \tag{8–12}$$

respectively.

Lemma 8.1. *Consider a signed graph $\mathcal{G}$ modeled by a simplicial complex $X_{\mathcal{G}}$. Suppose that there exists a circular subgraph in $\mathcal{G}$ composed of three vertices $\{v_i, v_j, v_k\}$, which corresponds to an oriented 2-simplex $[v_i, v_j, v_k]$ in $X_{\mathcal{G}}$. The circular subgraph is positive if and only if $\varphi([v_i, v_j]) \in \ker \delta^2$.*

Proof. To prove the sufficient condition, if $\varphi([v_i, v_j]) \in \ker \delta^2$, the definition of cocycles in (8–10) implies $\delta^2\varphi([v_i, v_j]) = 1$. Since $[v_i, v_j, v_k]$ is a 2-simplex containing $[v_i, v_j]$, the homomorphism yields

$$\begin{aligned}
\delta^2\varphi([v_i, v_j]) &= \varphi([v_i, v_j, v_k]) \\
&= \varphi([v_j, v_k])\varphi^{-1}([v_i, v_k])\varphi([v_i, v_j]) \\
&= \varphi([v_j, v_k])\varphi([v_k, v_i])\varphi([v_i, v_j]) = 1,
\end{aligned}$$

where $\varphi^{-1}([v_i, v_k]) = \varphi([v_k, v_i])$ is due to the change of the ordering of vertices. Since φ maps an edge in $\mathcal{G}$ to its edge weight, $\varphi([v_j, v_k])\varphi([v_k, v_i])\varphi([v_i, v_j]) = 1$ indicates that the product

of the edge weights is one. Therefore, the circular subgraph composed of $\{v_i, v_j, v_k\}$ is a positive cycle.

To prove the necessary condition, if the circular subgraph with nodes $\{v_i, v_j, v_k\}$ in $\mathcal{G}$ is positive,

$$\begin{aligned} 1 &= \varphi\left([v_j, v_k]\right) \varphi\left([v_k, v_i]\right) \varphi\left([v_i, v_j]\right) \\ &= \varphi\left([v_j, v_k]\right) \varphi^{-1}\left([v_i, v_k]\right) \varphi\left([v_i, v_j]\right) \\ &= \delta^2 \varphi\left([v_i, v_j]\right), \end{aligned}$$

which indicates that $\varphi\left([v_i, v_j]\right) \in \ker \delta^2$. □

Theorem 8.1. *Given the simplicial complex $X_{\mathcal{G}}$ modeling the signed graph $\mathcal{G}$, $\mathcal{G}$ is structurally balanced if all 3-node circular subgraphs (i.e., circles composed of three vertices $\{v_i, v_j, v_k\}$) are positive and the first cohomology satisfies $\mathcal{H}^1\left(X_{\mathcal{G}}; \mathbb{Z}_2\right) = 0$.*

Proof. According to (8–12), the first cohomology $\mathcal{H}^1\left(X_{\mathcal{G}}; \mathbb{Z}_2\right)$ is defined as a quotient vector space of $\ker \delta^2$ and $\mathrm{img}\delta^1$. If $\mathcal{H}^1 = 0$, then

$$\ker \delta^2 = \mathrm{img}\delta^1, \tag{8–13}$$

which indicates that the set of 1-cocycles (i.e., $\ker \delta^2$) coincides with the set of 1-coboundaries (i.e., $\mathrm{img}\delta^1$). If all 3-node circular graphs $\{v_i, v_j, v_k\}$ in $\mathcal{G}$ are positive, by Lemma 8.1, we know that $\varphi\left([v_j, v_k]\right) \varphi\left([v_k, v_i]\right) \varphi\left([v_i, v_j]\right) = 1$ and $\varphi\left([v_i, v_j]\right) \in \ker \delta^2$. From (8–13), $\varphi\left([v_i, v_j]\right)$ also belongs to $\mathrm{img}\delta^1$. Therefore, there exists a 0-simplex v_i that can be mapped to $[v_i, v_j]$ by the definition of k-coboundary in (8–11).

Due to the consideration of $\left(\mathbb{Z}_2, \times\right)$, the homomorphism $\varphi\left(v_i\right)$ also maps the 0-simplex v_i in $X_{\mathcal{G}}$ (i.e., the node v_i in $\mathcal{G}$) to either -1 or 1. Clearly, $C^0\left(X_{\mathcal{G}}; \mathbb{Z}_2\right)$ is an abelian group with $\varphi\left(v_i\right)$ as its basis. Suppose that the node set $\mathcal{V}$ in $\mathcal{G}$ can be partitioned into two sets $\mathcal{V}_1$ and $\mathcal{V}_2$, where $\mathcal{V}_1 \cap \mathcal{V}_2 = \emptyset$ and $\mathcal{V}_1 \cup \mathcal{V}_2 = \mathcal{V}$. Without loss of generality, let $\varphi\left(v_i\right) = 1$ if $v_i \in \mathcal{V}_1$ and $\varphi\left(v_i\right) = -1$ otherwise. If an edge $\left(v_i, v_j\right)$ in $\mathcal{G}$ is positive, its corresponding 1-simplex $[v_i, v_j]$ in

$X_{\mathcal{G}}$ satisfies

$$\varphi\left([v_i, v_j]\right) = \varphi\left(v_i\right)\varphi\left(v_j\right) = 1, \tag{8–14}$$

which can only be true when $\varphi\left(v_i\right)$ and $\varphi\left(v_j\right)$ are both positive or both negative. Therefore, $\varphi\left([v_i, v_j]\right) = 1$ in (8–14) indicates that v_i and v_j are from the same set, i.e., either both from $\mathcal{V}_1$ or both from $\mathcal{V}_2$. Analogously, if an edge (v_i, v_j) in $\mathcal{G}$ is negative, $\varphi\left([v_i, v_j]\right) = -1$ indicates that v_i and v_j are from different sets. Therefore, positive neighbors only exist in the same subset (i.e., either $\mathcal{V}_1$ or $\mathcal{V}_2$), while negative neighbors come from different subsets, which indicates that the signed graph $\mathcal{G}$ is structurally balanced by Def. 2.2. □

Note that homology and cohomology are computable topological invariants and various existing methods can be used to verify if the first homology or cohomology is vanishing [123]. Theorem 8.1 indicates that, if a simplicial complex $X_{\mathcal{G}}$ has a vanishing first cohomology $\mathcal{H}^1\left(X_{\mathcal{G}}; \mathbb{Z}_2\right) = 0$, the existence of the structural balance in $\mathcal{G}$ can be verified by only checking whether all 3-node circular subgraphs are positive. In addition, the developed characterization based on the vanishing cohomology in Theorem 8.1 unravels the fundamental relationship between the structural balance and the network structure from a global topological perspective. Since homology has an intuitive interpretation as "holes" in the constructed simplicial complex, the following corollary shows how Theorem 8.1 can be extended based on the first homology.

Corollary 8.1. *The signed graph $\mathcal{G}$ is structurally balanced if all 3-node circular subgraphs are positive and the first homology satisfies $\mathcal{H}_1\left(X_{\mathcal{G}}; \mathbb{Z}\right) = 0$, where $X_{\mathcal{G}}$ is the simplicial complex constructed from $\mathcal{G}$.*

The universal coefficient theorem for cohomology in [87] indicates that, if the first homology satisfies $\mathcal{H}_1\left(X_{\mathcal{G}}; \mathbb{Z}\right) = 0$, the first cohomology must have $\mathcal{H}^1\left(X_{\mathcal{G}}; \mp\right) = 0$, where $\mp$ is an abelian group. Therefore, Corollary 8.1 is a direct consequence of Theorem 8.1, where the abelian group $\mp$ takes a particular form of $\mathbb{Z}_2$.

Remark 8.1. Compared to the condition of $\mathcal{H}^1\left(X_{\mathcal{G}}; \mathbb{Z}_2\right) = 0$ in Theorem 8.1, a stronger condition of $\mathcal{H}_1\left(X_{\mathcal{G}}; \mathbb{Z}\right) = 0$ is required in Corollary 8.1. Note that $\mathcal{H}_1\left(X_{\mathcal{G}}; \mathbb{Z}\right) = 0$ can be true for a

variety of networks. For instance, there is a high probability that the first homology vanishes in large random graphs [124].

Corollary 8.2. *A complete signed graph $\mathcal{G}$ is structurally balanced if all 3-node circular subgraphs are positive.*

It is well known that a complete graph always has vanishing homologies [87]. Therefore, when considering a complete signed graph $\mathcal{G}$, the condition of $\mathcal{H}_1(X_{\mathcal{G}};\mathbb{Z}) = 0$ in Corollary 8.1 can be further relaxed in Corollary 8.2. When $\mathcal{G}$ is complete, the verification of the structural balance boils down to checking whether all 3-node circular subgraphs in $\mathcal{G}$ are positive.

Theorem 8.2. *Consider a signed graph $\mathcal{G}$ modeled by a simplicial complex $X_{\mathcal{G}}$, where the first homology $\mathcal{H}_1(X_{\mathcal{G}};\mathbb{Z})$ is nonzero. The signed graph $\mathcal{G}$ is structurally balanced if and only if all 3-node circular subgraphs are positive and the circular subgraphs corresponding to the nonzero $\mathcal{H}_1(X_{\mathcal{G}};\mathbb{Z})$ are also positive.*

Proof. Since $\mathcal{H}_1(X_{\mathcal{G}};\mathbb{Z})$ is nonzero, there must exist concatenated 1-simplices (e.g., a path in $\mathcal{G}$) forming one-dimensional holes in $X_{\mathcal{G}}$. Without loss of generality, only 1 one-dimensional hole is considered in the following analysis. For the case of multiple one-dimensional holes, the same analysis can be repeated for each hole.

Let $\mathcal{G}_{\mathcal{H}} = (\mathcal{V}_{\mathcal{H}}, \mathcal{E}_{\mathcal{H}}, \mathcal{A}_{\mathcal{H}})$ be the circular subgraph in $\mathcal{G}$ corresponding to the one-dimensional hole in $X_{\mathcal{G}}$. If $\mathcal{G}_{\mathcal{H}}$ is positive, $\mathcal{G}_{\mathcal{H}}$ is structurally balanced [2], which indicates that $\mathcal{V}_{\mathcal{H}}$ can be divided into two sets $\mathcal{V}_{\mathcal{H}1}$ and $\mathcal{V}_{\mathcal{H}2}$ with $\mathcal{V}_{\mathcal{H}1} \cup \mathcal{V}_{\mathcal{H}2} = \mathcal{V}_{\mathcal{H}}$ and $\mathcal{V}_{\mathcal{H}1} \cap \mathcal{V}_{\mathcal{H}2} = \emptyset$ such that edges within each set are positive and edges connecting different sets are negative. Note that $\mathcal{G}_{\mathcal{H}}$ remains structurally balanced by Def. 2.2, if $\mathcal{G}_{\mathcal{H}}$ is augmented to a complete graph $\mathcal{G}'_{\mathcal{H}}$ by adding positive edges to nodes that are not connected in the same set, and negative edges between nodes from different sets. Since $\mathcal{G}'_{\mathcal{H}}$ is a complete graph, $\mathcal{G}'_{\mathcal{H}}$ is contractible and thus has the vanishing first homology, which indicates all circular subgraphs in $\mathcal{G}'_{\mathcal{H}}$ are positive. Together with the condition that all 3-node circular subgraphs are positive, the original graph $\mathcal{G}$ is also structurally balanced by Theorem 8.1.

To prove the necessary condition, note that a connected signed graph $\mathcal{G}$ is structurally balanced if and only if all circular subgraphs of $\mathcal{G}$ are positive, i.e., the product of edge weights on any circular subgraph is positive [2]. Consequently, all 3-node circular subgraphs and the circular subgraphs corresponding to the nonzero $\mathcal{H}_1(X_{\mathcal{G}};\mathbb{Z})$ are all positive. □

Theorem 8.2 develops a necessary and sufficient condition to characterize the structural balance. Specifically, Theorem 8.2 relates the structure balance to the 3-node circular subgraphs, which provides insights into the key topological structures that result in the structural balance. If a graph does not have 3-node circular subgraphs, Theorem 2 is relaxed to only require that the circular subgraphs corresponding to the nonzero $\mathcal{H}_1(X_{\mathcal{G}};\mathbb{Z})$ are all positive. Note that the developed characterizations are only applicable to undirected graphs, since Theorem 8.1 and 8.2 are developed based on a multiplicative abelian group $(\mathbb{Z}_2,\times)$, where only the product of edge weights matters in characterizing the structural balance. The direction of edges are not accounted for in the considered multiplicative abelian group. Ongoing research will consider other abelian groups taking into account the direction of edges if directed graphs are considered. Nevertheless, the revealed key topological structures can be leveraged in topology design (see Section 8.2.3 for an illustrative example).

Example 8.3. Fig. 8-3 is provided to illustrate the general ideas in the proof of Theorem 8.2. Consider a simplicial complex $X_{\mathcal{G}}$ consisting of six vertices (0-simplices), eight edges (1-simplices), and two 2-simplices (filled triangles) in Fig. 8-3 (a). The vertices $\{1,2,3\}$ and $\{2,4,5\}$ form two positive 3-node circular subgraphs, while the vertices $\{2,3,6,5\}$ form a one-dimensional hole in $X_{\mathcal{G}}$, indicating $\mathcal{H}_1(X_{\mathcal{G}};\mathbb{Z}) \neq 0$. Fig. 8-3 (b) shows the construction of a complete subgraph over $\{2,3,6,5\}$, which can be verified to be structurally balanced. Note that, in Fig. 8-3 (b), its first homology $\mathcal{H}_1$ becomes zero due to the absence of the 1 dimensional hole, where Theorem 8.1 can be invoked to show that both Fig. 8-3 (a) and (b) are structurally balanced.

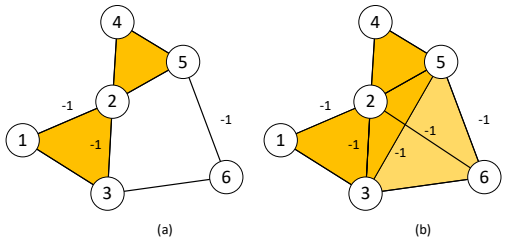

Figure 8-3. The illustration of the proof of Theorem 8.2.

8.2.3 Topology Design

In this section, we will demonstrate the effectiveness of the developed topological characterizations of the structural balance and how the characterizations can be potentially extended to construct structurally balanced graphs via topology design.

Consider a signed graph $\mathcal{G}$ in Fig. 8-4 (a), where negative edges are marked by -1. The signed graph $\mathcal{G}$ is initially structurally unbalanced. To demonstrate the developed topological characterizations of the structural balance in Section 8.2.2, $\mathcal{G}$ is represented by a simplicial complex $X_{\mathcal{G}}$ in Fig. 8-4 (b), which consists of 10 0-simplices (nodes), 18 1-simplices (edges), 9 2-simplices (triangles), and 1 3-simplex (tetrahedron). It can be verified that all 2-simplices (i.e., 3-node circular subgraphs) are positive, while the vertices $\{3, 2, 6, 7\}$ form a one-dimensional hole (dashed lines), which indicates a non-vanishing first homology $\mathcal{H}_1\left(X_{\mathcal{G}}; \mathbb{Z}\right) \neq 0$. Since the one-dimensional hole formed by $\{3, 2, 6, 7\}$ is indeed a negative 4-node circular subgraph, the conditions in Theorem 8.2 are not satisfied, which is consistent with the fact that $\mathcal{G}$ is structurally unbalanced.

In $X_{\mathcal{G}}$, all 2-simplices are positive, and the only violation to Theorem 8.2 is the non-vanishing $\mathcal{H}_1$ formed by the vertices $\{3, 2, 6, 7\}$. If $\mathcal{G}$ is modified by removing the edge $\{3, 7\}$, the vertices $\{3, 2, 6, 7\}$ no longer form a one-dimensional hole, and thus $\mathcal{H}_1\left(X_{\mathcal{G}}; \mathbb{Z}\right) = 0$, which indicates that the modified $\mathcal{G}$ becomes structurally balanced by Corollary 8.1. Note that the removal of $\{3, 7\}$ is not the only way to construct a structurally balanced graph from $\mathcal{G}$. An alternative is to switch the edge weight of $\{3, 7\}$ from $+1$ to -1, resulting in a positive circular

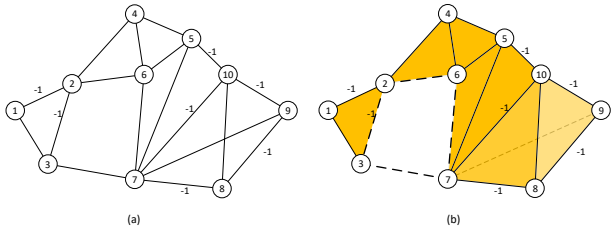

Figure 8-4. (a) The structurally unbalanced signed graph $\mathcal{G}$. (b) The simplicial complex $X_{\mathcal{G}}$ constructed from $\mathcal{G}$, where the dashed lines indicate a one-dimensional hole.

subgraph of $\{3, 2, 6, 7\}$. Theorem 8.2 can then be invoked to indicate that the modified $\mathcal{G}$ with a negative weight on $\{3, 7\}$ is also structurally balanced.

Remark 8.2. The developed algebraic topological characterizations can not only verify the structural balance, but also provide insights on how to tweak the network topology to yield structural balance. What makes the topological characterizations powerful is their capability to identify the key structures (i.e., one-dimensional holes) or key components (i.e., certain edges) in the graph, such that a minor modification on these key structures or components can result in a significant change of network topology structures, e.g., a change from structural unbalance to structural balance. Such insights are generally not obtainable from standard graphical methods and conventional analysis tools. The key enablers in our approach are the use of the novel simplicial-complex-based modeling approach capturing the global topological structure of the signed graph, and tools such as homology and cohomology to extract topological properties crucial to the structural balance.

8.3 Summary

Algebraic topological characterizations of the structural balance in signed graphs are developed in this Chapter. Leveraging tools from algebraic topology, simplicial complexes are used to model signed graphs, upon which simplicial homology and cohomology based characterizations are developed to capture the topological properties of the structural balance. The effectiveness of the developed topological characterizations is demonstrated via examples. Additional research will continue along this direction and further explore how the developed topological characterizations can be utilized in topology design for desired network performance.

Specifically, based on [121], additional research will investigate the potential extension of the developed cycle based topological characterizations in measuring partial balance in signed graphs. Future research will also consider extending the work of [125] and investigate the topological characterizations of generalized structural balance of graphs with complex edge weights.

CHAPTER 9
CONCLUSION AND FUTURE WORK

9.1 Conclusion

Topological characterizations of controllability of complex networks are investigated in this dissertation. Particularly, a leader-follower framework is adopted on networked control systems. Controllability, energy-related controllability and herdability are explored through various graph characteristics. Controllability ensures a leader-follower networked control system to enjoy the property, that the system can be driven into any desired state through designed control input. However, a lot of controllable networked systems could potentially be unrealizable in practice. This comes from the difference between traditional control systems and large-scaled networked control systems in terms of energy-related performance. Energy-related controllability provides a networked control system with the capability to be controllable and to have a better system performance in terms of energy-related metrics. Further, to require a system to be fully controllable might be unnecessary under certain situations. Herdability of a networked control system can be interpreted as the ability to drive the states of the system above a positive threshold, which is applicable in social and biological networked systems. Since controllability, energy-related controllability and herdability are all related to performance of driving system states, this dissertation treats them as generalized controllability and tries to bridge the gap between generalized controllability and network topology. Specific contributions of each chapter are summarized as follows.

In Chapter 2, classical controllability of networked control systems with Laplacian dynamics are considered. Leader selection to ensure controllability of signed networks with unit edge weight is investigated through partitioning the network into signed path and cycle networks, based on the developed condition that controllability is invariant under alterations of leader-to-leader connections. Sufficient conditions to ensure signed path and cycle networks to be controllable are developed via graph topology to facilitate the development of leader selection algorithm.

In Chapter 3, energy-related controllability is investigated through the structure of signed Laplacian matrix on general signed weighted networks. A nodal metric capturing energy-related performance of networked control system is defined. Average controllability, average control energy and volumetric control energy are discovered to be related to the defined nodal metric. This relates the performance of networked control systems to the contribution of individual leader. Further, structural balance is found to play an important role in network controllability, that controllability and energy-related controllability of a signed network are equivalent to the corresponding unsigned cases if the network is structurally balanced.

In Chapter 4, one type of energy-related controllability, average controllability, is investigated on signed acyclic networks with unit edge weights. For this particular network structure, nodal metric defined in Chapter 3 is found to be related to resistance distance and graph distance. Utilizing results developed in Chapter 2 and Chapter 3, leader selection algorithm via graph topology is developed to ensure network controllability with better average controllability.

In Chapter 5, energy-related controllability on signed weighted composite networks are investigated through their factor networks, through the construction of composite networks via graph product. Average controllability, average control energy and volumetric control energy of composite networks constructed through Cartesian product are found to be closely related to the energy-related metrics of the factor networks. These results are further extended to one type of layered control system. Then, energy-related metrics of composite networks constructed through direct product and strong product are tackled. Besides, the connection between composite networks and factor networks on structural balance are revealed.

In Chapter 6, herdability of signed weighted networks are revealed through a generalized equitable partition. Different from previous chapters, network dynamics are captured directly through the underlying network topology. Controllable subspace is captured through the generalized equitable partition defined in this Chapter. Through the partition, a quotient network structure is exploited to represent the dynamics of the original network while the herdability of

the system is remained. This provides a way of lowering the dimension of a networked system when checking herdability.

In Chapter 7, graph walks are used to capture the structure of controllability matrix. This indicates the connection between graph walks and network herdability. Graph 1-walks and 2-walks are utilized to reveal herdability of generalized signed weighted networks. For structurally balanced networks, leader selection methods are developed to ensure network herdability. The developed leader selection methods are further refined through graph walks.

In Chapter 8, simplicial complex is utilized to model signed graphs. Necessary and sufficient conditions for structural balance is developed through 3-cycles and first homology groups of the constructed simplicial complex, revealing a novel method to testify structural balance of signed graphs.

9.2 Future Work

Recently, modelings of complex networks and networked dynamical systems are not limited to engineering areas, such as multi-agent systems, power networks and transportation networks but extended to filed as biology and economics. With the wide-spreading of applications of complex networks, analyzing properties of networked control systems becomes more important. This section shows potential research directions of each chapter in the dissertation.

Chapter 2 discusses classical controllability of complex networks. Signed networks with unit edge weights is considered. However, topological characterizations of controllability of signed networks with other dynamics is still an open problem. A few work considers building the gap between graph structure and network controllability on network dynamics described by adjacency matrix. Despite of classical controllability, structurally controllability is also a popular topic on networked control systems. Future research can also be expanded to build the connection between structurally controllability and network topology.

Chapter 3 to Chapter 5 reveal energy-related controllability of complex networks with Laplacian dynamics. Two main research directions can be followed in the future. The one is to bridge the gap between the nodal metric developed in Chapter 3 and the underlying graph

structure. Although the nodal metric is captured by graph distance in Chapter 4 on structurally balanced networks, the gap between the defined nodal metric and graph topology on structurally unbalanced networks is still unfilled. Followed by this direction, definition on resistance distance on signed graphs is still an open problem which might endow the nodal metric a topological interpretation. The other limitation of the work from Chapter 3 to Chapter 5 is that all of the energy-related controllability are developed on infinite-time controllability Gramian. In reality, plenty of state transfer should be completed within finite time. In the future, relationship between energy-related controllability and network topology will be investigated on finite-time controllability Gramian.

Chapter 6 and Chapter 7 analyze herdability of signed networks with network dynamics captured by adjacency matrix. Graph partition and graph walks are exploited to unveil the relation between network structure and herdability. However, compared to previous chapters, system performance in related to driving the states above a positive threshold remains to be explored, i.e., energy-related herdability.

Chapter 8 indicates that higher order interactions among network units can be modeled through simplicial complex. This paves a way to analyze complex networks with more sophisticated dynamics. Controllability, control energy metrics and herdability analysis of networked control systems could be extend to networked systems with higher order interactions constructed through simplicial complex in the future.

REFERENCES

[1] W. Ren, R. W. Beard, and E. M. Atkins, "Information consensus in multi-vehicle cooperative control," *IEEE Control Syst. Mag.*, vol. 27, pp. 71–82, April 2007.

[2] C. Altafini, "Consensus problems on networks with antagonistic interactions," *IEEE Trans. Autom. Control*, vol. 58, no. 4, pp. 935–946, 2013.

[3] G. Facchetti, G. Iacono, and C. Altafini, "Computing global structural balance in large-scale signed social networks," *Proc. Nat. Acad. Sci.*, vol. 108, no. 52, pp. 20 953–20 958, 2011.

[4] L. Tian, Z. Ji, T. Hou, and K. Liu, "Bipartite consensus on coopetition networks with time-varying delays," *IEEE Access*, vol. 6, pp. 10 169–10 178, 2018.

[5] H. G. Tanner, "On the controllability of nearest neighbor interconnections," in *Proc. IEEE Conf. Decis. Control*, vol. 3, 2004, pp. 2467–2472.

[6] A. Rahmani, M. Ji, M. Mesbahi, and M. Egerstedt, "Controllability of multi-agent systems from a graph-theoretic perspective," *SIAM J. Control Optim*, vol. 48, no. 1, pp. 162–186, 2009.

[7] Z. Ji and H. Yu, "A new perspective to graphical characterization of multi-agent controllability," *IEEE Trans. Cybern.*, vol. 47, no. 6, pp. 1471–1483, 2017.

[8] R. Haghighi and C. C. Cheah, "Topology-based controllability problem in network systems," *IEEE Trans. Syst. Man Cybern: Syst.*, vol. 47, no. 11, pp. 3077–3088, 2017.

[9] A. Yazıcıoğlu, W. Abbas, and M. Egerstedt, "Graph distances and controllability of networks," *IEEE Trans. Autom. Control*, vol. 61, no. 12, pp. 4125–4130, 2016.

[10] Z. Ji, H. Lin, and H. Yu, "Leaders in multi-agent controllability under consensus algorithm and tree topology," *Syst. Control Lett.*, vol. 61, no. 9, pp. 918–925, 2012.

[11] G. Notarstefano and G. Parlangeli, "Controllability and observability of grid graphs via reduction and symmetries," *IEEE Trans. Autom. Control*, vol. 58, no. 7, pp. 1719–1731, 2013.

[12] G. Parlangeli and G. Notarstefano, "On the reachability and observability of path and cycle graphs," *IEEE Trans. Autom. Control*, vol. 57, no. 3, pp. 743–748, 2012.

[13] X. Liu, H. Lin, and B. M. Chen, "Structural controllability of switched linear systems," *Automatica*, vol. 49, no. 12, pp. 3531–3537, 2013.

[14] C.-T. Lin, "Structural controllability," *IEEE Trans. Autom. Control*, vol. 19, no. 3, pp. 201–208, 1974.

[15] R. Shields and J. Pearson, "Structural controllability of multi-input linear systems," *IEEE Trans Autom Control*, vol. 21, no. 2, pp. 203–212, 1976.

[16] X. Liu, H. Lin, and B. M. Chen, "Graph-theoretic characterisations of structural controllability for multi-agent system with switching topology," *Int. J. Control*, vol. 86, no. 2, pp. 222–231, 2013.

[17] Y. Tang, Z. Wang, H. Gao, H. Qiao, and J. Kurths, "On controllability of neuronal networks with constraints on the average of control gains," *IEEE Trans. Cybern.*, vol. 44, no. 12, pp. 2670–2681, Dec 2014.

[18] S. Zhao and F. Pasqualetti, "Networks with diagonal controllability gramian: Analysis, graphical conditions, and design algorithms," *Automatica*, vol. 102, pp. 10–18, 2019.

[19] F. Liu and A. S. Morse, "A graphical characterization of structurally controllable linear systems with dependent parameters," *IEEE Trans. on Autom. Control*, 2019.

[20] J. Jia, H. L. Trentelman, W. Baar, and M. K. Camlibel, "Strong structural controllability of systems on colored graphs," *IEEE Trans. on Autom. Control*, 2019.

[21] Y. Hao, Z. Duan, G. Chen, and F. Wu, "New controllability conditions for networked identical LTI systems," *IEEE Trans. Autom. Control*, vol. 64, no. 10, pp. 4223–4228, 2019.

[22] C. O. Aguilar and B. Gharesifard, "Graph controllability classes for the Laplacian leader-follower dynamics," *IEEE Trans. Autom. Control*, vol. 60, no. 6, pp. 1611–1623, 2015.

[23] C. Commault and J.-M. Dion, "Input addition and leader selection for the controllability of graph-based systems," *Automatica*, vol. 49, no. 11, pp. 3322–3328, 2013.

[24] Z. Ji, Z. Wang, H. Lin, and Z. Wang, "Interconnection topologies for multi-agent coordination under leader–follower framework," *Automatica*, vol. 45, no. 12, pp. 2857–2863, 2009.

[25] A. Olshevsky, "Minimal controllability problems," *IEEE Trans. Control Network Syst.*, vol. 1, no. 3, pp. 249–258, 2014.

[26] M. Van De Wal and B. De Jager, "A review of methods for input/output selection," *Automatica*, vol. 37, no. 4, pp. 487–510, 2001.

[27] B. Marx, D. Koenig, and D. Georges, "Optimal sensor and actuator location for descriptor systems using generalized gramians and balanced realizations," in *Am. Control Conf.*, vol. 3. IEEE, 2004, pp. 2729–2734.

[28] H. R. Shaker and M. Tahavori, "Optimal sensor and actuator location for unstable systems," *J. Vib. Control*, vol. 19, no. 12, pp. 1915–1920, 2013.

[29] K. Lim, "Method for optimal actuator and sensor placement for large flexible structures," *J. Guid. Control Dyn.,*, vol. 15, no. 1, pp. 49–57, 1992.

[30] G. Yan, J. Ren, Y.-C. Lai, C.-H. Lai, and B. Li, "Controlling complex networks: How much energy is needed?" *Phys Rev Lett*, vol. 108, no. 21, p. 218703, 2012.

[31] T. H. Summers, F. L. Cortesi, and J. Lygeros, "On submodularity and controllability in complex dynamical networks," *IEEE Trans. Control Network Syst.*, vol. 3, no. 1, pp. 91–101, 2016.

[32] F. Pasqualetti, S. Zampieri, and F. Bullo, "Controllability metrics, limitations and algorithms for complex networks," *IEEE Trans. Control Network Syst.*, vol. 1, no. 1, pp. 40–52, 2014.

[33] A. Olshevsky, "Eigenvalue clustering, control energy, and logarithmic capacity," *Syst. Control Lett.*, vol. 96, pp. 45–50, 2016.

[34] N. Bof, G. Baggio, and S. Zampieri, "On the role of network centrality in the controllability of complex networks," *IEEE Trans. Control Network Syst.*, vol. 4, no. 3, pp. 643–653, 2017.

[35] V. Tzoumas, M. A. Rahimian, G. J. Pappas, and A. Jadbabaie, "Minimal actuator placement with bounds on control effort," *IEEE Trans. Control Network Syst.*, vol. 3, no. 1, pp. 67–78, 2016.

[36] S. Pequito, S. Kar, and A. P. Aguiar, "Minimum cost input/output design for large-scale linear structural systems," *Automatica*, vol. 68, pp. 384–391, 2016.

[37] A. Clark, B. Alomair, L. Bushnell, and R. Poovendran, "Input selection for performance and controllability of structured linear descriptor systems," *SIAM J. Control Optim.*, vol. 55, no. 1, pp. 457–485, 2017.

[38] K. Fitch and N. E. Leonard, "Joint centrality distinguishes optimal leaders in noisy networks," *IEEE Trans. Control Network Syst.*, vol. 3, no. 4, pp. 366–378, 2016.

[39] J. Z. Kim, J. M. Soffer, A. E. Kahn, J. M. Vettel, F. Pasqualetti, and D. S. Bassett, "Role of graph architecture in controlling dynamical networks with applications to neural systems," *Nat. Phys.*, vol. 14, no. 1, pp. 91–98, 2018.

[40] B. She, S. Mehta, J. C. Emily Doucette, and Z. Kan, "Leader group selection for energy-related controllability of signed acyclic graphs," in *Proc. Am. Control Conf.*, 2019, pp. 133–138.

[41] C. O. Becker, S. Pequito, G. J. Pappas, and V. M. Preciado, "Network design for controllability metrics," in *IEEE Conf. Decis. Control*, 2017, pp. 4193–4198.

[42] R. Dhal and S. Roy, "Vulnerability of network synchronization processes: A minimum energy perspective," *IEEE Trans. Autom. Control*, vol. 61, no. 9, pp. 2525–2530, 2015.

[43] G. Lindmark and C. Altafini, "Combining centrality measures for control energy reduction in network controllability problems," in *Europ. Control Conf.*, 2019, pp. 1518–1523.

[44] E. Nozari, F. Pasqualetti, and J. Cortés, "Time-invariant versus time-varying actuator scheduling in complex networks," in *Am. Control Conf.*, 2017, pp. 4995–5000.

[45] S. Zhao and F. Pasqualetti, "Controllability degree of directed line networks: Nodal energy and asymptotic bounds," in *Europ. Control Conf.*, 2018, pp. 1857–1862.

[46] Y. Zhao and J. Cortés, "Gramian-based reachability metrics for bilinear networks," *IEEE Trans. Control Netw. System*, vol. 4, no. 3, pp. 620–631, 2016.

[47] T. Summers and J. Ruths, "Performance bounds for optimal feedback control in networks," in *Am. Control Conf.*, 2018, pp. 203–209.

[48] C. Enyioha, M. A. Rahimian, G. J. Pappas, and A. Jadbabaie, "Controllability and fraction of leaders in infinite networks," in *Proc. IEEE Conf. Decis. Control*. IEEE, 2014, pp. 1359–1364.

[49] G. Lindmark and C. Altafini, "Minimum energy control for complex networks," *Sci Rep*, vol. 8, no. 1, p. 3188, 2018.

[50] J. Ding, C. Wen, and G. Li, "Key node selection in minimum-cost control of complex networks," *Physica A*, vol. 486, pp. 251–261, 2017.

[51] K. Fitch and N. E. Leonard, "Optimal leader selection for controllability and robustness in multi-agent networks," in *Eur. Control Conf.* IEEE, 2016, pp. 1550–1555.

[52] E. Davison and S. Wang, "New results on the controllability and observability of general composite systems," *IEEE Trans. Autom. Control*, vol. 20, no. 1, pp. 123–128, 1975.

[53] W. M. Haddad and V. Chellaboina, *Nonlinear dynamical systems and control: a Lyapunov-based approach*. Princeton university press, 2011.

[54] A. Chapman, M. Nabi-Abdolyousefi, and M. Mesbahi, "Controllability and observability of network-of-networks via Cartesian products," *IEEE Trans. Autom. Control*, vol. 59, no. 10, pp. 2668–2679, 2014.

[55] Y. Hao, Q. Wang, Z. Duan, and G. Chen, "Controllability of Kronecker product networks," *Automatica*, vol. 110, p. 108597, 2019.

[56] L. Pan, H. Shao, and M. Mesbahi, "Verification and prediction of structural balance: A data-driven perspective," in *Proc. Am. Control Conf.* IEEE, 2016, pp. 2858–2863.

[57] T. N. Tran and A. Chapman, "Generalized graph product: Spectrum, trajectories and controllability," in *Proc. IEEE Conf. Decis. Control*. IEEE, 2018, pp. 5358–5363.

[58] Y.-Y. Liu, J.-J. Slotine, and A.-L. Barabási, "Controllability of complex networks," *Nature*, vol. 473, no. 7346, pp. 167–173, 2011.

[59] C. Sun, G. Hu, and L. Xie, "Controllability of multi-agent networks with antagonistic interactions," *IEEE Trans. Autom. Control*, vol. 62, no. 10, pp. 5457–5462, 2017.

[60] S. Alemzadeh, M. H. de Badyn, and M. Mesbahi, "Controllability and stabilizability analysis of signed consensus networks," in *IEEE Conf. Control Technol. Appl.* IEEE, 2017, pp. 55–60.

[61] Y. Guan and L. Wang, "Controllability of multi-agent systems with directed and weighted signed networks," *Syst. Control Lett.*, vol. 116, pp. 47–55, 2018.

[62] C. Godsil and G. Royle, *Algebraic Graph Theory*, ser. Graduate Texts in Mathematics. Springer, 2001.

[63] D. M. Cardoso, C. Delorme, and P. Rama, "Laplacian eigenvectors and eigenvalues and almost equitable partitions," *Eur. J. Combinatorics*, vol. 28, no. 3, pp. 665–673, 2007.

[64] M. Egerstedt, S. Martini, M. Cao, K. Camlibel, and A. Bicchi, "Interacting with networks: How does structure relate to controllability in single-leader, consensus networks?" *IEEE Control Syst.*, vol. 32, no. 4, pp. 66–73, 2012.

[65] C. O. Aguilar and B. Gharesifard, "Almost equitable partitions and new necessary conditions for network controllability," *Automatica*, vol. 80, pp. 25–31, 2017.

[66] S. Zhang, M. Cao, and M. K. Camlibel, "Upper and lower bounds for controllable subspaces of networks of diffusively coupled agents," *IEEE Trans. Autom. control*, vol. 59, no. 3, pp. 745–750, 2014.

[67] M. T. Schaub, N. O'Clery, Y. N. Billeh, J.-C. Delvenne, R. Lambiotte, and M. Barahona, "Graph partitions and cluster synchronization in networks of oscillators," *Chaos*, vol. 26, no. 9, p. 094821, 2016.

[68] N. OClery, Y. Yuan, G.-B. Stan, and M. Barahona, "Observability and coarse graining of consensus dynamics through the external equitable partition," *Pyhs. Rev. E*, vol. 88, no. 4, p. 042805, 2013.

[69] S. F. Ruf, M. Egerstedt, and J. S. Shamma, "Herdable systems over signed, directed graphs," in *Proc. Am. Control Conf.*, 2018.

[70] L. Farina and S. Rinaldi, *Positive linear systems: theory and applications*. John Wiley & Sons, 2011, vol. 50.

[71] S. F. Ruf, M. Egersted, and J. S. Shamma, "Herding complex networks," *arXiv preprint arXiv:1804.04449*, 2018.

[72] S. F. Ruf, M. Egerstedt, and J. S. Shamma, "Herdability of linear systems based on sign patterns and graph structures," *arXiv preprint arXiv:1904.08778*, 2019.

[73] F. Harary *et al.*, "On the notion of balance of a signed graph." *The Michigan Math. J.*, vol. 2, no. 2, pp. 143–146, 1953.

[74] Y. Jiang, H. Zhang, and J. Chen, "Sign-consensus of linear multi-agent systems over signed directed graphs," *IEEE Trans. Ind. Electron.*, vol. 64, no. 6, pp. 5075–5083, 2017.

[75] D. Meng, Z. Meng, and Y. Hong, "Uniform convergence for signed networks under directed switching topologies," *Automatica*, vol. 90, pp. 8–15, 2018.

[76] H. Zhang and J. Chen, "Bipartite consensus of multi-agent systems over signed graphs: State feedback and output feedback control approaches," *Int. J. Robust Nonlinear Control*, vol. 27, no. 1, pp. 3–14, 2017.

[77] Y. Wu, Y. Zhao, and J. Hu, "Bipartite consensus control of high-order multi-agent systems with unknown disturbances," *IEEE Trans Syst Man Cybern Syst.*, 2017.

[78] S. A. Marvel, J. Kleinberg, R. D. Kleinberg, and S. H. Strogatz, "Continuous-time model of structural balance," *Proc. Natl. Acad. Sci.*, vol. 108, no. 5, pp. 1771–1776, 2011.

[79] T. Antal, P. L. Krapivsky, and S. Redner, "Dynamics of social balance on networks," *Phys. Rev. E*, vol. 72, no. 3, p. 036121, 2005.

[80] A. V. Proskurnikov, A. S. Matveev, and M. Cao, "Opinion dynamics in social networks with hostile camps: Consensus vs. polarization," *IEEE Trans. Autom. Control*, vol. 61, no. 6, pp. 1524–1536, 2016.

[81] J. Kunegis, "Applications of structural balance in signed social networks," *arXiv preprint arXiv:1402.6865*, 2014.

[82] J. Liu, X. Chen, and T. Başar, "Stability of the continuous-time altafini model," in *Am. Control Conf.* IEEE, 2016, pp. 1930–1935.

[83] M. H. de Badyn, S. Alemzadeh, and M. Mesbahi, "Controllability and data-driven identification of bipartite consensus on nonlinear signed networks," *arXiv preprint arXiv:1709.06679*, 2017.

[84] W. Xiao and I. Gutman, "Resistance distance and Laplacian spectrum," *Theor. Chem. Acc.*, vol. 110, no. 4, pp. 284–289, 2003.

[85] S. Gu, F. Pasqualetti, M. Cieslak, Q. K. Telesford, B. Y. Alfred, A. E. Kahn, J. D. Medaglia, J. M. Vettel, M. B. Miller, S. T. Grafton *et al.*, "Controllability of structural brain networks," *Nat Commun*, vol. 6, 2015.

[86] S. Jafari, A. Ajorlou, and A. G. Aghdam, "Leader localization in multi-agent systems subject to failure: A graph-theoretic approach," *Automatica*, vol. 47, no. 8, pp. 1744–1750, 2011.

[87] A. Hatcher, *Algebraic topology*. New York:Cambridge University Press, 2001.

[88] A. Tahbaz-Salehi and A. Jadbabaie, "Distributed coverage verification in sensor networks without location information," *IEEE Trans. Autom. Control*, vol. 55, no. 8, pp. 1837–1849, 2010.

[89] V. De Silva and R. Ghrist, "Coordinate-free coverage in sensor networks with controlled boundaries via homology," *Int. J. Robot. Res.*, vol. 25, no. 12, pp. 1205–1222, 2006.

[90] H. Chintakunta and H. Krim, "Distributed localization of coverage holes using topological persistence." *IEEE Trans. Signal Processing*, vol. 62, no. 10, pp. 2531–2541, 2014.

[91] Z. Han, L. Wang, Z. Lin, and R. Zheng, "Formation control with size scaling via a complex Laplacian-based approach," *IEEE Trans Cybern*, vol. 46, no. 10, pp. 2348–2359, 2016.

[92] H. G. Tanner, A. Jadbabaie, and G. J. Pappas, "Flocking in fixed and switching networks," *IEEE Trans. Autom. Control*, vol. 52, no. 5, pp. 863–868, May 2007.

[93] L. Cheng, Y. Wang, W. Ren, Z.-G. Hou, and M. Tan, "Containment control of multi-agent systems with dynamic leaders based on a PI^n-type approach," *IEEE Trans Cybern*, vol. 46, no. 12, pp. 3004–3017, 2016.

[94] K. Ogata and Y. Yang, "Modern control engineering," 1970.

[95] M. Nabi-Abdolyousefi and M. Mesbahi, "On the controllability properties of circulant networks," *IEEE Trans. Autom. Control*, vol. 58, no. 12, pp. 3179–3184, 2013.

[96] R. Olfati-Saber, J. A. Fax, and R. M. Murray, "Consensus and cooperation in networked multi-agent systems," *Proc. IEEE*, vol. 95, no. 1, pp. 215–233, Jan. 2007.

[97] G. Steiner, "On the k-path partition of graphs," *Theor. Comput. Sci.*, vol. 290, no. 3, pp. 2147–2155, 2003.

[98] Z. Hu and H. Li, "Partition of a graph into cycles and vertices," *Discrete Math.*, vol. 307, no. 11-12, pp. 1436–1440, 2007.

[99] H. Enomoto, "Graph partition problems into cycles and paths," *Discrete Math.*, vol. 233, no. 1-3, pp. 93–101, 2001.

[100] S. Pequito, G. Ramos, S. Kar, A. P. Aguiar, and J. Ramos, "The robust minimal controllability problem," *Automatica*, vol. 82, pp. 261–268, 2017.

[101] T. Kailath, *Linear systems*. Prentice-Hall Englewood Cliffs, NJ, 1980, vol. 156.

[102] M. Pirani, E. M. Shahrivar, B. Fidan, and S. Sundaram, "Robustness of leader–follower networked dynamical systems," *IEEE Trans. on Control of Network Syst.*, vol. 5, no. 4, pp. 1752–1763, 2017.

[103] P. Barooah and J. P. Hespanha, "Graph effective resistance and distributed control: Spectral properties and applications," in *Proc. IEEE Conf. Decis. Control*, 2006, pp. 3479–3485.

[104] O. Romero and S. Pequito, "Actuator placement for symmetric structural controllability with heterogeneous costs," *IEEE Control Syst. Lett.*, vol. 2, no. 4, pp. 821–826, 2018.

[105] B. She, S. Mehta, C. Ton, and Z. Kan, "Topological characterizations of leader-follower controllability on signed path and cycle networks," in *Proc. IEEE Conf. Decis. Control*. IEEE, 2018, pp. 6157–6162.

[106] W. Imrich and S. Klavzar, *Product graphs: structure and recognition*. Wiley, 2000.

[107] R. A. Horn and C. R. Johnson, *Topics in matrix analysis*. New York: Cambridge Univ. Press, 1991.

[108] A. Olshevsky, "On (non) supermodularity of average control energy," *IEEE Trans. Control Network Syst.*, 2017.

[109] I. Poulakakis, G. F. Young, L. Scardovi, and N. E. Leonard, "Information centrality and ordering of nodes for accuracy in noisy decision-making networks," *IEEE Trans. Autom. Control*, vol. 61, no. 4, pp. 1040–1045, 2015.

[110] M. Fiedler, "Algebraic connectivity of graphs," *Czechoslovak Math. J.*, vol. 23, no. 2, pp. 298–305, 1973.

[111] D. S. Bernstein, *Matrix mathematics: theory, facts, and formulas*. Princeton university press, 2009.

[112] J. Leskovec, A. Krause, C. Guestrin, C. Faloutsos, C. Faloutsos, J. VanBriesen, and N. Glance, "Cost-effective outbreak detection in networks," in *Proc. ACM SIGKDD Int. Conf. Knowledge Discovery Data Mining*. ACM, 2007, pp. 420–429.

[113] D. Burgarth, D. D'Alessandro, L. Hogben, S. Severini, and M. Young, "Zero forcing, linear and quantum controllability for systems evolving on networks," *IEEE Tran. Autom. Control*, vol. 58, no. 9, pp. 2349–2354, 2013.

[114] V. Gupta, M. Sharma, and N. Thakur, "Optimization criteria for optimal placement of piezoelectric sensors and actuators on a smart structure: a technical review," *J. Intell. Mater. Syst. and Struct.*, vol. 21, no. 12, pp. 1227–1243, 2010.

[115] S. Barik, R. B. Bapat, and S. Pati, "On the laplacian spectra of product graphs," *Appli. Analy. and Discr. Math.*, pp. 39–58, 2015.

[116] M. Mesbahi and M. Egerstedt, *Graph theoretic methods in multiagent networks*. Princeton University Press, 2010.

[117] J. P. Hespanha, *Linear systems theory*. Princeton university press, 2018.

[118] P. De Leenheer and D. Aeyels, "Stabilization of positive linear systems," *Syst. control lett.*, vol. 44, no. 4, pp. 259–271, 2001.

[119] F. Harary and J. A. Kabell, "A simple algorithm to detect balance in signed graphs," 1980.

[120] F. Harary, "A matrix criterion for structural balance," *Naval Research Logistics (NRL)*, vol. 7, no. 2, pp. 195–199, 1960.

[121] S. Aref and M. C. Wilson, "Measuring partial balance in signed networks," *J. Complex Networks*, vol. 6, no. 4, pp. 566–595, 2017.

[122] J. R. Durbin, *Modern algebra: An introduction*. John Wiley & Sons, 2008.

[123] H. Edelsbrunner and J. Harer, *Computational topology: an introduction*. American Mathematical Soc., 2010.

[124] M. Kahle, "Topology of random clique complexes," *Discrete Math.*, vol. 309, no. 6, pp. 1658–1671, 2009.

[125] F. A. Yaghmaie, R. Su, F. L. Lewis, and L. Xie, "Multiparty consensus of linear heterogeneous multiagent systems," *IEEE Trans. on Autom. Control*, vol. 62, no. 11, pp. 5578–5589, 2017.